

Aspects of string theory compactifications:  
D-brane statistics and generalised geometry

---

Florian Gmeiner



Munich 2006



# Aspects of string theory compactifications: D-brane statistics and generalised geometry

---

Dissertation  
an der Fakultät für Physik  
Ludwig-Maximilians-Universität München

vorgelegt von  
Florian Gmeiner  
aus Berlin

München, den 26. Mai 2006

## Gutachter

---

1. Gutachter: Prof. Dr. Dieter Lüst
2. Gutachter: Dr. habil. Johanna Erdmenger

Datum der mündlichen Prüfung: 13. Juli 2006

## Abstract

In this thesis we investigate two different aspects of string theory compactifications.

The first part deals with the issue of the huge amount of possible string vacua, known as the landscape. Concretely we investigate a specific well defined subset of type II orientifold compactifications. We develop the necessary tools to construct a very large set of consistent models and investigate their gauge sector on a statistical basis. In particular we analyse the frequency distributions of gauge groups and the possible amount of chiral matter for compactifications to six and four dimensions. In the phenomenologically relevant case of four-dimensional compactifications, special attention is paid to solutions with gauge groups that include those of the standard model, as well as Pati-Salam,  $SU(5)$  and flipped  $SU(5)$  models. Additionally we investigate the frequency distribution of coupling constants and correlations between the observables in the gauge sector. These results are compared with a recent study of Gepner models. Moreover, we elaborate on questions concerning the finiteness of the number of solutions and the computational complexity of the algorithm.

In the second part of this thesis we consider a new mathematical framework, called generalised geometry, to describe the six-manifolds used in string theory compactifications. In particular, the formulation of T-duality and mirror symmetry for nonlinear topological sigma models is investigated. Therefore we provide a reformulation and extension of the known topological A- and B-models to the generalised framework. The action of mirror symmetry on topological D-branes in this setup is presented and the transformation of the boundary conditions is analysed. To extend the considerations to D-branes in type II string theory, we introduce the notion of generalised calibrations. We show that the known calibration conditions of supersymmetric branes in type IIA and IIB can be obtained as special cases. Finally we investigate the action of T-duality on the generalised calibrations.

## Zusammenfassung

In dieser Arbeit werden zwei unterschiedliche Aspekte von Kompaktifizierungen in der Stringtheorie untersucht.

Der erste Teil beschäftigt sich mit dem unter dem Namen “Landscape” bekannten Phänomen, das die sehr große Zahl von Vakuumlösungen in der Stringtheorie thematisiert. Konkret beschäftigen wir uns mit einer speziellen wohldefinierten Untermenge von Orientifold-Kompaktifizierungen in Stringtheorie vom Typ II. Wir entwickeln die notwendigen Methoden, um eine große Anzahl von konsistenten Modellen zu berechnen und deren Eichsektoren einer statistischen Analyse zu unterziehen. Diese beinhaltet eine Untersuchung der Häufigkeitsverteilungen einzelner Eichgruppen, sowie der Verteilung chiraler Materie in Kompaktifizierungen von zehn sowohl auf sechs, als auch auf vier Dimensionen. Der vierdimensionale Fall ist unter phänomenologischen Gesichtspunkten interessanter, und wir vertiefen daher unsere Analyse des Eichsektors in diesem Fall durch das Betrachten von Lösungen, die spezielle Eichgruppen, wie die des Standardmodells, von Pati-Salam,  $SU(5)$  und flipped  $SU(5)$  Modellen, aufweisen. Darüber hinaus untersuchen wir die Häufigkeitsverteilung von Kopplungskonstanten und Korrelationen zwischen den Observablen im Eichsektor der Modelle. Diese Ergebnisse werden mit einer Untersuchung von Gepner-Modellen verglichen. Wir beschäftigen uns ferner mit der Endlichkeit der Lösungen im Raum der von uns betrachteten Orientifold-Modelle, sowie der Komplexität der verwendeten Algorithmen.

Im zweiten Teil dieser Arbeit wird untersucht, wie ein neues Konzept der Mathematik, die sogenannte generalisierte Geometrie, zur Beschreibung der kompakten, sechsdimensionalen Mannigfaltigkeiten, welche in Kompaktifizierungen von Stringtheorie Verwendung finden, genutzt werden kann. Die Formulierung von T-Dualität und Mirror-Symmetrie für topologische Sigma-Modelle wird thematisiert und eine neue Formulierung und Erweiterung der bekannten topologischen A- und B-Modelle wird entwickelt. Wir untersuchen die Wirkung von Mirror-Symmetrie auf topologische D-Branen und die Transformation der Randbedingungen dieser Branen. Um die Analyse auf D-Branen in Stringtheorie vom Typ II zu erweitern, führen wir das Konzept generalisierter Kalibrierungen ein und zeigen, dass diese die bekannten Kalibrierungsbedingungen von D-Branen in Stringtheorie vom Typ IIA und IIB als Spezialfälle enthalten. Abschließend wird die Wirkung von T-Dualität auf die generalisierten Kalibrierungen untersucht.

## Acknowledgements

First of all I would like to thank Dieter Lüst for giving me the opportunity to work on this thesis under his supervision and member of his group. He never failed to support and encourage me during the last three years.

I would like to express my gratitude to all members of the string group in Munich, especially to Ralph Blumenhagen, not only for the fruitful collaboration, but also for his encouragement and his dedication to make the string group at the MPI such an inspiring place to be. Special thanks goes as well to Johanna Erdmenger for refereeing this work.

I owe a lot to my collaborators on the research projects presented in this thesis, namely Ralph Blumenhagen, Stefano Chiantese, Gabriele Honecker, Claus Jeschek, Maren Stein, Timo Weigand and especially Frederik Witt for explaining me the mysteries of generalised geometry.

It is a pleasure to thank Carlo Angelantonj, Mirjam Cvetič, Louise Dolan, Michael Douglas, Tianjun Li and Stefan Stieberger for interesting discussions.

Since the landscape project involved a considerable amount of computer business, I am grateful to the people at the Max-Planck-Rechenzentrum in Garching, Andreas Wisskirchen at Bonn University, as well as Thomas Hahn and Peter Breitenlohner at the MPI für Physik.

I am happy to thank all the people who shared my office during the last years and my fellow PhD students for making this time rich of experience, interesting discussions and fun. Thanks to Stefano Chiantese, Claus Jeschek, Dan Oprisa, Erik Plauschinn, Susanne Reffert, Maximilian Schmidt-Sommerfeld, Christoph Sieg and Timo Weigand.

Last but not least I would like to thank my parents and my friends for their love and support.





# Contents

<b>1</b>	<b>Introduction</b>	<b>1</b>
1.1	The Landscape . . . . .	2
1.2	Generalised Geometry . . . . .	4
1.3	Outline . . . . .	5
<b>I</b>	<b>D-brane statistics</b>	<b>7</b>
<b>2</b>	<b>Models and methods</b>	<b>9</b>
2.1	Orientifold models . . . . .	9
2.1.1	Chiral matter . . . . .	11
2.1.2	Tadpole cancellation conditions . . . . .	11
2.1.3	Supersymmetry conditions . . . . .	12
2.1.4	Anomalies and K-theory constraints . . . . .	13
2.2	Methods of D-brane statistics . . . . .	14
2.2.1	Introduction to the saddle point approximation . . . . .	14
2.2.2	A first application of the saddle point approximation . . . . .	18
2.2.3	Exact computations . . . . .	22
2.3	Finiteness of solutions . . . . .	25
2.3.1	The six-dimensional case . . . . .	25
2.3.2	Compactifications to four dimensions . . . . .	27
<b>3</b>	<b>Statistical analysis of orientifold models</b>	<b>31</b>
3.1	Statistics of six-dimensional models . . . . .	32
3.1.1	Distributions of gauge group observables . . . . .	32
3.1.2	Chirality . . . . .	34
3.1.3	Correlations . . . . .	35
3.2	Statistics of four-dimensional models . . . . .	36
3.2.1	Properties of the gauge sector . . . . .	36
3.2.2	Chirality . . . . .	37
3.3	Standard model constructions . . . . .	38
3.3.1	Number of generations . . . . .	41
3.3.2	Hidden sector . . . . .	43
3.3.3	Gauge couplings . . . . .	44
3.3.4	Comparison with the statistics of Gepner models . . . . .	46

3.4	Pati-Salam models . . . . .	47
3.5	SU(5) models . . . . .	48
3.5.1	Construction . . . . .	49
3.5.2	General results . . . . .	50
3.5.3	Restriction to three branes in the hidden sector . . . . .	53
3.5.4	Comments . . . . .	55
3.6	Correlations . . . . .	55
3.6.1	Rank and chirality . . . . .	56
3.6.2	Estimates . . . . .	57

## II Generalised geometry 61

### 4 Concepts 63

4.1	The space $T \oplus T^*$ . . . . .	63
4.2	Spinors and forms . . . . .	64
4.2.1	The action of 2-forms on spinors . . . . .	65
4.2.2	Pure spinors and maximally isotropic subspaces . . . . .	66
4.3	The Courant bracket and integrability . . . . .	67
4.4	Generalised complex structures . . . . .	67
4.5	Generalised metrics . . . . .	68
4.5.1	Generalised Kähler structures . . . . .	71
4.5.2	Generalised $G$ -structures . . . . .	72

### 5 Applications 75

5.1	T-duality and mirror symmetry . . . . .	76
5.1.1	T-duality action on spinors . . . . .	78
5.1.2	Geometric aspects of T-duality . . . . .	78
5.2	The mirror map for generalised Kähler structures . . . . .	79
5.2.1	Description in terms of pure spinors . . . . .	81
5.3	Topological sigma models . . . . .	84
5.3.1	Definition of generalised topological sigma models . . . . .	84
5.3.2	BRST operators . . . . .	86
5.3.3	The action of mirror symmetry . . . . .	87
5.4	Topological branes . . . . .	88
5.4.1	Transformation under mirror symmetry . . . . .	90
5.5	Generalised Calibrations . . . . .	90
5.5.1	Definition . . . . .	90
5.5.2	Connection with $G$ -structures . . . . .	92
5.5.3	Examples . . . . .	96
5.5.4	Calibrations over manifolds . . . . .	98
5.5.5	Adding R-R fields . . . . .	99
5.5.6	T-duality transformation of calibrations . . . . .	100

<b>Appendix</b>	<b>103</b>
<b>A Orientifold models</b>	<b>103</b>
A.1 $T^2$ . . . . .	103
A.2 $T^4/\mathbb{Z}_2$ . . . . .	104
A.2.1 Multiple wrapping . . . . .	105
A.3 $T^6/\mathbb{Z}_2 \times \mathbb{Z}_2$ . . . . .	105
A.3.1 Multiple wrapping . . . . .	106
<b>B Partition algorithm</b>	<b>109</b>
B.1 Implementation . . . . .	110
<b>Bibliography</b>	<b>113</b>
<b>Curriculum Vitae</b>	<b>125</b>



# Chapter 1

## Introduction

Our current understanding of the fundamental forces of the universe is governed by two of the most successful theories in the history of science. On the one hand, the standard model of particle physics, formulated in the framework of quantum field theory, provides a description of the strong and electroweak interactions. On the other hand, general relativity explains the gravitational force in a beautiful geometric manner. The predictions of both theories are experimentally confirmed to a very high accuracy. Nevertheless, there are several issues concerning both, the mathematical structure as well as the impossibility to describe important phenomena, which convince us that the standard model and general relativity can only be low energy limits of a more fundamental theory, that would provide us with a unified description of all forces of nature.

Within the framework of the standard model, we are not able to describe the reason why there exist exactly three families of quarks and leptons, why the coupling constants of the electroweak and the strong interactions show the tendency to unify at high energies, why there is such a large hierarchy between the electroweak and the Planck scale and why the cosmological constant has such a small positive value. Concerning the structure of the standard model, the large number of free parameters, including such important quantities as the masses of fundamental particles, is not very appealing. Furthermore, general relativity, being a classical theory, cannot be formulated within the framework of quantum field theory. It loses its predictive power at the order of the Planck scale, where quantum effects would dominate. A quantum theory of gravity is therefore absolutely necessary to describe phenomena at high curvature, as in the case of black holes.

The best candidate for a fundamental theory that includes quantum gravity is string theory (for standard textbooks see [101, 102, 135, 145, 146, 172]). It is based on the idea that the fundamental constituents of matter are not described by point particles, but by one-dimensional objects. What might look like a minor change at first glance implies major changes in the mathematical description, as well as in the possible formulation of consistent theories. It turns out that the quantisation of string theory leads to five different theories, which are connected by dualities. In this way they

can be seen as special limits of one and the same underlying theory, which has been dubbed M-theory. The low energy limit of this still unknown fundamental theory is the maximal, eleven-dimensional supergravity [141, 53]. A consistent quantisation of string theory leads, besides others, to two fundamental predictions. The first one is that the dimension of the target space manifold has to be ten, the second one is supersymmetry. The latter is actually good news, since for phenomenological reasons we expect supersymmetry to be realised in nature, although it is broken at low energy. Since we do not observe a ten-dimensional space-time, we are necessarily led to the conclusion that six dimensions have to be invisible at low energies, which can be accommodated for by a compactification. The geometry of the compact manifold determines many properties of the low energy effective theory, in particular the amount of observed supersymmetry.

The first attempts to obtain consistent effective low energy theories that resemble the standard model have been made in heterotic string theory (see for example [37, 113, 112]). These methods have been refined over the years and are used presently to obtain the most realistic constructions of the standard model available (recent work includes [32, 29, 27]). With the advent of D-branes [143] many new possibilities for string model building have been discovered. In particular the notion of intersecting D-branes [18] proved to be very fruitful to construct models with realistic properties (see e.g. [134, 21] and references therein).

There are several open questions concerning compactifications in string theory and in this thesis we elaborate on two of them. Therefore this work is divided into two parts. In the first part we discuss aspects of the so-called landscape problem, which concerns the overwhelming abundance of possibilities to construct consistent low energy theories. In the second part we switch to a less phenomenological topic and investigate how a new mathematical structure, called generalised complex geometry, can deepen our understanding of the possible compactification spaces and the connection of string theories via dualities.

## 1.1 The Landscape

Starting from early observations of Lerche, Lüst and Schellekens [130], it has become clear over the years that string theory does provide us not only with one consistent low energy effective theory, but with a multitude of solutions. This phenomenon has been given the name “the landscape” [150, 155] (for a recent essay on the subject see also [76]).

It was known from the very first approaches to compactification of string theory to four dimensions that there exist many families of solutions due to the so-called moduli. These scalar fields parametrise the geometric properties of different possible compactification manifolds and their values are generically not fixed. It was believed for a long time that some stabilisation mechanism for these moduli would finally lead to only one consistent solution. Even though it is way too early to completely

abandon this idea, recent developments suggest that even after moduli stabilisation there exist a very large number of consistent vacuum solutions. Especially the studies of compactifications with fluxes (see e.g. [95] and references therein) clarified the situation. The effective potential induced by these background fluxes, together with non-perturbative effects, allow to fix the values of some or even all of the moduli at a supersymmetric minimum. What is surprising is the number of possible minima, which has been estimated [30]<sup>1</sup> to be of the order of  $10^{500}$ . So it seems very likely that there exists a very large number of stable vacua in string theory that give rise to low energy theories which meet all our criteria on physical observables.

After the initial work of Douglas [75], who pointed out that facing these huge numbers the search for *the* vacuum is no longer feasible, recent research has started to focus on the statistical distributions of string vacua. This approach relies on the conjecture that, given such a huge number of possible vacua, our world can be realized in many different ways and only a statistical analysis might be possible. Treating physical theories on a statistical basis is a provocative statement and it has given rise to a sometimes very emotional debate. Basic criticism is expressed in [12, 11], where the authors emphasise the point that, as long as we do not have a non-perturbative description of string theory, such reasoning seems to be premature. Moreover such an approach immediately rises philosophical questions. How can we talk seriously about the idea to abandon unambiguous predictions of reality and replace it with statistical reasoning? One is reminded to similar questions concerning quantum mechanics, but there is a major difference to this problem. In the case of quantum mechanics there is a clean definition of observer and measurement. Most importantly, measurements can be repeated and therefore we can make sense out of a statistical statement. In the case of our universe we have just one measurement and there is no hope to repeat the experiment.

At the moment there are two roads visible that might lead to a solution of these problems. One of them is based on anthropic arguments [155], which have already been used outside string theory to explain the observed value of the cosmological constant [159]. Combined with the landscape picture this gives rise to the idea of a multiverse, where all possible solutions for a string vacuum are actually realised [119] (for a recent essay on the cosmological constant problem and the string landscape see also [147]). Anthropic reasoning is not very satisfactory, especially within the framework of a theory that is believed to be unique. Another possible way to deal with the landscape might therefore be the assignment of an entropy to the different vacuum solutions and their interpretation in terms of a Hartle-Hawking wave function [142, 39]. A principle of extremisation of the entropy could then be used to determine the correct vacuum.

We do not dwell into philosophical aspects of the landscape problem in this thesis, but rather take a very pragmatic point of view, following Feynman's "shut up and calculate" attitude. In this endeavour a lot of work has been done to analyse the

---

<sup>1</sup>Note that in this estimate not all effects from the process of moduli stabilisation have been taken into account.

properties and define a suitable statistical measure in the closed string sector of string theory [8, 61, 64, 90, 73, 140, 50, 62, 66, 69, 72, 1, 74, 77, 125]. In this work we are focusing on the statistics of the open string sector [23, 126, 127, 7, 157, 92, 91, 93, 128, 67, 68]. We are not trying to take the most general point of view and analyse a generic statistical distribution, but focus instead on a very specific class of models. In this small region of the landscape we are going to compute almost all possible solutions and give an estimate for those solutions we were not able to take into account.

There are several interesting questions one can ask, given a large set of possible models. One of them concerns the frequency distribution of properties, like the total rank of the gauge group or the occurrence of certain gauge factors. Another question concerns the correlation of observables in these models. This question is particularly interesting, since a non-trivial correlation of properties could lead to the exclusion of certain regions of the landscape or give hints where to look for realistic models. It should be stressed that in our analysis of realistic four-dimensional compactifications we are not dealing with an abstract statistical measure, but with explicit constructions.

## 1.2 Generalised Geometry

From a mathematical point of view, the problem of compactifications in string theory can be regarded as the task to classify six-manifolds with special properties. In particular, demanding supersymmetry in the four-dimensional space-time leads to the requirement of a covariantly constant spinor to exist on the target space manifold [162]. For special cases and minimal supersymmetry in four dimensions, this reasoning leads to spaces with  $SU(3)$  holonomy, so called Calabi-Yau manifolds [37]. However, Calabi-Yau spaces are not the most general possible target space manifolds. As has been realised in [153], one can treat non-trivial NS-NS background fields as torsion of the internal manifold. The search for possible solutions for internal fields (fluxes) that preserve a certain amount of supersymmetry can be performed using the mathematical tool of  $G$ -structures [85, 38]. Considering  $G$ -structures with  $G = SU(3)$  contains Calabi-Yaus as a special case, when all background fields except the metric are set to zero. The method of  $G$ -structures cannot only be applied to string theory compactifications, but also to eleven-dimensional supergravity. In the simplest case the structure group of the seven-dimensional compact space is  $G_2$ .

More recently, the development of generalised complex geometry by Hitchin [109] and his students [103, 41, 161] turned out to be very suitable to describe the target space manifolds of string theory. The basic idea of generalised geometry is to replace the tangent bundle of the manifold under consideration with the sum of the tangent and cotangent bundle. The  $G$ -structure of a manifold is thereby replaced with a  $G \times G$ -structure, that contains the classical case as a special limit. The formulation of string theory problems using generalised geometry is useful for several reasons. First of all the antisymmetric two-form, the  $B$ -field can be incorporated in a very natural way. Secondly, as has been shown in [116], it is possible to include the R-R fields



in the classification of target spaces as well. This is an important step towards a sensible description of R-R fluxes in string theory compactifications. Specifically in compactifications of type II string theories the new mathematical tools have already found many applications [97, 98, 115, 99, 100, 96].

Another important aspect of generalised geometry is a natural description of T-duality and mirror symmetry [154]. Under the action of mirror symmetry the complex structure of one manifold gets exchanged with the symplectic structure of the dual manifold. The notion of a generalised complex structure unifies both, complex and symplectic structures, and provides therefore a good framework to describe mirror symmetry. In the context of nonlinear sigma models an important insight was gained in [103], where it has been proven that the most general target space structure for  $\mathcal{N} = (2, 2)$  theories, which has been found to be a bi-hermitian geometry in [84], is equivalent to a generalised Kähler structure. This was the motivation for the authors of [120, 122] to introduce a generalised topological B-model. In [49] this has been extended to the A-model case and the action of T-duality on these generalised models has been investigated. As a non-trivial test of the new ideas it can be shown that the classical topological A- and B-models [164] are recovered in special limits of the generalised models. Related work on nonlinear sigma models in the context of generalised geometry includes [131, 132, 169, 167, 133, 170, 171, 33].

With respect to the theory of D-branes, generalised geometry provides new insights as well. In [166] boundary conditions for branes in nonlinear sigma models with generalised target spaces have been formulated. As has been shown in [49], these conditions for generalised topological A- and B-branes get interchanged by mirror symmetry. Turning from the topological branes to D-branes in type II string theory, the well-known conditions for D-branes on Calabi-Yau manifolds to preserve a certain amount of supersymmetry [137], namely to wrap special Lagrangian cycles in type IIA and holomorphic cycles in type IIB, can be combined and extended in the framework of generalised complex geometry [124, 139, 138, 94]. The classical conditions can be formulated mathematically using the notion of calibrated submanifolds [107]. Including non-trivial background fluxes changes these calibrations and has led the authors of [123] to discover a new type of A-branes, the so-called coisotropic branes, which obey a modified calibration condition [121]. Together with all known classical calibrations these can be unified in the notion of a generalised calibration, which contains the different cases as special limits.

## 1.3 Outline

Corresponding to the two topics addressed in this thesis, the text is divided into two parts. In part one we deal with some aspects of the landscape problem and in part two we occupy ourselves with generalised geometry.

Part one is structured as follows. In chapter 2 we prepare the stage, introducing the special class of type II orientifold models that are our objects of interest. Moreover

we explain the two methods we use to analyse these models. On the one hand, the saddle point approximation and on the other hand a brute force algorithm for explicit calculations. Concerning this algorithm, we comment on its computational complexity, which touches a more general issue about computations in the landscape. In the last section we discuss another fundamental problem of the statistical analysis, namely the finiteness of vacua. An analytic proof of finiteness seems to be out of reach, but we give several numerical arguments that support the conjecture that the total number of solutions is indeed finite.

In chapter 3 we apply the described methods to type II orientifold models. We begin with general questions about the frequency distributions of properties of the gauge sector in compactifications to six and four dimensions. After that we pick several subsets of models for a more detailed analysis. We choose those subsets that could provide us with a phenomenologically interesting low energy gauge group. This includes first of all the standard model, but in addition constructions of Pati-Salam,  $SU(5)$  and flipped  $SU(5)$  models. In the case of standard model-like constructions we investigate the relations and frequency distributions of the gauge coupling constants and compare the results with a recent analysis of Gepner models. In the last section of this chapter the question of correlations of gauge sector observables is explored.

With chapter 4 we begin the second part of this thesis. We give a brief introduction to the mathematical concepts of generalised geometry, focusing on the topics we need for applications to string theory. In particular we explain the notions of generalised complex and Kähler structures and their classical limits. The extension of classical  $G$ -structures to the new setting is presented as well.

In chapter 5 we focus on two aspects of string theory where generalised complex geometry has useful applications. In the first section we demonstrate the natural description of T-duality and mirror symmetry in this context. The results established in this section are then applied to topological nonlinear sigma models. We define the generalisation of the classical A- and B-models and show their mutual relation under mirror symmetry. Turning to D-branes, we show that the boundary conditions of topological A- and B-branes get interchanged by the action of mirror symmetry. In the last section of this chapter we turn to D-branes in type II string theory and define the analog of the classical calibration condition in the generalised framework. After showing that the well-known calibrations for branes in type IIA and type IIB can be found as classical limits, we investigate the action of T-duality on the generalised calibration condition.

In appendix A we summarise some useful formulae for the different orientifold models. Appendix B contains details about the implementation of the computer algorithm, used to construct the models we analysed in part I.

# Part I

## D-brane statistics



# Chapter 2

## Models and methods

As explained in the introduction, our program to classify a subset of the landscape of string vacua is performed on a very specific set of models. In this chapter, we want to set the stage for the analysis, explain the construction and the constraints on possible solutions. Moreover, we have to develop the necessary tools of analysis.

In the first part of this chapter we give a general introduction to the orientifolds we are planning to analyse. We focus on the consistency conditions that have to be met by any stable solution. In particular these are the tadpole conditions for the R-R fields, the supersymmetry conditions on the three-cycles wrapped by D-branes and orientifold planes and restrictions coming from the requirement of anomaly cancellation.

In the second part we develop the tools for a statistical analysis and test them on a very simple compactification to eight dimensions. There are two methods that we use for six- and four-dimensional models in the next chapter, namely an approximative method and a direct, brute force analysis. The first method relies on the saddle point approximation, which we explain in detail and compare it with known results from number theory. For the second method we describe an algorithm that can be used for a large scale search performed on several computer clusters. To estimate the amount of time needed to generate a suitable amount of solutions, we analyse the computational complexity of this algorithm.

In the last part of this chapter we investigate the problem of finiteness of the number of solutions, an issue that is important to judge the validity of the statistical statements.

### 2.1 Orientifold models

Let us give a brief introduction to the orientifold models we use in the following to do a statistical analysis. We will not try to give a complete introduction to the subject, for readers with interest in more background material, we refer to the available textbooks [145, 146, 117] and reviews [148, 144, 81] for a general introduction and the

recent review [21] for an account of orientifold models and their phenomenological aspects.

Our analysis is based on the study of supersymmetric toroidal type II orientifold models with intersecting D-branes [18, 6, 10, 151]. These models are, of course, far from being the most general compactifications, but they have the great advantage of being very well understood. In particular, the basic constraints for model building, namely the tadpole cancellation conditions, the supersymmetry and K-theory constraints, are well known. It is therefore possible to classify almost all possible solutions for these constructions.

The orientifold models we consider can be described in type IIB string theory using space-filling D9-branes with background gauge fields on their worldvolume. An equivalent description can be given in the T-dual type IIA picture, where the D9-branes are replaced by D6-branes, which intersect at non-trivial angles. This point of view is geometrically appealing and goes under the name of intersecting D6-branes. We use this description in the following.

The orientifold projection is given by  $\Omega\bar{\sigma}(-1)^{F_L}$ , where  $\Omega : (\sigma, \tau) \rightarrow (-\sigma, \tau)$  defines the world-sheet parity transformation and  $\bar{\sigma}$  is an isometric anti-holomorphic involution, which we choose to be simply complex conjugation in local coordinates:  $\bar{\sigma} : z \rightarrow \bar{z}$ .  $F_L$  denotes the left-moving space-time fermion number. This projection introduces topological defects in the geometry, the so-called orientifold O6-planes. These are non-dynamical objects, localised at the fixed point locus of  $\bar{\sigma}$ , which carry tension and charge under the R-R seven-form, opposite to those of the D6-branes<sup>1</sup>.

Both, the O6-planes and D6-branes wrap three-cycles  $\pi \in H_3(M, \mathbb{Z})$  in the internal Calabi-Yau manifold  $M$ , which, in order to preserve half of the supersymmetry, have to be special Lagrangian. In mathematical terms this is a calibration condition, which we will meet again as a special case of generalised calibrations in chapter 5. Since the charge of the orientifolds is fixed and we are dealing with a compact manifold, the induced R-R and NS-NS tadpoles have to be cancelled by a choice of D6-branes. These two conditions, preserving supersymmetry and cancelling the tadpoles, are the basic model building constraints we have to take into account.

The homology group  $H_3(M, \mathbb{Z})$  of three-cycles in the compact manifold  $M$  splits under the action of  $\Omega\bar{\sigma}$  into an even and an odd part, such that the only non-vanishing intersections are between odd and even cycles. We can therefore choose a symplectic basis  $(\alpha_I, \beta_I)$  and expand  $\pi_a$  and  $\pi'_a$  as

$$\begin{aligned}\pi_a &= \sum_{I=1}^{b_3/2} (X_a^I \alpha_I + Y_a^I \beta_I), \\ \pi'_a &= \sum_{I=1}^{b_3/2} (X_a^I \alpha_I - Y_a^I \beta_I),\end{aligned}\tag{2.1}$$

---

<sup>1</sup>It is also possible to introduce orientifold planes with different charges, but we consider only those with negative tension and charge in this thesis.

and  $\pi_{O6}$  as

$$\pi_{O6} = \frac{1}{2} \sum_{I=1}^{b_3/2} L^I \alpha_I, \quad (2.2)$$

where  $b_3$  is the third Betti-Number of  $M$ , counting the number of three-cycles.

### 2.1.1 Chiral matter

Chiral matter arises at the intersection of branes wrapping different three-cycles. Generically we get bifundamental representations  $(\mathbf{N}_a, \overline{\mathbf{N}}_b)$  and  $(\mathbf{N}_a, \mathbf{N}_b)$  of  $U(N_a) \times U(N_b)$  for two stacks with  $N_a$  and  $N_b$  branes. The former arise at the intersection of brane  $a$  and brane  $b$ , the latter at the intersection of brane  $a$  and the orientifold image of brane  $b$ , denoted by  $b'$ . An example is shown in figure 2.1.

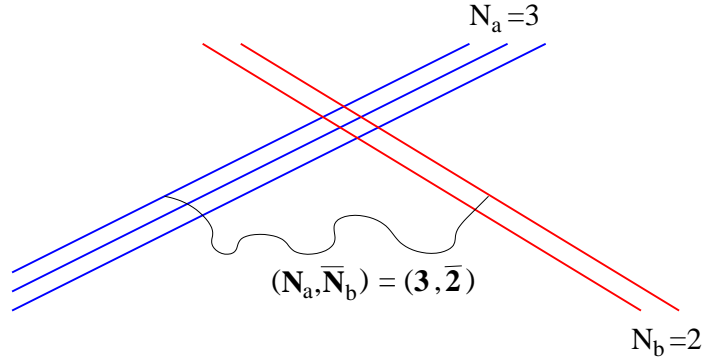


Figure 2.1: We find chiral matter at the intersection of two stacks of branes. The representation is given in terms of the number of branes of each stack.

In addition we get matter transforming in symmetric or antisymmetric representations of the gauge group for each individual stack. The multiplicities of these representations are given by the intersection numbers of the three-cycles,

$$I_{ab} := \pi_a \circ \pi_b = \sum_{I=1}^{b_3/2} (X_a^I Y_b^I - X_b^I Y_a^I). \quad (2.3)$$

The possible representations are summarized in table 2.1, where  $\mathbf{Sym}_a$  and  $\mathbf{Anti}_a$  are the symmetric and antisymmetric representations of  $U(N_a)$ .

### 2.1.2 Tadpole cancellation conditions

The D6-branes in our models are charged under a R-R seven-form [143]. Since the internal manifold is compact, as a simple consequence of the Gauss law, all R-R charges have to add up to zero. These so-called tadpole cancellation conditions can be obtained considering the part of the supergravity Lagrangian that contains the

representations	multiplicity
$(\mathbf{N}_a, \bar{\mathbf{N}}_b)$	$\pi_a \circ \pi_b = I_{ab}$
$(\mathbf{N}_a, \mathbf{N}_b)$	$\pi'_a \circ \pi_b = I_{ab'}$
<b>Sym</b> <sub><i>a</i></sub>	$\frac{1}{2} (\pi_a \circ \pi'_a - \pi_a \circ \pi_{O6}) = \frac{1}{2} (I_{aa'} - I_{aO6})$
<b>Anti</b> <sub><i>a</i></sub>	$\frac{1}{2} (\pi_a \circ \pi'_a + \pi_a \circ \pi_{O6}) = \frac{1}{2} (I_{aa'} + I_{aO6})$

Table 2.1: Multiplicities of the chiral spectrum.

corresponding contributions. In particular we do not only get contributions from  $k$  stacks of branes, wrapping cycles  $\pi_a$ , but in addition terms from the orientifold mirrors of these branes, wrapping cycles  $\pi'_a$ , and the O6-planes.

$$S = -\frac{1}{4\kappa^2} \int_{X \times M} dC_7 \wedge \star dC_7 + \mu_6 \sum_{a=1}^k N_a \left( \int_{X \times \pi_a} C_7 + \int_{X \times \pi'_a} C_7 \right) - 4\mu_6 \int_{X \times \pi_{O6}} C_7, \quad (2.4)$$

where the ten dimensional gravitational coupling is given by  $\kappa^2 = \frac{1}{2}(2\pi)^7(\alpha')^4$ , the R-R charge is denoted by  $\mu_6 = (\alpha')^{-\frac{7}{2}}(2\pi)^{-6}$  and  $X$  denotes the uncompactified space-time.

From this we can derive the equations of motion for the R-R field strength  $G_8 = dC_7$  to be

$$d \star G_8 = \kappa^2 \mu_6 \left( \sum_{a=1}^k N_a (\delta(\pi_a) + \delta(\pi'_a)) - 4\delta(\pi_{O6}) \right). \quad (2.5)$$

In this equation  $\delta(\pi)$  denotes the Poincaré dual three form of a cycle  $\pi$ . Noticing that the left hand side of (2.5) is exact, we can rewrite this as a condition in homology as

$$\sum_{a=1}^k N_a (\pi_a + \pi'_a) = 4\pi_{O6} \quad (2.6)$$

We do not have to worry about the NS-NS tadpoles, as long as we are considering supersymmetric models, since the supersymmetry conditions together with R-R tadpole cancellation ensure that there are no NS-NS tadpoles. In this thesis we consider supersymmetric models only.

### 2.1.3 Supersymmetry conditions

Since we want to analyse supersymmetric models, it is crucial that the D-branes and O-planes preserve half of the target-space supersymmetry. It can be shown [137] that



this requirement is equivalent to a calibration condition on the cycles,

$$\begin{aligned}\Im(\Omega_3)|_{\pi_a} &= 0, \\ \Re(\Omega_3)|_{\pi_a} &> 0.\end{aligned}\tag{2.7}$$

where  $\Omega_3$  is the holomorphic 3-form. The second equation in (2.7) excludes anti-branes from the spectrum.

Written in the symplectic basis (2.1), these equations read

$$\begin{aligned}\sum_{I=1}^{b_3/2} Y_a^I f_I &= 0, \\ \sum_{I=1}^{b_3/2} X_a^I u_I &> 0,\end{aligned}\tag{2.8}$$

where we defined

$$f_I := \int_{\beta_I} \Omega_3, \quad u_I := \int_{\alpha_I} \Omega_3.$$

#### 2.1.4 Anomalies and K-theory constraints

If the tadpole cancellation conditions (2.6) are satisfied, there are no cubic anomalies of  $SU(N)$  gauge groups in our models. What we do have to worry about are mixed anomalies, containing abelian factors. The mixed anomaly for branes stretching between two stacks  $a$  and  $b$  with  $N_a = 1$  and  $N_b > 1$  branes per stack, looks like

$$\begin{aligned}\mathcal{A}_{U(1)_a-SU(N)_b} &\simeq N_a(I_{ab} + I_{ab'})c_2(N_b) \\ &= -2N_a\vec{Y}_a\vec{X}_bc_2(N_b),\end{aligned}\tag{2.9}$$

where  $c_2(N_b)$  denotes the value of the quadratic Casimir operator for the fundamental representation of  $SU(N_b)$ .

The cubic anomaly consisting of three abelian factors is cancelled by the Green-Schwarz mechanism. This makes these  $U(1)$ s massive and projects them out of the low energy spectrum. But in some cases, for example in the case of a standard model-like gauge group or for flipped  $SU(5)$  models, we want to get a massless  $U(1)$  factor. A sufficient condition to get such a massless  $U(1)$  in one of our models is that the anomaly (2.9) vanishes.

This can be achieved, if the  $U(1)$ , defined in general by a combination of several  $U(1)$  factors as

$$U(1) = \sum_{a=1}^k x_a U(1)_a,\tag{2.10}$$

fulfills the following relations,

$$\sum_{a=1}^k x_a N_a \vec{Y}_a = 0. \quad (2.11)$$

Inserting this into (2.9) shows that  $\mathcal{A}$  vanishes.

Besides these local gauge anomalies, there is also the potential danger of getting a global gauge anomaly, which would make the whole model inconsistent. This anomaly arises if a  $\mathbb{Z}_2$ -valued K-theory charge is not conserved [156]. In our case this anomaly can be derived by introducing  $Sp(2)$  probe branes on top of the orientifold planes and compute their intersection numbers with all branes in the model. This intersection number has to be even, otherwise we would get an odd number of fermions, transforming in the fundamental representation of  $Sp(2)$  [163].

## 2.2 Methods of D-brane statistics

To analyse a large class of models in the orientifold setting described in the last section, we have to develop some tools that allow us to generate as many solutions to the supersymmetry, tadpole and K-theory conditions as possible. It turns out that the most difficult part of this problem can be reduced to a purely number theoretical question, namely the problem of counting partitions of natural numbers. This insight allows us to use an approximative method, the saddle point approximation that we introduce in section 2.2.1 and apply to a simple toy-model in 2.2.2. Unfortunately it turns out that this method is not very well suited to study the most interesting compactifications, namely those down to four dimensions. Therefore we have to change the method of analysis in that case to a more direct one, using a brute force, exact computer analysis. The algorithm used to do so is described in section 2.2.3.

### 2.2.1 Introduction to the saddle point approximation

As an approximative method to analyse the gauge sector of type II orientifolds, the saddle point approximation has been introduced in [23]. In the following we begin with a very simple, eight-dimensional model, in order to explain the method.

Let us recall the basic constraints on type IIA orientifold models, the tadpole and supersymmetry conditions from section 2.1.2<sup>2</sup>,

$$\sum_{a=1}^k N_a X_a^I = L^I, \quad \sum_{I=1}^{b_3/2} Y_a^I f_I = 0, \quad \sum_{I=1}^{b_3/2} X_a^I u_I > 0. \quad (2.12)$$

In the most simple case, a compactification to eight dimensions on  $T^2$ , the susy conditions reduce to  $Y_a = 0$  and  $X_a > 0$  and the tadpole cancellation conditions are given

---

<sup>2</sup>For the moment we are going to ignore the constraints from K-theory, we come back to this point later, since they are of significance in the four-dimensional compactifications.

by

$$\sum_{a=1}^k N_a X_a = 16, \quad (2.13)$$

as shown in appendix A.1.

The task to count the number of solutions to this equation for an arbitrary number of stacks  $k$  is a combination of a partitioning and factorisation problem. Let us take things slowly and start with a pure partitioning problem, namely to count the unordered solutions of

$$\sum_{a=1}^k N_a = L. \quad (2.14)$$

This is nothing else but the number of unordered partitions of  $L$ . Since we are not interested in an exact solution, but rather an approximative result, suitable for a statistical analysis and further generalisation to the more ambitious task of solving the tadpole equation, let us attack this by means of the saddle point approximation [4, 165].

### Counting partitions

As a first step to solve (2.14), let's consider

$$\sum_{k=1}^{\infty} k n_k = L, \quad (2.15)$$

where we do not have to worry about the ordering problem. We can rewrite this as

$$\begin{aligned} \mathcal{N}(L) &= \sum_{all} \delta_{\sum_k k n_k - L, 0} \\ &= \frac{1}{2\pi i} \oint dq \frac{1}{q^{L+1}} \sum_{n_k=0}^{\infty} q^{\sum_k k n_k} \\ &= \frac{1}{2\pi i} \oint dq \frac{1}{q^{L+1}} \prod_{k=1}^{\infty} \left( \frac{1}{1 - q^k} \right). \end{aligned} \quad (2.16)$$

To evaluate integrals of this type in an asymptotic expansion, the saddle point method is a commonly used tool. In the following we describe its application in detail. The last line of (2.16) can be written as

$$\begin{aligned} \mathcal{N}(L) &= \frac{1}{2\pi i} \oint dq \exp(f(q)), \\ \text{with } f(q) &= - \sum_{k=1}^{\infty} \log(1 - q^k) - (L + 1) \log q. \end{aligned} \quad (2.17)$$

Now we are going to assume that the main contributions to this integral come from saddle points  $q_i$ , determined by  $df/dq|_{q_i} = 0$ . In the following we work with only one saddle point at  $q = q_0$ , the generalisation to many points is always straightforward. Using the decomposition  $q = \rho \exp(i\varphi)$  we get

$$\mathcal{N}(L) = \frac{1}{2\pi} \int_{-\pi}^{\pi} d\varphi q \exp(f(q)). \quad (2.18)$$

Performing a Taylor expansion in  $\varphi$

$$f(\rho_0, \varphi) = f(q_0) + \frac{1}{2} \left. \frac{\partial^2 f}{\partial \varphi^2} \right|_{q_0} \varphi^2 + \dots, \quad (2.19)$$

we can compute (2.18) to arbitrary order by inserting the corresponding terms from (2.19).

The leading order term is simply given by

$$\mathcal{N}^{(0)}(L) = \exp(f(q_0)), \quad (2.20)$$

and the first correction at next-to-leading order by

$$\mathcal{N}_{corr}^{(2)}(L) = \frac{1}{2\pi} \int_{-q_0\pi}^{q_0\pi} dx \exp\left(-\frac{1}{2} \left. \frac{\partial^2 f}{\partial q^2} \right|_{q_0} x^2\right), \quad (2.21)$$

where we defined  $x := q_0\varphi$  and used that  $(\partial^2 f / \partial \varphi^2)_{q_0} = -q^2 (\partial^2 f / \partial q^2)_{q_0}$ . For  $\partial^2 f / \partial q^2$  large enough we finally obtain the result for the saddle point approximation including next-to-leading order corrections

$$\mathcal{N}^{(2)}(L) = \frac{1}{2\pi} \exp(f(q_0)) \left( \left. \frac{\partial^2 f}{\partial q^2} \right|_{q_0} \right)^{-1/2}. \quad (2.22)$$

The same procedure can also be performed for functions of several variables. The integral to approximate this situation looks like

$$\mathcal{N}(\vec{L}) = \frac{1}{2\pi^i} \oint \prod_{I=1}^n d\vec{q} \exp(f(\vec{q})), \quad (2.23)$$

with  $f$  being of the form

$$f(\vec{q}) = g(\vec{q}) - \sum_{I=1}^N (L_I + 1) \log q_I. \quad (2.24)$$

We can perform the saddle point approximation around  $\nabla f(\vec{q})|_{\vec{q}_0} = 0$  in the same way as above and obtain the following result at next-to-leading order

$$\mathcal{N}^{(2)}(\vec{L}) = (2\pi)^{-n/2} \exp(f(\vec{q}_0)) \left( \det \text{Hess} f(\vec{q})|_{\vec{q}_0} \right)^{-1/2}. \quad (2.25)$$

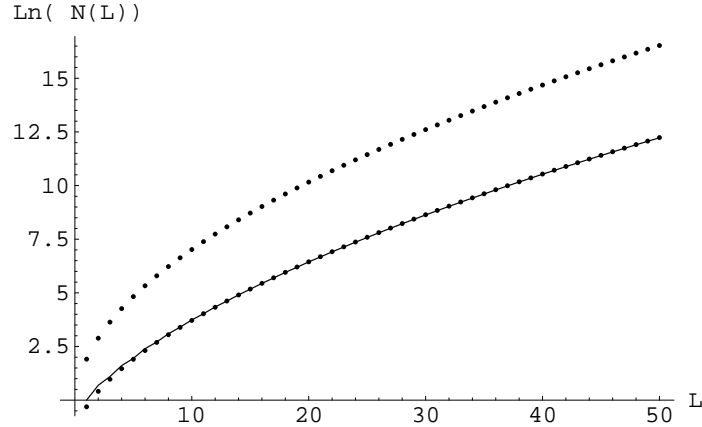


Figure 2.2: Comparison of the number of partitions obtained by an exact calculation (solid line) and a saddle point approximation to leading (upper dotted line) and next-to-leading order (lower dotted line).

### Comparison with the Hardy-Ramanujan formula and the exact result

In the simple case discussed so far, contrary to the more complicated cases we encounter later, an analytic evaluation of the leading order contribution is possible. For large  $L$  the integrand of (2.16) quickly approaches infinity for  $q < 1$  and  $q \simeq 1$ . One expects a sharp minimum close to 1, which would be the saddle point we are looking for.

Close to  $q \simeq 1$  we can write the first term in (2.17) as

$$\begin{aligned}
 - \sum_{k=1}^{\infty} \log(1 - q^k) &= \sum_{k,m>0} \frac{1}{m} q^{km} \\
 &\simeq \frac{1}{1-q} \sum_{m>0} \frac{1}{m^2} = \frac{\pi^2}{6} \frac{1}{1-q},
 \end{aligned} \tag{2.26}$$

such that we can approximate  $f(q)$  by

$$f(q) \simeq \frac{\pi^2}{6} \frac{1}{1-q} - (L+1) \log q. \tag{2.27}$$

For large values of  $L$ , the minimum of this function is approximately at  $q_0 \simeq 1 - \sqrt{\frac{\pi^2}{6L}}$  which leads to  $f(q_0) \simeq \pi\sqrt{2L/3}$ . Inserting this into (2.20) gives a first estimate of the growth of the partitions for large  $L$  to be

$$\mathcal{N}(L) \simeq \exp\left(\pi\sqrt{2L/3}\right). \tag{2.28}$$

This is precisely the leading term in the Hardy-Ramanujan formula [106] for the asymptotic growth of the number of partitions

$$\mathcal{N}(L)^{(HR)} \simeq \frac{1}{4L\sqrt{3}} \exp\left(\pi\sqrt{2L/3}\right). \tag{2.29}$$

In figure 2.2 the results of an exact calculation, using the partition algorithm described in appendix B, and the saddle point approximation in leading and next-to-leading order are shown.

### 2.2.2 A first application of the saddle point approximation

After this introduction to the saddle point method let us come back to our original problem. To solve equation (2.13), we first have to transfer our approximation method to (2.14) and then include the factorisation in the computation. This last step turns out not to be too difficult, but in order to use the technique developed above, we have to be a bit careful about the ordering of solutions.

#### Solving the tadpole equation for eight-dimensional compactifications

In the example we presented to introduce the method, we did not have to worry about the ordering, since it was solved implicitly by the definition of the partition function. This is not the case for (2.14), such that by simply copying from above the result is too large. We should divide the result by the product of the number of possibilities to order each partition. Obtaining this factor precisely is very difficult and since we are only interested in an approximative result anyway, we should try to estimate the term. Such an estimate can be made dividing by  $k!$ , where  $k$  is the total number of stacks. This restricts the number of solutions more than necessary, because the factor is too high for partitions that contain the same element more than once. Let us nevertheless calculate the result with this rough estimate and see what comes out.

Repeating the steps from above, we can rewrite (2.14) to obtain

$$\begin{aligned}
\tilde{\mathcal{N}}(L) &\simeq \frac{1}{2\pi i} \oint dq \frac{1}{q^{L+1}} \sum_{k=1}^{\infty} \frac{1}{k!} \prod_{i=1}^k \left( \sum_{N_i=1}^{\infty} q^{\sum_a N_a} \right) \\
&= \frac{1}{2\pi i} \oint dq \frac{1}{q^{L+1}} \sum_{k=1}^{\infty} \frac{1}{k!} \left( \sum_{N=1}^{\infty} q^N \right)^k \\
&= \frac{1}{2\pi i} \oint dq \frac{1}{q^{L+1}} \sum_{k=1}^{\infty} \frac{1}{k!} \left( \frac{q}{1-q} \right)^k \\
&= \frac{1}{2\pi i} \oint dq \frac{1}{q^{L+1}} \exp \left( \frac{q}{1-q} \right). \tag{2.30}
\end{aligned}$$

Applying the saddle point approximation as explained above for the function

$$\tilde{f}(q) = \frac{q}{1-q} - (L+1) \log q, \tag{2.31}$$

we get for the number of solutions of (2.14) the estimate

$$\tilde{\mathcal{N}}(L) \simeq \exp(2\sqrt{L}). \tag{2.32}$$

Comparing this result with (2.28) shows that we get the correct exponential growth, but the coefficient is too small by a factor

$$\frac{\log \mathcal{N}}{\log \tilde{\mathcal{N}}} = \frac{\pi}{\sqrt{6}} \simeq 1.28. \quad (2.33)$$

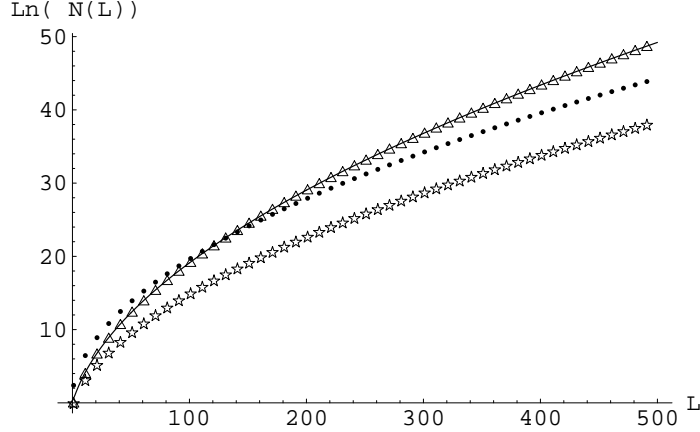


Figure 2.3: Comparing the results for the number of partitions of  $L$ . The solid line is the exact result, the dotted line is the saddle point approximation to leading order. The stars and triangles show the next-to-leading order result, without and including the additional analytic factor 1.28, respectively.

In figure 2.3 we compare the results for the leading and next-to-leading order results of the computation above with the exact result. As already expected, the value for the second order approximation is too small, since our suppression factor  $k!$  is too big. Nevertheless, qualitatively the results are correct. Since we are not aiming at exact results, but rather at an approximative method to get an idea of the frequency distributions of properties of the models under consideration, this is not a big problem.

Let us finally come back to the full tadpole equation (2.13). It can be treated in the same way as the pure partition problem and analogous to (2.30) we can write

$$\mathcal{N}(L) \simeq \frac{1}{2\pi i} \oint dq \frac{1}{q^{L+1}} \sum_{k=1}^{\infty} \frac{1}{k!} \prod_{i=1}^k \left( \sum_{N_i=1}^{\infty} \sum_{X_i=1}^L q^{\sum_a N_a X_a} \right) \quad (2.34)$$

$$= \frac{1}{2\pi i} \oint dq \frac{1}{q^{L+1}} \sum_{k=1}^{\infty} \frac{1}{k!} \left( \sum_{X=1}^L \frac{q^X}{1-q^X} \right)^k, \quad (2.35)$$

such that we obtain for  $f$

$$f(q) = \sum_{X=1}^L \frac{q^X}{1-q^X} - (L+1) \log q. \quad (2.36)$$

Close to  $q \simeq 1$  we can approximate this to

$$f(q) \simeq \frac{1}{1-q} \sum_{X=1}^L \frac{1}{X} - L \log q \simeq \frac{\log L}{1-q} - L \log q. \quad (2.37)$$

The minimum can then be found at  $q_0 \simeq 1 - \sqrt{\frac{\log L}{L}}$ , which gives for the number of solutions

$$\mathcal{N}(L) \simeq \exp(2\sqrt{L \log L}). \quad (2.38)$$

The additional factor of  $\log L$  in the scaling behaviour compared to (2.32) can be explained by a result from number theory. It is known that the function  $\sigma_0(n)$ , counting number of divisors of an integer  $n$ , has the property

$$\frac{1}{L} \sum_{n=1}^L \sigma_0(n) \simeq \log L + (2\gamma_E - 1), \quad (2.39)$$

where  $\gamma_E$  is the Euler-Mascheroni constant.

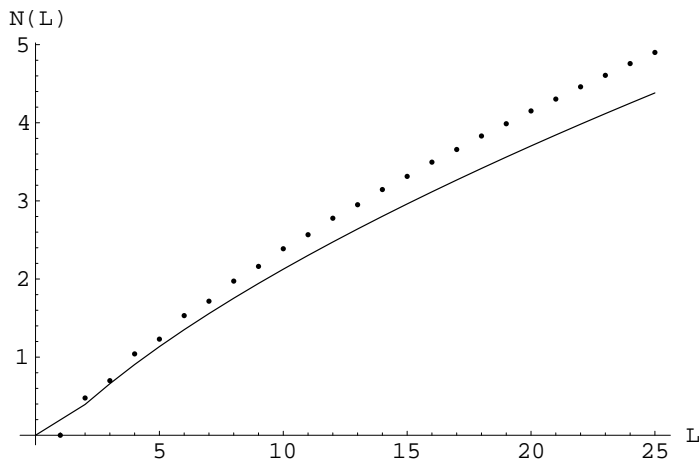


Figure 2.4: Logarithmic plot of the number of solutions to the supersymmetry and tadpole equations for compactifications on  $T^2$ . The dotted line shows the exact results, the solid line is the result of a next-to-leading order saddle point approximation.

Let us compare the result (2.38) with the exact number of solutions, obtained with a brute force computer analysis. This is shown in figure 2.4. As expected from the discussion above, the estimate using the saddle point approximation is too small, but it has the correct scaling behaviour and should therefore be suitable to qualitatively analyse the properties of the solutions.

### Analysing properties of the gauge sector

We can use the saddle point approximation method introduced above to analyse several properties of the gauge sector of the models. To show how this works, we



present two examples in the simple eight-dimensional case, before applying these methods in section 3.1 to models on  $T^4/\mathbb{Z}_2$ .

One interesting observable is the probability to find an  $SU(M)$  gauge factor in the total set of models. Using the same reasoning as in the computation of the number of models this is given by

$$\begin{aligned} P(M, L) &\simeq \frac{1}{2\pi i \mathcal{N}(L)} \oint dq \frac{1}{q^{L+1}} \sum_{k=1}^{\infty} \frac{1}{(k-1)!} \left( \sum_{X=1}^L \frac{q^X}{1-q^X} \right)^{k-1} \sum_{X=1}^L \sum_{N=1}^{\infty} q^{NX} \delta_{N,M} \\ &= \frac{1}{2\pi i \mathcal{N}(L)} \oint dq \frac{1}{q^{L+1}} \exp \left( \sum_{X=1}^L \frac{q^X}{1-q^X} \right) q^M \frac{1-q^{ML}}{1-q^M}. \end{aligned} \quad (2.40)$$

The saddle point function is therefore given by

$$f(q) = \sum_{X=1}^L \frac{q^X}{1-q^X} + \log \left( q^M \frac{1-q^{ML}}{1-q^M} \right) - (L+1) \log q. \quad (2.41)$$

A comparison between exact computer results and the saddle point approximation to second order is shown in figure 2.5(a).

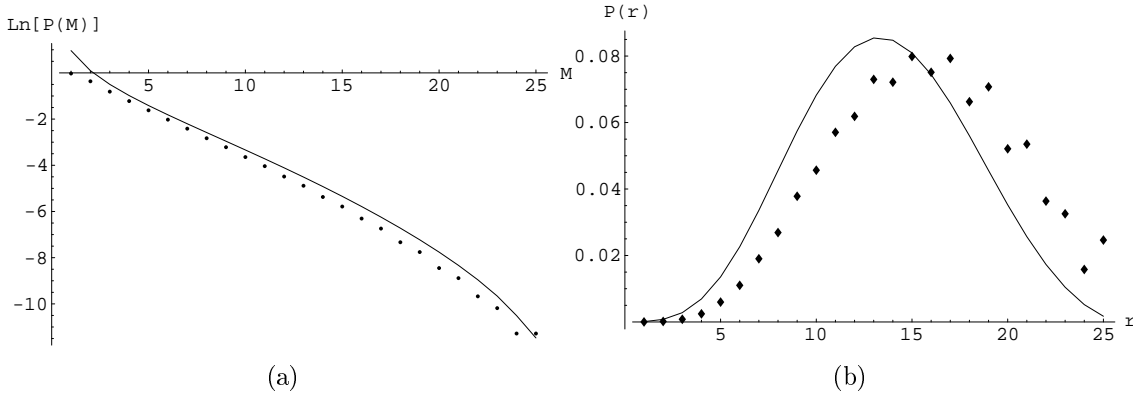


Figure 2.5: Distributions for compactifications on  $T^2$ . The solid lines are the exact result, the dotted lines represent the second order saddle point approximation. (a) Probability to find at least one  $SU(M)$  gauge factor. (b) Frequency distribution of the total rank.

Another observable we are interested in is the distribution of the total rank of the gauge group in our models. This amounts to including a constraint

$$\sum_{a=1}^{\infty} N_a = r, \quad (2.42)$$

that fixes the total rank to a specific value  $r$ . This constraint can be accounted for by adding an additional delta-function, represented by an additional contour integral to

our formula. We obtain

$$\begin{aligned}
P(r, L) &\simeq \frac{1}{2\pi i \mathcal{N}(L)} \oint dq \frac{1}{q^{L+1}} \oint dz \frac{1}{z^{r+1}} \sum_{k=1}^{\infty} \frac{1}{k!} \prod_{i=1}^k \left( \sum_{N_i=1}^{\infty} \sum_{X_i=1}^L q^{\sum_a N_a X_a} z^{\sum_a N_a} \right) \\
&= \frac{1}{2\pi i \mathcal{N}(L)} \oint dq \frac{1}{q^{L+1}} \oint dz \frac{1}{z^{r+1}} \exp \left( \sum_{X=1}^L \frac{zq^X}{1-zq^X} \right), \tag{2.43}
\end{aligned}$$

with saddle point function

$$f(q, z) = \sum_{X=1}^L \frac{zq^X}{1-zq^X} - (L+1) \log q - (r+1) \log z. \tag{2.44}$$

As we can see in figure 2.5(b), where we also show the exact computer result, we get a Gaussian distribution.

### 2.2.3 Exact computations

Instead of using an approximative method, it is also possible to directly calculate possible solutions to the constraining equations. At least for models on  $T^2$  or  $T^4/\mathbb{Z}_2$ , this is much more time-consuming than the saddle point approximation, and, what is even more important, cannot be done completely for models on  $T^6/\mathbb{Z}_2 \times \mathbb{Z}_2$ . The reason why a complete classification is not possible has to do with the fact that the problem to find solutions to the supersymmetry and tadpole equations belongs to the class of NP-complete problems, an issue that we elaborate on in section 2.3. Despite these difficulties, it turns out to be necessary to use an explicit calculation for four-dimensional compactifications, the ones we are most interested in, since the saddle point method does not lead to reliable results in that case.

#### Compactifications to six and eight dimensions

In the eight-dimensional case the algorithmic solution to the tadpole equation

$$\sum_a N_a X_a = L, \tag{2.45}$$

can be formulated as a two-step algorithm. First calculate all possible unordered partitions of  $L$ , then find all possible factorisations to obtain solutions for  $X$  and  $N$ . The task of partitioning is solved by the algorithm explained in appendix B, the factorisation can only be handled by brute force. In this way we are not able to calculate solutions up to very high values for  $L$ , but for our purposes, namely to check the validity of the saddle point approximation (see section 2.2.2), the method is sufficient.

In the case of compactifications to six dimensions we can still use the same method, although we now have to take care of two additional constraints. First of all we exclude

multiple wrapping, which gives an additional constraint on the wrapping numbers  $X_1, X_2, Y_1$  and  $Y_2$ , defined in appendix A.3. This constraint can be formulated in terms of the greatest common divisors of the wrapping numbers – we will come back to this issue in section 3.1. Another difference compared to the eight dimensional case is that we have to take different values for the complex structure parameters  $U_1$  and  $U_2$  (see appendix A.3 for a definition) into account. As it is shown in section 2.3, these are bounded from above and we have to sum over all possible values, making sure that we are not double counting solutions with wrapping numbers which allow for different values of the complex structures.

### An algorithm for four-dimensional models

In (A.14) the wrapping numbers  $\vec{X}$  and  $\vec{Y}$  are defined as integer valued quantities in order to implement the supersymmetry (A.18) and tadpole (A.17) conditions in a fast computer algorithm. From the equations we can derive the following inequalities

$$0 < \sum_{I=0}^3 X^I U_I \leq \sum_{I=0}^3 L^I U_I. \quad (2.46)$$

The algorithm to find solutions to these equations and the additional K-theory constraints (A.20) consists of four steps.

1. First we choose a set of complex structure variables  $U_I$ . This is done systematically and leads to a loop over all possible values. Furthermore, we have to check for redundancies, which might exist because of trivial symmetries under the exchange of two of the three two-tori.
2. In a second step we determine all possible values for the wrapping numbers  $X^I$  and  $Y^I$ , using (2.46) for the given set of complex structures, thereby obtaining all possible supersymmetric branes. In this step we also take care of the multiple wrapping constraint, which can be formulated, analogously to the six dimensional case, in terms of the greatest common divisors of the wrapping numbers.
3. In the third and most time-consuming part, we use the tadpole equations (A.17), which after a summation can be written as

$$\sum_{a=0}^k S_a = \Lambda \quad \text{with} \quad S_a := \sum_{I=0}^3 N_a U_I X_a^I \quad \text{and} \quad \Lambda := \sum_I L^I U_I. \quad (2.47)$$

To solve this equation, we note that all  $S_a$  and  $\Lambda$  are positive definite integers, which allows us to use the partition algorithm to obtain all possible combinations. The algorithm is improved by using only those values for the elements of the partition which are in the list of values we computed in the second step. For a detailed description of the explicit algorithm we used, see appendix B. Having obtained the possible  $S_a$ , we have to factorise them into values for  $N_a$  and  $X_a^I$ .

4. Since (2.47) is only a necessary but no sufficient condition, we have to check in the fourth and last step, if the obtained results indeed satisfy all constraints, especially the individual tadpole cancellation conditions and the restrictions from K-theory, which up to this point have not been accounted for at all.

The described algorithm has been implemented in C and was put on several high-performance computer clusters, using a total CPU-time of about  $4 \times 10^5$  hours. The solutions obtained in this way have been saved in a database for later analysis.

### Complexity

The main problem of the algorithm described in the last section lies in the fact that its complexity scales exponentially with the complex structure parameters. Therefore we are not able to compute up to arbitrarily high values for the  $U_I$ . Although we tried our best, it may of course be possible to improve the algorithm in many ways, but unfortunately the exponential behaviour cannot be cured unless we might have access to a quantum computer. This is due to the fact that the problem of finding solutions to the Diophantine equations we are considering falls into the class of NP complete problems [83], which means that they cannot be reduced to problems which are solvable in polynomial time.

In fact, this is quite a severe issue since the Diophantine structure of the tadpole equations encountered here is not at all exceptional, but very generic for the topological constraints also in other types of string constructions. The problem seems indeed to appear generically in computations of landscape statistics, see [63] for a general account on this issue.

As we outlined in the previous section, the computational effort to generate the solutions to be analysed in the next chapter took a significant amount of time, although we used several high-end computer clusters. To estimate how many models could be computed in principle, using a computer grid equipped with contemporary technology in a reasonable amount of time, the exponential behaviour of the problem has to be taken into account. Let us be optimistic and imagine that we would have a total number of  $10^5$  processors at our disposal which are twice as fast as the ones we have been using. Expanding our analysis to cover a range of complex structures which is twice as large as the one we considered would, in a very rough estimate, still take us of the order of 500 years.

Note that in principle there can be a big difference in the estimated computing time for the two computational problems of finding all string vacua in a certain class on the one hand, and of looking for configurations with special properties, that lead to additional constraints, on the other hand. As we explore in section 3.5.3 the computing time can be significantly reduced if we restrict ourselves to a maximum number of stacks in the hidden sector and take only configurations of a specific visible sector into account (in the example we consider we look for grand unified models with an  $SU(5)$  gauge group). Nevertheless, although a much larger range of complex structures can be

covered, the scaling of the algorithm remains unchanged. This means in particular that a cutoff on the  $U_I$ , even though it might be at higher values, has to be imposed.

## 2.3 Finiteness of solutions

It is an important question whether or not the number of solutions is infinite. Making statistical statements about an infinite set of models is much more difficult than to deal with a finite sample, because we would have to rely on properties that reoccur at certain intervals, in order to be able to make any valuable statements at all. If instead the number of solutions is finite, and we can be sure that the solutions we found form a representative sample, it is possible to draw conclusions by analysing the frequency distributions of properties without worrying about their pattern of occurrence within the space of solutions.

In the case of compactifications to eight dimensions, the results are clearly finite, as can be seen directly from the fact that the variables  $X$  and  $N$  have to be positive and  $L$  has a fixed value. Note however, although such an eight-dimensional model is clearly not realistic, that the complex structures are unconstrained. This means that if we do not invoke additional methods to fix their values, each solution to the tadpole equation represents in fact an infinite family of solutions.

### 2.3.1 The six-dimensional case

In the six dimensional case, the finiteness of the number of solutions is not so obvious, but it can be rigorously proven. In order to do so, we have to show that possible values for the complex structure parameters  $U_1$  and  $U_2$  are bounded from above. If this were not be the case, we could immediately deduce from equations (A.18) that infinitely many brane configurations would be possible.

In contrast to the eight-dimensional toy-model that we explored in section 2.2.2, in this case, and also for the four-dimensional compactifications, we do not want to allow branes that wrap the torus several times. To exclude this, we can derive the following condition on the wrapping numbers (for details see appendix A.2.1),

$$\gcd(X^1, Y^2) \gcd(X^2, Y^2) = Y^2. \quad (2.48)$$

This condition implies that all  $\vec{X}$  and  $\vec{Y}$  are non-vanishing. Additional branes, which wrap the same cycles as the orientifold planes, are given by  $\vec{X} \in \{(1, 0), (0, 1)\}$ , with  $\vec{Y} = \vec{0}$  in both cases.

From (A.18) we conclude that all non-trivial solutions have to obey  $U_1/U_2 \in \mathbb{Q}$ . Therefore we can restrict ourselves to coprime values

$$(u_1, u_2) \quad \text{with} \quad u_i := \frac{U_i}{\gcd(U_1, U_2)}. \quad (2.49)$$

With these variables we find from the supersymmetry conditions that  $Y^1 = u_2 \alpha$ , for some  $\alpha \in \mathbb{Z}$ . Now we can use the relation (A.5) to get

$$X^1 X^2 = u_1 u_2 \alpha^2. \quad (2.50)$$

In total we get two classes of possible branes, those where  $X^1$  and  $X^2$  are both positive and those where one of them is 0. The latter are those where the branes lie on top of the orientifold planes.

For fixed values of  $u_1$  and  $u_2$  the tadpole cancellation conditions (A.7) admit only a finite set of solutions. Since all quantities in these equations are positive, we can furthermore deduce from (2.50) that solutions which contain at least one brane with  $X^1, X^2 > 0$  are only possible if the complex structures satisfy the bound

$$u_1 u_2 \leq L_1 L_2. \quad (2.51)$$

In figure 2.6 we show the allowed values for  $u_1$  and  $u_2$  that satisfy equation (2.51).



Figure 2.6: Allowed values for the complex structure parameters  $u_1$  and  $u_2$  for compactifications to six dimensions.

In the case that only branes with one of the  $X^i$  vanishing are present in our model, the complex structures are not bounded from above, but since there exist only two such branes in the case of coprime wrapping numbers, all solutions of this type are already contained in the set of solutions which satisfy (2.51). Therefore we can conclude that the overall number of solutions to the constraining equations in the case of compactifications to six dimensions is finite<sup>3</sup>.

<sup>3</sup>Note however, that in the case where all branes lie on top of the orientifold planes, we are in an analogous situation for the eight-dimensional compactifications. Unless we invoke additional methods of moduli stabilisation, the complex structure moduli represent flat directions and we get infinite families of solutions.

### 2.3.2 Compactifications to four dimensions

The four dimensional case is very similar to the six-dimensional one discussed above, but some new phenomena appear. In particular, we see that the wrapping numbers can have negative values, which is the crucial point that prevents us from proving the finiteness of solutions. Although we were not able to obtain an analytic proof, we present some arguments and numerical results, which provide evidence and make it very plausible that the number of solutions is indeed finite.

#### Conditions on the wrapping numbers

As in the  $T^4/\mathbb{Z}_2$  case, we can derive a condition on the (rescaled) wrapping numbers  $\vec{X}$  and  $\vec{Y}$ , defined by (A.24), to exclude multiple wrapping. The derivation is given in appendix A.3.1 and the result is<sup>4</sup>

$$\prod_{i=1}^3 \gcd(\tilde{Y}^0, \tilde{X}^i) = (\tilde{Y}^0)^2. \quad (2.52)$$

From the relations (A.15), it follows that either one, two or all four  $X^I$  can be non-vanishing. The case with only one of them vanishing is excluded. Let us consider the three possibilities in turn and see what we can say about the number of possible solutions in each case.

1. In the case that only one of the  $X^I \neq 0$ , the corresponding brane lies on top of one of the orientifold planes on all three  $T^2$ . This situation is equivalent to the eight-dimensional case and can be included in the discussion of the next possibility.
2. If two  $X^I \neq 0$ , we are in the situation discussed for the compactification to six dimensions. The two  $X^I$  have to be positive by means of the supersymmetry condition and one of the complex structures is fixed at a rational number. Together with the eight-dimensional branes, the same proof of finiteness we have given for the  $T^4/\mathbb{Z}_2$ -case can be applied.
3. A new situation arises for those branes where all  $X^I \neq 0$ . Let us discuss this a bit more in detail.

From the relations (A.15) we deduce that an odd number of them has to be negative. In the case that three would be negative and one positive – let us without loss of generality choose  $X_0 > 0$  – we can write the supersymmetry condition (A.18) as

$$\sum_{I=0}^3 Y^I \frac{1}{U_I} = \frac{Y^0}{U_0} \left( 1 + \sum_{i=1}^3 \frac{X^i U_0}{X^i U_i} \right) = 0, \quad (2.53)$$

---

<sup>4</sup>We have to use rescaled wrapping numbers, as defined by (A.24), to write the solution in this simple form.

which implies  $X^i U_i < -X^0 U_0 \forall i \in \{1, 2, 3\}$ . This contradicts the second supersymmetry condition,

$$X^0 U_0 \left( 1 + \sum_{i=1}^3 \frac{X^i U_i}{X^0 U_0} \right) > 0. \quad (2.54)$$

Therefore, we conclude that the only remaining possibility is to have one of the  $X^I < 0$ . Again we choose  $X^0$  without loss of generality. We can now use (2.53) to express  $X^0$  in terms of the other three wrapping numbers as

$$X^0 = - \left( \sum_i \frac{U_0}{U_i X^i} \right)^{-1}. \quad (2.55)$$

Furthermore, we can use the inequality (2.46) and derive an upper bound

$$\sum_{I=0}^3 L_I U_I \geq X^0 U_0 + \sum_{i=1}^3 X^i U_i > X^j U_j > 0, \quad \forall j \in \{1, 2, 3\}. \quad (2.56)$$

As in the six-dimensional case, we can use the argument that the complex structures are fixed at rational values, as long as we take a sufficient number of branes. So we can write them, in analogy to (2.49) as  $u_{I,2}/u_{I,1}$ . Using this definition, we can write (2.56) as

$$1 \leq X_i \leq \frac{\sum_{P=0}^3 u_{P,2} u_{Q,1} u_{R,1} u_{S,1} L_P}{u_{i,2} u_{J,1} u_{K,1} u_{L,1}}, \quad (2.57)$$

for  $P \neq Q \neq R \neq S \neq P$  and  $i \neq J \neq K \neq L \neq i$ .

From this we conclude that as long as the complex structures are fixed, we have only a finite number of possible brane configurations, i.e. only a finite number of solutions. This is unfortunately not enough to conclude that we have only a finite number of solutions in general. We would have to show, as in the six-dimensional case, that there exists an upper bound on the complex structures. Since we were not able to find an analytic proof that such a bound exists, we have to rely on some numerical hints that it is in fact the case. We present some of these hints in the following.

### Numerical analysis

Figure 2.7 shows how the total number of mutually different brane configurations for  $L = 2$  increases and saturates, as we include more and more combinations of values for the complex structures  $U_I$  into the set for which we construct solutions. For this small value of  $L$  our algorithm actually admits pushing the computations up to those complex structures where obviously no additional brane solutions exist.

For the physically relevant case of  $L = 8$  the total number of models compared to the absolute value  $|U|$  of the complex structure variables scales as displayed in figure 2.8. The plot shows all complex structures we have actually been able to analyse systematically. We find that the number of solutions falls logarithmically for



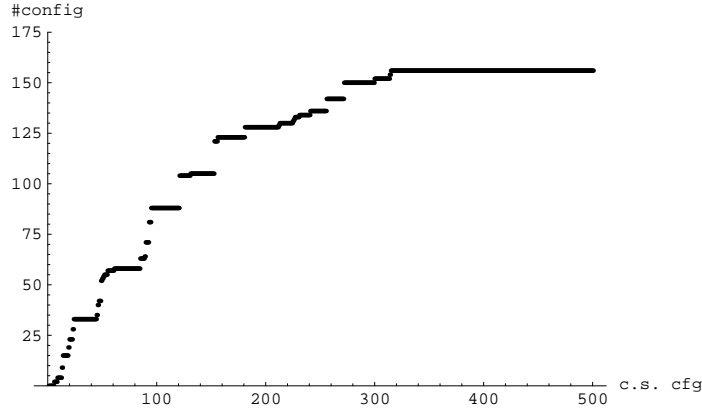


Figure 2.7: The number of unique solutions for compactifications on  $T^6/\mathbb{Z}_2 \times \mathbb{Z}_2$ , taking  $L_I = 2 \forall I \in \{0, \dots, 3\}$ . The horizontal axis shows combinations of the  $U_I$ , ordered by their absolute value  $|U|$ . For each of these values we plotted the cumulative set of solutions obtained up to this point.

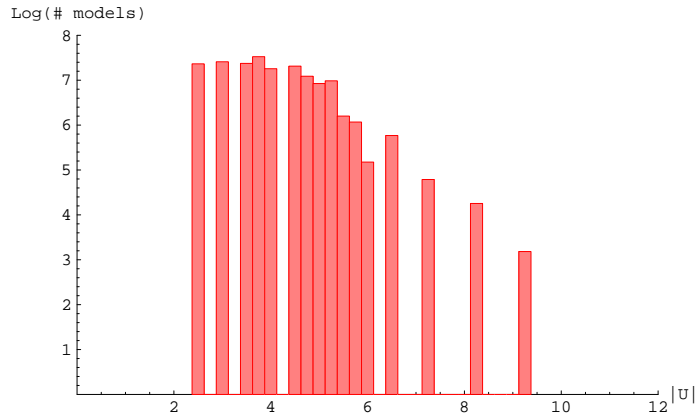


Figure 2.8: Logarithmic plot of the absolute number of solutions for compactifications on  $T^6/\mathbb{Z}_2 \times \mathbb{Z}_2$  using the physical values  $L_I = 8 \forall I \in \{0, \dots, 3\}$  against the absolute value  $|U|$ . The cutoff is set at  $|U| = 12$ . In this plot, as in all other plots of this thesis, we use a decadic logarithm.

increasing values of  $|U|$ . In order to interpret this result, we observe that the complex structure moduli  $U_I$  are only defined up to an overall rescaling by the volume modulus of the compact space. We have chosen all radii and thereby also all  $U_I$  to be integer valued, which means that large  $|U|$  correspond to large coprime values of  $R_1^{(i)}$  and  $R_2^{(i)}$ . This comprises on the one hand decompactification limits which have to be discarded in any case for phenomenological reasons, but on the other hand also tori which are slightly distorted, e.g. almost square tori with  $R_2^{(i)}/R_1^{(i)} = 0.99$ .

Combining the results of the two numerical tests, we have reason to hope that we can indeed make a convincing statistical statement using the analysed data. Nevertheless,

at this point it should be mentioned that we cannot fully exclude that a large number of new solutions appears at those values for the complex structures which we have not analysed. A hint that this problem should not occur is given in section 3.5.3, where we performed a restricted analysis of  $SU(5)$  models up to values of  $|U| \approx 250$ .

# Chapter 3

## Statistical analysis of orientifold models

After preparing the stage in the last chapter, introducing the models and methods of analysis, we are now going to analyse some specific constructions of phenomenological interest. At the end of this chapter we want to arrive at a point where we can make some meaningful statistical statements about the probability to find realisations of the standard model or GUT models in the specific set of models we are considering.

However, it is important to mention, that our results cannot be regarded to be complete. First of all we neglect the impact of fluxes, which does not change the distributions completely, but definitely has some influence. Secondly, we are considering only very specific geometries. Since the construction of the orientifolds, especially the choice of the orbifold group which in our case is always  $\mathbb{Z}_2$ , has a strong impact on the constraining equations, it is very probable that the results change significantly once we use a different compactification space. Nevertheless we think that these results are one step towards a deeper understanding of open string statistics.

In the first part of this chapter we discuss some general aspects of compactifications to six and four dimensions. We analyse the properties of the gauge groups, including the occurrence of specific individual gauge factors and the total rank. With respect to the chiral matter content, we establish the notion of a mean chirality and discuss their frequency distribution.

In a second part we perform a search for models with the properties of a supersymmetric standard model. Besides the frequency distributions in the gauge sector we analyse the values of the gauge couplings and compare our results to those of a recent statistical analysis of Gepner models [70, 71]. In addition to standard model gauge groups we look also for models with a Pati-Salam,  $SU(5)$  and flipped  $SU(5)$  structure.

In the last part we consider different aspects of the question of correlations of observables in the gauge sector and give an estimate how likely it is to find a three generation standard model in our setup.

### 3.1 Statistics of six-dimensional models

Before considering the statistics of realistic four-dimensional models, let us start with a simpler construction to test the methods of analysis developed in chapter 2. We will use a compactification to six dimensions on a  $T^4/\mathbb{Z}_2$  orientifold, defined in appendix A.2. The important question about the finiteness of solutions has been settled in section 2.3, so we can be confident that the results we obtain will be meaningful. To use the saddle point approximation in this context, we have to generalise from the eight-dimensional example in 2.2.2 to an approximation in several variables, as described by equations (2.23) and (2.24). In our case we will have to deal with two variables  $\vec{q} = (q_1, q_2)$ , corresponding to the two wrapping numbers  $\vec{X} = (X^1, X^2)$ .

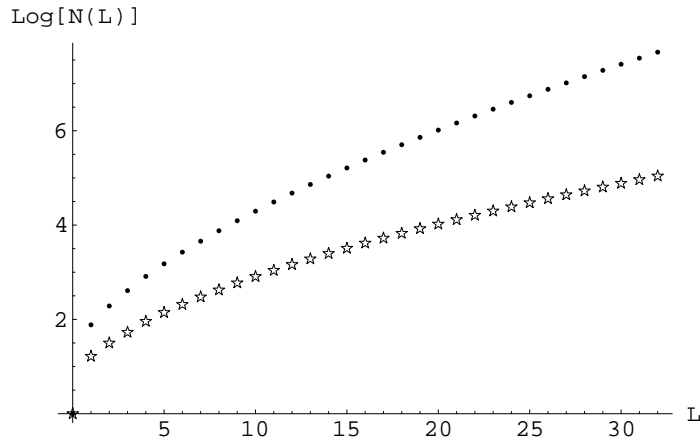


Figure 3.1: Logarithmic plot of the number of solutions for compactifications on  $T^4/\mathbb{Z}_2$  for  $L^2 = 8$  and different values of  $L \equiv L^1$ . The complex structures are fixed to  $u_1 = u_2 = 1$ . The dotted line shows the result with multiple wrapping, the starred line gives the result with coprime wrapping numbers.

Let us briefly consider the question of multiple wrapping. As shown in appendix A.2.1, we can derive a constraint on the wrapping numbers  $\vec{X}$  and  $\vec{Y}$ , such that multiply wrapping branes are excluded. To figure out what impact this additional constraint has on the distributions, let us compare the number of solutions for different values of  $L^1$  and  $L^2$ , with and without multiple wrapping. The result is shown in figure 3.1. As could have been expected, the number of solutions with coprime wrapping numbers grows less fast than the one where multiple wrapping is allowed.

#### 3.1.1 Distributions of gauge group observables

Using the saddle point method, introduced in section 2.2.1, we can evaluate the distributions for individual gauge group factors and total rank of the gauge group in analogy to the simple eight-dimensional example we pursued in section 2.2.2. Therefore we will fix the orientifold charges to their physical values,  $\vec{L} = (L_1, L_2) = (8, 8)$ .

The probability to find one  $U(M)$  gauge factor can be written similar to (2.40) as

$$P(M, \vec{L}) \simeq \frac{1}{\mathcal{N}(\vec{L})(2\pi i)^2} \oint d\vec{q} \exp \left[ \sum_{\vec{X} \in S_U} \frac{q_1^{X_1} q_2^{X_2}}{1 - q_1^{X_1} q_2^{X_2}} + \log \left( \sum_{\vec{X} \in S_U} q_1^{MX_1} q_2^{MX_2} \right) - (L_1 + 1) \log q_1 - (L_2 + 1) \log q_2 \right], \quad (3.1)$$

where we denoted with  $S_U$  the set of all values for  $\vec{X}$  that are compatible with the supersymmetry conditions and the constraints on multiple wrapping. The number of solution  $\mathcal{N}(\vec{L})$  is given by

$$\mathcal{N}(\vec{L}) \simeq \frac{q}{(2\pi i)^2} \oint d\vec{q} \exp \left[ \sum_{\vec{X} \in S_U} \frac{q_1^{X_1} q_2^{X_2}}{1 - q_1^{X_1} q_2^{X_2}} - (L_1 + 1) \log q_1 - (L_2 + 1) \log q_2 \right]. \quad (3.2)$$

The resulting distribution for the probability of an  $U(M)$  factor, compared to the results of an exact computer search, is shown in figure 3.2(a).

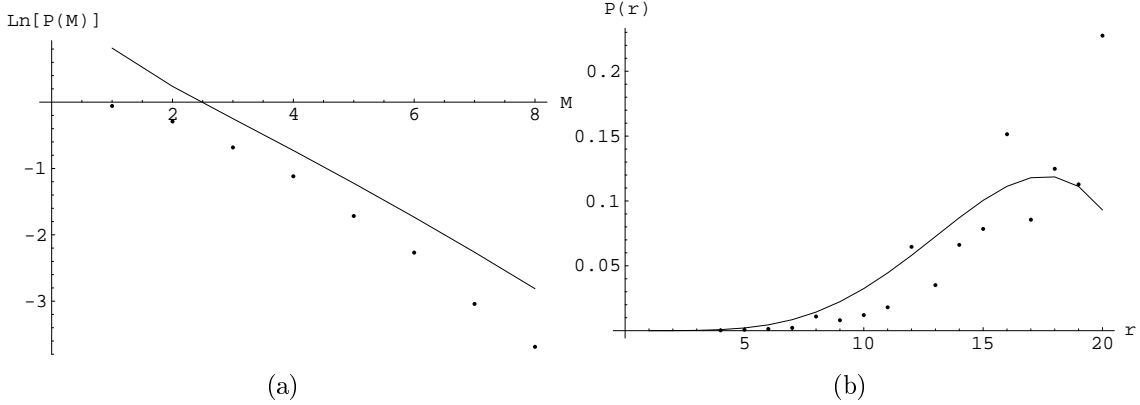


Figure 3.2: Distributions in the gauge sector of a compactification on  $T^4/\mathbb{Z}_2$ . The complex structures are fixed to  $u_1 = u_2 = 1$ . The dotted line is the result of an exact computation, the solid line shows the saddle point approximation to second order. (a) Probability to find an  $U(M)$  gauge factor, (b) Distribution of the total rank of the gauge group.

As in the eight-dimensional example we can evaluate the distribution of the total rank (2.42). As a generalisation of (2.43) we obtain the following formula

$$P(r, \vec{L}) \simeq \frac{1}{\mathcal{N}(\vec{L})(2\pi i)^3} \oint d\vec{q} dz \exp \left[ \sum_{\vec{X} \in S_U} \frac{z q_1^{X_1} q_2^{X_2}}{1 - z q_1^{X_1} q_2^{X_2}} - (L_1 + 1) \log q_1 - (L_2 + 1) \log q_2 - (r + 1) \log z \right]. \quad (3.3)$$

Figure 3.2(b) shows the resulting distribution of the total rank, compared to the exact result. As one can see, the results of the saddle point analysis are much smoother than the exact results, which show a more jumping behaviour, resulting from number theoretical effects. These are strong at low  $L$ , which is also the reason that our saddle point approximation is not very accurate. In the present six-dimensional case the deviations are not too strong, but in the four-dimensional case their impact is so big that the result cannot be trusted anymore. These problems can be traced back to the small values of  $L$  we are working with, but since these are the physical values for the orientifold charge, we cannot do much about it.

### 3.1.2 Chirality

Since we are ultimately interested in calculating distributions for models with gauge groups and matter content close to the standard model, it would be interesting to have a measure for the mean chirality of the matter content in our models.

A good quantity to consider for this purpose would be the distribution of intersection numbers  $I_{ab}$  between different stacks of branes. This is precisely the quantity we choose later in the four-dimensional compactifications. In the present case we use a simpler definition for chirality, given by

$$\chi := X^1 X^2. \quad (3.4)$$

This quantity counts the net number of chiral fermions in the antisymmetric and symmetric representations.

Using the saddle point method, we can compute the distribution of values for  $\chi$ , using

$$\begin{aligned} P(\chi, \vec{L}) = & \frac{1}{\mathcal{N}(\vec{L})(2\pi i)^2} \oint d\vec{q} \exp \left[ \sum_{\vec{X} \in S_U} \frac{q_1^{X_1} q_2^{X_2}}{1 - q_1^{X_1} q_2^{X_2}} \right. \\ & - \log \left( \sum_{\vec{X} \in S_U} \frac{q_1^{X_1} q_2^{X_2}}{1 - q_1^{X_1} q_2^{X_2}} \right) + \log \left( \sum_{\vec{X} \in S_{U,\chi}} \frac{q_1^{X_1} q_2^{X_2}}{1 - q_1^{X_1} q_2^{X_2}} \right) \\ & \left. - (L_1 + 1) \log q_1 - (L_2 + 1) \log q_2 \right], \quad (3.5) \end{aligned}$$

where  $S_{U,\chi} \subset S_U$  is the set of wrapping numbers that fulfills (3.4).

The resulting distribution is shown in figure 3.3. For the used values of  $u_1, u_2 = 1$ ,  $\chi$  has to be a square, which can be directly deduced from the supersymmetry conditions (A.8). The scaling turns out to be roughly  $P(\chi) \simeq \exp(-c\sqrt{\chi})$ . From this result we can conclude that non-chiral models are exponentially more frequent than chiral ones. This turns out to be a general property of the orientifold models that also holds in the four-dimensional case.

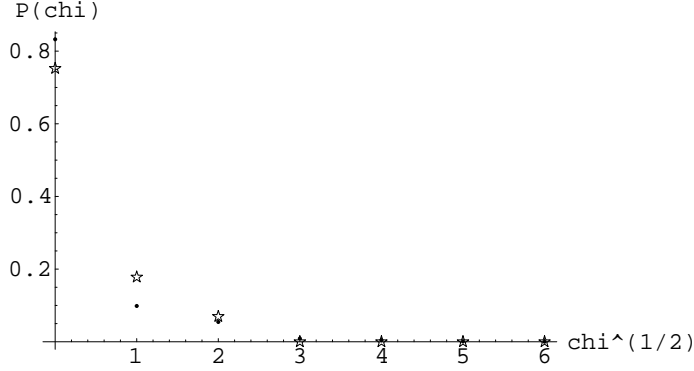


Figure 3.3: Distribution of the mean chirality for  $T^4/\mathbb{Z}_2$ ,  $L^1 = L^2 = 8$ ,  $u_1 = u_2 = 1$ .

### 3.1.3 Correlations

In this section we would like to address the question of correlations between observables for the first time. We come back to this issue in section 3.6. The existence of such correlations can be seen in figure 3.4, where we plotted the distributions of models with specific total rank and chirality. The connection between both variables is given by the tadpole cancellation conditions, which involve the  $N_a$  used for the definition of the total rank in (2.42) and the wrapping numbers  $\vec{X}_a$ , which appear in the definition of the mean chirality  $\chi$  in (3.4). The distribution can be obtained from

$$\begin{aligned}
P(\chi, r, \vec{L}) \simeq & \frac{1}{\mathcal{N}(\vec{L})(2\pi i)^3} \oint d\vec{q} dz \exp \left[ \sum_{\vec{X} \in S_U} \frac{z q_1^{X_1} q_2^{X_2}}{1 - z q_1^{X_1} q_2^{X_2}} \right. \\
& - \log \left( \sum_{\vec{X} \in S_U} \frac{z q_1^{X_1} q_2^{X_2}}{1 - z q_1^{X_1} q_2^{X_2}} \right) + \log \left( \sum_{\vec{X} \in S_{U,\chi}} \frac{z q_1^{X_1} q_2^{X_2}}{1 - z q_1^{X_1} q_2^{X_2}} \right) \\
& \left. - (L_1 + 1) \log q_1 - (L_2 + 1) \log q_2 - (r + 1) \log z \right], \quad (3.6)
\end{aligned}$$

which is a straightforward combination of (3.3) and (3.5).

In figure 3.4(a) one can see that the maximum of the rank distribution is shifted to smaller values for larger values of  $\chi$ . This could have been expected, since larger values of  $\chi$  imply larger values for the wrapping numbers  $\vec{X}$ , which in turn require lower values for the number of branes per stack  $N_a$ , in order to fulfill the tadpole conditions. The shift of the maximum depending of  $\chi$ , can be seen more directly in figure 3.4(b).

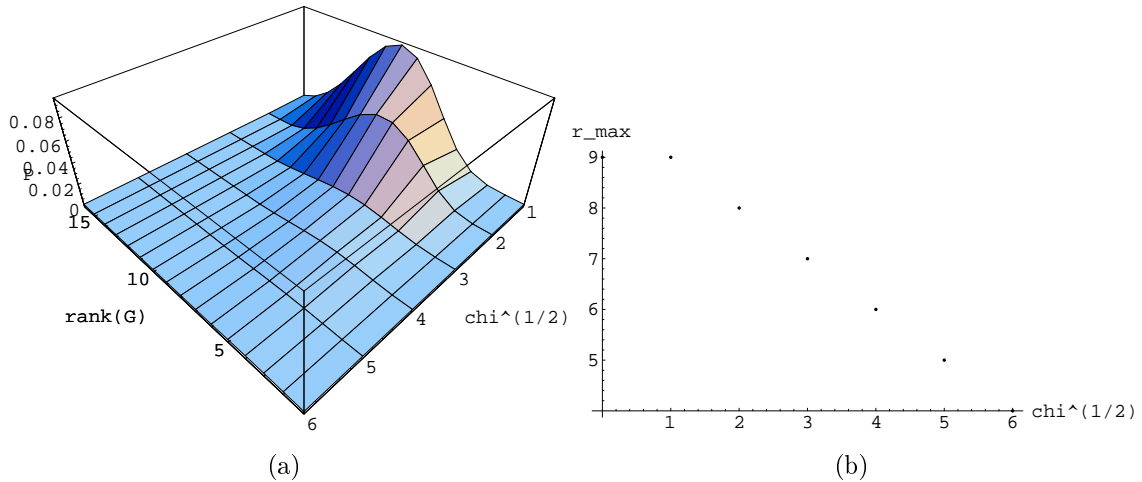


Figure 3.4: Correlation between total rank and chirality for  $L_1 = L_2 = 8$  and  $u_1 = u_2 = 1$  for a compactification on  $T^4/\mathbb{Z}_2$ . (b) shows the maximum of the total rank distribution depending on  $\chi$ .

## 3.2 Statistics of four-dimensional models

Having tried our methods in compactifications down to six dimensions, let us now switch to the phenomenologically more interesting case of four-dimensional models. Unfortunately we can no longer use the saddle point approximation, since it turns out that in this more complicated case the approximation is no longer reliable. The results deviate significantly from what we see in exact computations. Furthermore the computer power needed to obtain the integrals numerically in the approximation becomes comparable to the effort needed to compute the solutions explicitly.

### 3.2.1 Properties of the gauge sector

Using several computer clusters and the specifically adapted algorithm described in section 2.2.3 for a period of several months, we produced explicit constructions of  $\approx 1.6 \times 10^8$  consistent compactifications on  $T^6/\mathbb{Z}_2 \times \mathbb{Z}_2$ . The results presented in the following have been published in [92, 91], see also the analysis in [127] and more recent results using brane recombination methods in [128].

Using this data we can proceed to analyse the observables of these models. The distribution of the total rank  $r$  of the gauge group is shown in figure 3.5(a). An interesting phenomenon is the suppression of odd values for the total rank. This can be explained by the K-theory constraints and the observation that the generic value for  $Y^I$  is 0 or 1. Branes with these values belong to the first class of branes in the classification of section 2.3.2 and are those which lie on top of the orientifold planes. Therefore equation (A.20) suppresses solutions with an odd value for  $r$ . This suppression from the K-theory constraints is quite strong, the total number of solutions



is reduced by a factor of six compared to the situation where these constraints are not enforced.

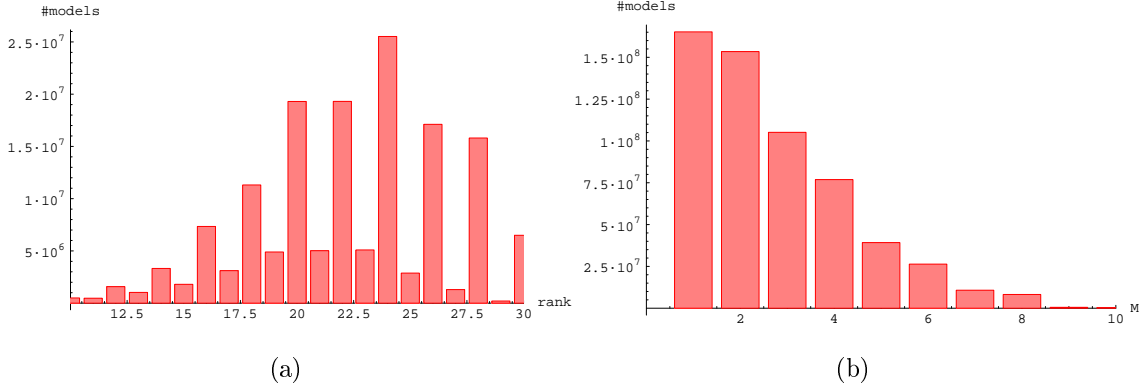


Figure 3.5: Frequency distributions of total rank and  $U(M)$  gauge groups of all models.

Another quantity of interest is the distribution of  $U(M)$  gauge groups, shown in figure 3.5(b). We find that most models carry at least one  $U(1)$  gauge group, corresponding to a single brane, and stacks with a higher number of branes become more and more unlikely. This could have been expected because small numbers occur with a much higher frequency in the partition and factorisation of natural numbers.

### 3.2.2 Chirality

As in the six-dimensional case we want to define a quantity that counts chiral matter in the models under consideration. In contrast to the very rough estimate we used in section 3.1.2, this time we are going to count all chiral matter states, such that our definition of mean chirality is now

$$\chi := \frac{2}{k(k+1)} \sum_{a,b=0,a<b}^k I_{a'b} - I_{ab} = \frac{4}{k(k+1)} \sum_{a,b=0,a<b}^k \vec{Y}_a \vec{X}_b. \quad (3.7)$$

In this formula the states from the intersection of two branes  $a$  and  $b$  are counted with a positive sign, while the states from the intersection of the orientifold image of brane  $a$ , denoted by  $a'$ , and brane  $b$  are counted negatively. As we explained in section 2.1.1 and summarised in table 2.1,  $I_{ab}$  gives the number of bifundamental representations  $(\mathbf{N}_a, \overline{\mathbf{N}}_b)$ , while  $I_{a'b}$  counts  $(\overline{\mathbf{N}}_a, \mathbf{N}_b)$ . Therefore we compute the net number of chiral representations with this definition of  $\chi$ . By summing over all possible intersections and normalising the result we obtain a quantity that is independent of the number of stacks and can be used for a statistical analysis.

A computation of the value of  $\chi$  according to (3.7) for all models leads to a frequency distribution of the mean chirality as shown in figure 3.6. This distribution is basically

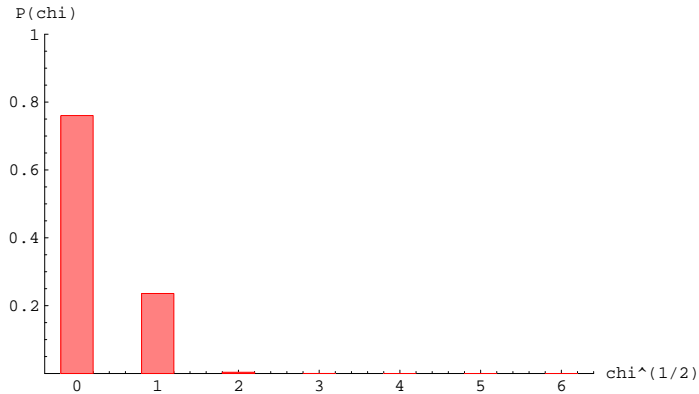


Figure 3.6: Distribution of the mean chirality  $\chi$  in compactification to four dimensions.

identical to the one we obtained in section 3.1.2, shown in figure 3.3. In particular we also find that models with a mean chirality of 0 dominate the spectrum and are exponentially more frequent than chiral ones.

From the similarity with the distribution of models on  $T^4/\mathbb{Z}_2$  we can also conjecture that there is a correlation between the mean chirality and the total rank, as we found it to be the case for the six-dimensional models in section 3.1.3. Let us postpone this question to section 3.6, where we give a more detailed account of several questions concerning the correlation of observables.

### 3.3 Standard model constructions

An important subset of the models considered in the previous section are of course those which could provide a standard model gauge group at low energies. More precisely, since we are dealing with supersymmetric models only, we are looking for models which might resemble the particle spectrum of the MSSM.

To realise the gauge group of the standard model we need generically four stacks of branes (denoted by a,b,c,d) with two possible choices for the gauge groups:

$$\begin{aligned}
 &U(3)_a \times U(2)_b \times U(1)_c \times U(1)_d, \\
 &U(3)_a \times Sp(2)_b \times U(1)_c \times U(1)_d.
 \end{aligned} \tag{3.8}$$

To exclude exotic chiral matter from the first two factors we have to impose the constraint that  $\#\mathbf{Sym}_{a/b} = 0$ , i.e. the number of symmetric representations of stacks  $a$  and  $b$  has to be zero. Models with only three stacks of branes can also be realised, but they suffer generically from having non-standard Yukawa couplings. Since we are not treating our models in so much detail and are more interested in their generic distributions, we include these three-stack constructions in our analysis.

Another important ingredient for standard model-like configurations is the existence of a massless  $U(1)_Y$  hypercharge. This is in general a combination

$$U(1)_Y = \sum_{a=1}^k x_a U(1)_a, \quad (3.9)$$

including contributions of several  $U(1)$ s. Since we would like to construct the matter content of the standard model, we are very constrained about the combination of  $U(1)$  factors. In order to obtain the right hypercharges for the standard model particles, there are three different combinations of the  $U(1)$ s used to construct the quarks and leptons possible,

$$\begin{aligned} U(1)_Y^{(1)} &= \frac{1}{6}U(1)_a + \frac{1}{2}U(1)_c + \frac{1}{2}U(1)_d, \\ U(1)_Y^{(2)} &= -\frac{1}{3}U(1)_a - \frac{1}{2}U(1)_b, \\ U(1)_Y^{(3)} &= -\frac{1}{3}U(1)_a - \frac{1}{2}U(1)_b + U(1)_d, \end{aligned} \quad (3.10)$$

where choices 2 and 3 are only available for the first choice of gauge groups. As explained in section 2.1.4, we can construct a massless combination of  $U(1)$  factors, if (2.11) is satisfied. This gives an additional constraint on the wrapping numbers  $\vec{Y}$ .

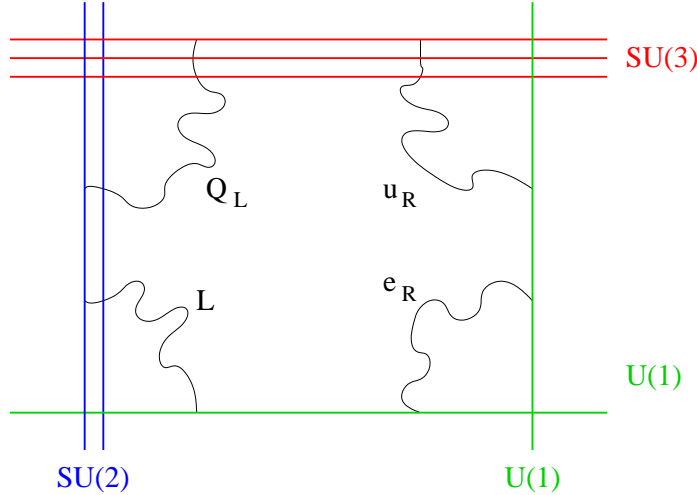


Figure 3.7: Assignment of brane intersections and chiral matter content for the first of the possible realisations of the standard model using intersecting branes.

For the different possibilities to construct the hypercharge this constraint looks different. In the case of  $U(1)_Y^{(1)}$  the condition can be formulated as

$$\vec{Y}_a + \vec{Y}_c + \vec{Y}_d = 0. \quad (3.11)$$

For  $Q_Y^{(2)}$ , where the right-handed up-type quarks are realised as antisymmetric representations of  $U(3)$  [5, 24], we obtain

$$\vec{Y}_a + \vec{Y}_b = 0, \quad (3.12)$$

and for  $Q_Y^{(3)}$ , where we also need antisymmetric representations of  $U(3)$  to realise the right-handed up-quarks, we get

$$\vec{Y}_a + \vec{Y}_b - \vec{Y}_d = 0. \quad (3.13)$$

In total we have found four ways to realise the standard model with massless hypercharge, summarised with the explicit realisation of the fundamental particles in tables 3.1 and 3.2. The chiral matter content arises at the intersection of the four stacks of branes. This is shown schematically for one of the four possibilities in figure 3.7.

particle	representation	mult.
$U(3)_a \times Sp(2)_b \times U(1)_c \times U(1)_d$ with $Q_Y^{(1)}$		
$Q_L$	$(\mathbf{3}, \mathbf{2})_{0,0}$	$I_{ab}$
$u_R$	$(\bar{\mathbf{3}}, \mathbf{1})_{-1,0} + (\bar{\mathbf{3}}, \mathbf{1})_{0,-1}$	$I_{a'c} + I_{a'd}$
$d_R$	$(\bar{\mathbf{3}}, \mathbf{1})_{1,0} + (\bar{\mathbf{3}}, \mathbf{1})_{0,1}$	$I_{a'c'} + I_{a'd'}$
$d_R$	$(\bar{\mathbf{3}}_A, \mathbf{1})_{0,0}$	$\frac{1}{2}(I_{aa'} + I_{aO6})$
$L$	$(\mathbf{1}, \mathbf{2})_{-1,0} + (\mathbf{1}, \mathbf{2})_{0,-1}$	$I_{bc} + I_{bd}$
$e_R$	$(\mathbf{1}, \mathbf{1})_{2,0}$	$\frac{1}{2}(I_{cc'} - I_{cO6})$
$e_R$	$(\mathbf{1}, \mathbf{1})_{0,2}$	$\frac{1}{2}(I_{dd'} - I_{dO6})$
$e_R$	$(\mathbf{1}, \mathbf{1})_{1,1}$	$I_{cd'}$
$U(3)_a \times U(2)_b \times U(1)_c \times U(1)_d$ with $Q_Y^{(1)}$		
$Q_L$	$(\mathbf{3}, \bar{\mathbf{2}})_{0,0}$	$I_{ab}$
$Q_L$	$(\mathbf{3}, \mathbf{2})_{0,0}$	$I_{ab'}$
$u_R$	$(\bar{\mathbf{3}}, \mathbf{1})_{-1,0} + (\bar{\mathbf{3}}, \mathbf{1})_{0,-1}$	$I_{a'c} + I_{a'd}$
$d_R$	$(\bar{\mathbf{3}}, \mathbf{1})_{1,0} + (\bar{\mathbf{3}}, \mathbf{1})_{0,1}$	$I_{a'c'} + I_{a'd'}$
$d_R$	$(\bar{\mathbf{3}}_A, \mathbf{1})_{0,0}$	$\frac{1}{2}(I_{aa'} + I_{aO6})$
$L$	$(\mathbf{1}, \mathbf{2})_{-1,0} + (\mathbf{1}, \mathbf{2})_{0,-1}$	$I_{bc} + I_{bd}$
$L$	$(\mathbf{1}, \bar{\mathbf{2}})_{-1,0} + (\mathbf{1}, \bar{\mathbf{2}})_{0,-1}$	$I_{b'c} + I_{b'd}$
$e_R$	$(\mathbf{1}, \mathbf{1})_{2,0}$	$\frac{1}{2}(I_{cc'} - I_{cO6})$
$e_R$	$(\mathbf{1}, \mathbf{1})_{0,2}$	$\frac{1}{2}(I_{dd'} - I_{dO6})$
$e_R$	$(\mathbf{1}, \mathbf{1})_{1,1}$	$I_{cd'}$

Table 3.1: Realisation of quarks and leptons for the two different choices of gauge groups (3.8) and hypercharge (1) in (3.10).

particle	representation	mult.
$U(3)_a \times U(2)_b \times U(1)_c \times U(1)_d$ with $Q_Y^{(2)}$		
$Q_L$	$(\mathbf{3}, \bar{\mathbf{2}})_{0,0}$	$I_{ab}$
$u_R$	$(\bar{\mathbf{3}}_A, \mathbf{1})_{0,0}$	$\frac{1}{2}(I_{aa'} + I_{aO6})$
$d_R$	$(\bar{\mathbf{3}}, \mathbf{1})_{-1,0} + (\bar{\mathbf{3}}, \mathbf{1})_{0,-1}$	$I_{a'c} + I_{a'd}$
$d_R$	$(\bar{\mathbf{3}}, \mathbf{1})_{1,0} + (\bar{\mathbf{3}}, \mathbf{1})_{0,1}$	$I_{a'c'} + I_{a'd'}$
$L$	$(\mathbf{1}, \mathbf{2})_{-1,0} + (\mathbf{1}, \mathbf{2})_{0,-1}$	$I_{bc} + I_{bd}$
$L$	$(\mathbf{1}, \mathbf{2})_{1,0} + (\mathbf{1}, \mathbf{2})_{0,1}$	$I_{bc'} + I_{bd'}$
$e_R$	$(\mathbf{1}, \bar{\mathbf{1}}_A)_{0,0}$	$-\frac{1}{2}(I_{bb'} + I_{bO6})$
$U(3)_a \times U(2)_b \times U(1)_c \times U(1)_d$ with $Q_Y^{(3)}$		
$Q_L$	$(\mathbf{3}, \bar{\mathbf{2}})_{0,0}$	$I_{ab}$
$u_R$	$(\bar{\mathbf{3}}_A, \mathbf{1})_{0,0}$	$\frac{1}{2}(I_{aa'} + I_{aO6})$
$d_R$	$(\bar{\mathbf{3}}, \mathbf{1})_{-1,0}$	$I_{a'c}$
$d_R$	$(\bar{\mathbf{3}}, \mathbf{1})_{1,0}$	$I_{a'c'}$
$L$	$(\mathbf{1}, \bar{\mathbf{2}})_{0,-1}$	$I_{b'd}$
$e_R$	$(\mathbf{1}, \bar{\mathbf{1}}_A)_{0,0}$	$-\frac{1}{2}(I_{bb'} + I_{bO6})$
$e_R$	$(\mathbf{1}, \mathbf{1})_{1,1}$	$I_{cd'}$
$e_R$	$(\mathbf{1}, \mathbf{1})_{-1,1}$	$I_{c'd'}$

Table 3.2: Realisation of quarks and leptons for hypercharges (2) and (3) of (3.10), which can only be realised for the first choice of gauge groups in (3.8).

### 3.3.1 Number of generations

The first question one would like to ask, after having defined what a "standard model" is in our setup, concerns the frequency of such configurations in the space of all solutions. Put differently: *How many standard models with three generations of quarks and leptons do we find?* The answer to this question is *zero*, even if we relax our constraints and allow for a massive hypercharge (which is rather fishy from a phenomenological point of view). The result of the analysis can be seen in figure 3.8.

To analyse this result more closely, we relaxed our constraints further and allowed for different numbers of generations for the quark and lepton sector. This is of course phenomenologically no longer relevant, but it helps to understand the structure of the solutions. The three-dimensional plot of this analysis is shown in figure 3.9. Actually there exist solutions with three generations of either quarks or leptons, where

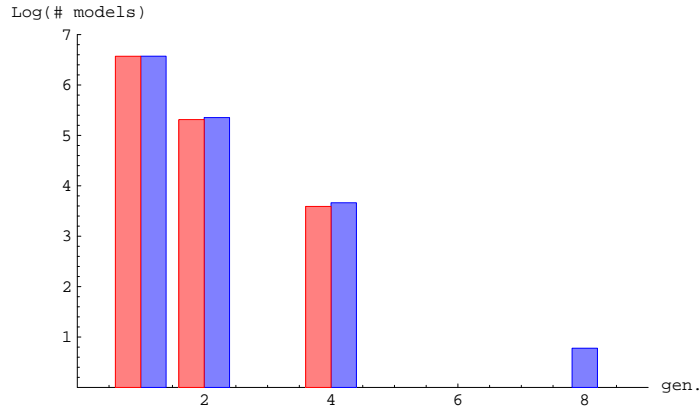


Figure 3.8: Number of quark and lepton generations with (red bars on the left) and without (blue bars on the right) enforcing a massless  $U(1)$ .

models with only one generation of quarks clearly dominate. The suppression of three generation models can therefore be pinned down to the construction of models with three generations of quarks, which arise at the intersection of the  $U(3)$  with the  $SU(2)/Sp(2)$  branes and the  $U(1)$  branes respectively. models with three generations of either quarks or leptons are shown in table 3.3.

# of quark gen.	# of lepton gen.	# of models
1	3	183081
2	3	8
3	4	136
4	3	48

Table 3.3: Number of models found with either three quark or three lepton generations.

This result is rather strange, since we know that models with three families of quarks and leptons have been constructed in our setup (e.g. in [26, 40, 136, 55]). A detailed analysis of the models in the literature shows that all models which are known use (in our conventions) large values for the complex structure variables  $U_I$  and therefore did not appear in our analysis (see section 2.2.3). On the other hand we know that the number of models decreases exponentially with higher values for the complex structures. Therefore we conclude that standard models with three generations are highly suppressed in this specific setup.

This brings up a natural question, namely: How big is this suppression factor? We postpone this question to section 3.6.2, where we analyse this issue more closely and finally give an estimate for the probability to find a three generation standard model

in our setup. For now let us just notice that this probability has to be smaller than the inverse of the total number of models we analysed, i.e.  $< 10^{-8}$ .

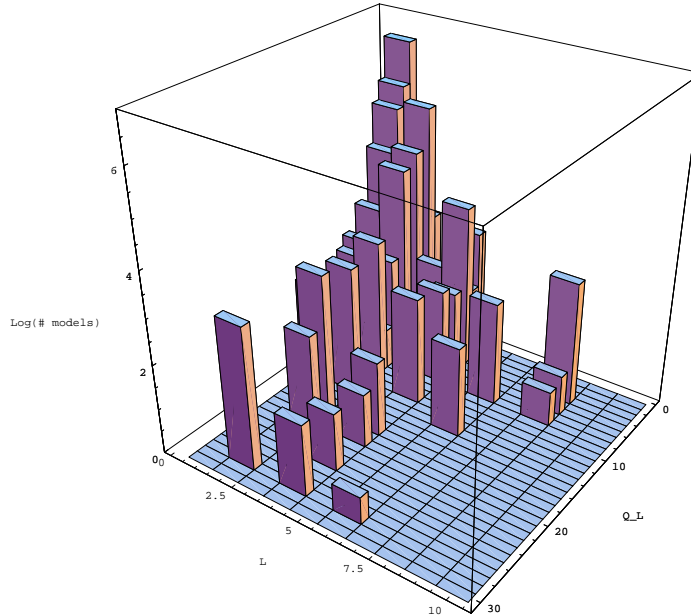


Figure 3.9: Logarithmic plot of the number of models with different numbers of generations of quarks and leptons.  $Q_L$  denotes the number of quark families,  $L$  is the number of lepton generations.

### 3.3.2 Hidden sector

Besides the so called “visible sector” of the model, containing the standard model gauge group and particles, we have generically additional chiral matter, transforming under different gauge groups. This sector is usually called the “hidden sector” of the theory, assuming that the masses of the additional particles are lifted and therefore unobservable at low energies.

In figure 3.10(a) we show the frequency distributions of the total rank of gauge groups in the hidden sector. In 3.10(b) we show the frequency distribution of individual gauge group factors. Comparing these results with the distributions of the full set of models in figure 3.5, we observe that at a qualitative level the restriction to the standard model gauge group in the visible sector did not change the distribution of gauge group observables. The number of constructions in the standard model case is of course much lower, but the frequency distributions of the hidden sector properties behave pretty much like those we obtained for the complete set of models.

As we argue in section 3.6, this is not a coincidence, but a generic feature of the class of models we analysed. Many of the properties of our models can be regarded to be

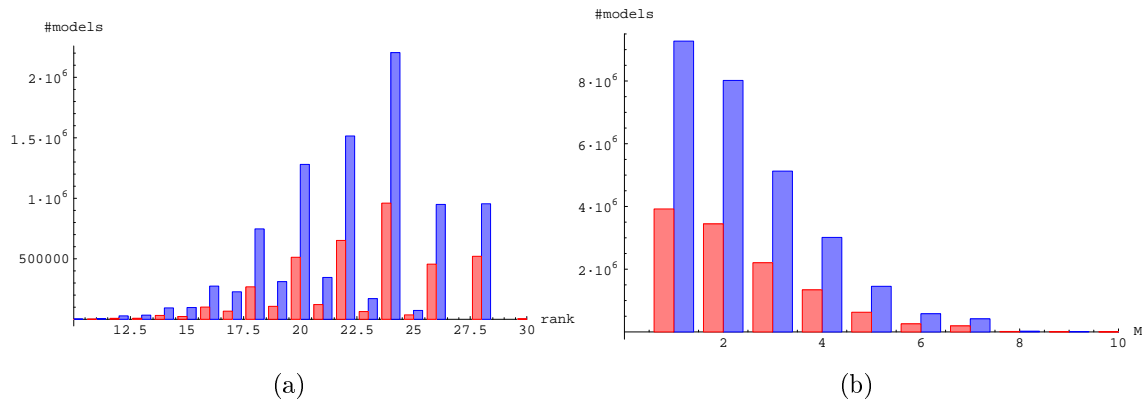


Figure 3.10: Frequency distributions of (a) total rank and (b) single gauge group factors in the hidden sector of MSSM-models (red bars on the left) and MSSM models with massive  $U(1)$  (blue bars on the right).

independent of each other, which means that the statistical analysis of the hidden sector of any model with specific visible gauge group leads to very similar results.

### 3.3.3 Gauge couplings

The gauge sector considered so far belongs to the topological sector of the theory, in the sense that its observables are defined by the wrapping numbers of the branes and independent of the geometric moduli. This does not apply to the gauge couplings, which explicitly do depend on the complex structures, following the derivation in [25], which in our conventions reads

$$\frac{1}{\alpha_a} = \frac{M_{Planck}}{2\sqrt{2}M_s\kappa_a} \frac{1}{c\sqrt{\prod_{i=1}^3 R_1^{(i)} R_2^{(i)}}} \sum_{I=0}^3 X^I U_I, \quad (3.14)$$

where  $\kappa_a = 1$  or  $2$  for an  $U(N)$  or  $Sp(2N)$  stack respectively.

If one wants to perform an honest analysis of the coupling constants, one would have to compute their values at low energies using the renormalization group equations. We are not going to do this, but look instead at the distribution of  $\alpha_s/\alpha_w$  at the string scale. A value of one at the string scale does of course not necessarily mean unification at lower energies, but it could be taken as a hint in this direction.

To calculate the coupling  $\alpha_Y$  we have to include contributions from all branes used for the definition of  $U(1)_Y$ . Therefore we need to distinguish the different possible constructions defined in (3.10). In general we have

$$\frac{1}{\alpha_Y} = \sum_{a=1}^k 2N_a x_a^2 \frac{1}{\alpha_a}, \quad (3.15)$$



which for the three different possibilities reads explicitly

$$\begin{aligned}\frac{1}{\alpha_Y^{(1)}} &= \frac{1}{6} \frac{1}{\alpha_a} + \frac{1}{2} \frac{1}{\alpha_c} + \frac{1}{2} \frac{1}{\alpha_d}, \\ \frac{1}{\alpha_Y^{(2)}} &= \frac{2}{3} \frac{1}{\alpha_a} + \frac{1}{\alpha_b}, \\ \frac{1}{\alpha_Y^{(3)}} &= \frac{2}{3} \frac{1}{\alpha_a} + \frac{1}{\alpha_b} + 2 \frac{1}{\alpha_d}.\end{aligned}\tag{3.16}$$

The result is shown in figure 3.11(a) and it turns out that only 2.75% of all models actually do show gauge unification at the string scale.

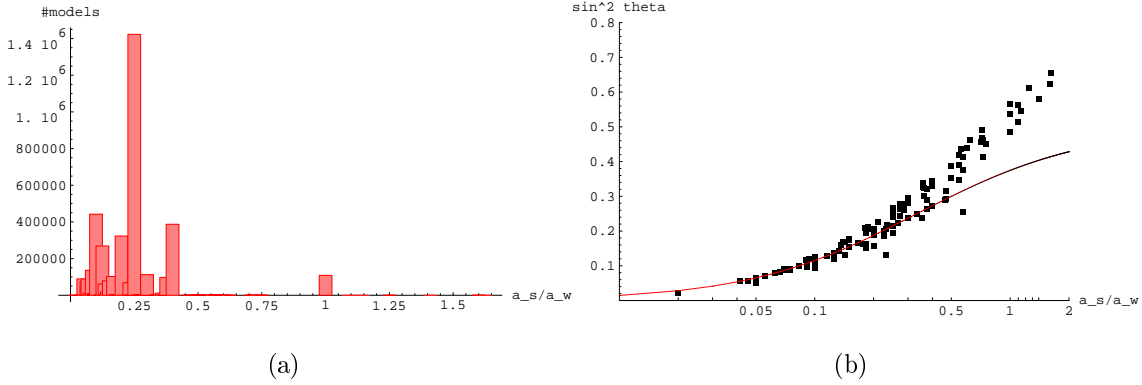


Figure 3.11: (a) Frequency distribution of  $\alpha_s/\alpha_w$  in standard model-like configurations. (b) Values of  $\sin^2\theta$  depending on  $\alpha_s/\alpha_w$ . Each dot represents a class of models with these values.

Furthermore we analyse the distribution of values for the Weinberg angle

$$\sin^2\theta = \frac{\alpha_Y}{\alpha_Y + \alpha_w},\tag{3.17}$$

which depends on the ratio  $\alpha_s/\alpha_w$ . We want to check the following relation between the three couplings, which was proposed in [25] and is supposed to hold for a large class of intersecting brane models

$$\frac{1}{\alpha_Y} = \frac{2}{3} \frac{1}{\alpha_s} + \frac{1}{\alpha_w}.\tag{3.18}$$

From this equation we can derive a relation for the weak mixing angle

$$\sin^2\theta = \frac{3}{2} \frac{1}{\alpha_w/\alpha_s + 3}.\tag{3.19}$$

The result is shown in figure 3.11(b), where we included a red line that represents the relation (3.18). The fact that actually 88% of all models obey this relation is a bit obscured by the plot, because each dot represents a class of models and small values for  $\alpha_s/\alpha_w$  are highly preferred, as can be seen from figure 3.11(a).

### 3.3.4 Comparison with the statistics of Gepner models

In this paragraph we would like to compare our results with the analysis of [70, 71], where a search for standard model-like features in Gepner model constructions [88, 87, 34, 28] has been performed.

To do so, we have to take only a subset of the data analysed in the previous sections, since the authors of [70, 71] restricted their analysis to a special subset of constructions. Due to the complexity of the problem they restricted their analysis to models with a maximum of three branes in the hidden sector and focussed on three-generation models only. Since the number of generations does not modify the frequency distributions and we obtained no explicit results for three generation models, we include models of an arbitrary number of generations in the analysis. To match the first constraint we filter our results and include only those models with a maximum of three hidden branes. But, as we will see, this does also not change the qualitative behaviour of the frequency distributions.

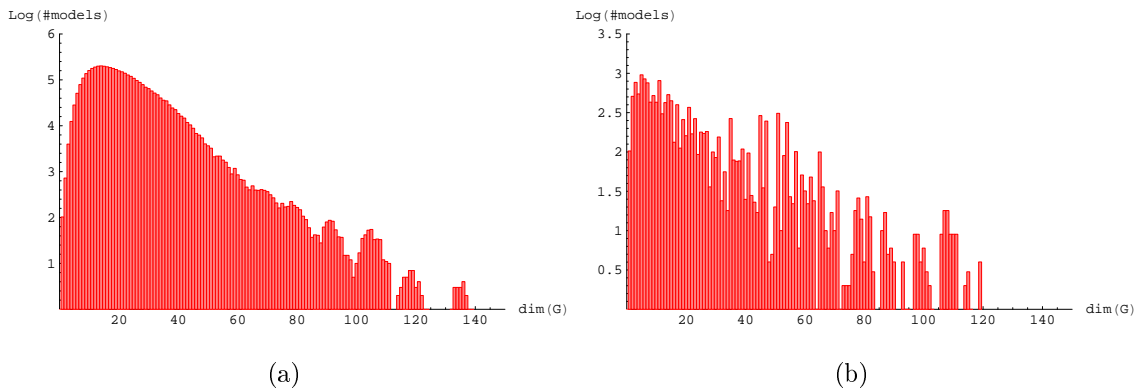


Figure 3.12: Frequency distribution of the dimension of the hidden sector gauge group. Figure (a) is the full set of models, figure (b) shows the subset of solutions with a maximum of three branes in the hidden sector.

In figure 3.12 we show the frequency distribution of the dimension of the hidden sector gauge group before (a) and after (b) the truncation to a maximum of three hidden branes. Obviously the number of models drops significantly, but the qualitative shape of the distribution remains the same. Figure 3.12(b) can be compared directly with figure 5 of [71]. From a qualitative point of view both distributions are very similar, which could have been expected since the Gepner model construction is from a pure topological point of view quite similar to intersecting D-branes. A major difference can be observed in the absolute values of models analysed. In the Gepner case the authors of [71] found a significantly larger amount of candidates for a standard model.

Besides the frequency distribution of gauge groups we can also compare the analysis of the distribution of gauge couplings. In particular, the distribution of values for  $\sin^2 \theta$  depending on the ratio  $\alpha_w/\alpha_s$ , figure 3.11(b), can be compared with figure 6

of [71]. We find, in contrast to the case of hidden sector gauge groups, very different distributions. While almost all of our models are distributed along one curve, in the Gepner case a much larger variety of values is possible. The fraction of models obeying (3.18) was found to be only about 10% in the Gepner model case, which can be identified as a very thin line in figure 6 of [71]. This discrepancy might be traced back to the observation that in contrast to the topological data of gauge groups we are dealing with geometrical aspects here.

As explained in the last paragraph, the gauge couplings do depend explicitly on the geometric moduli. A major difference between the Gepner construction and our intersecting D-brane models lies in the different regimes of internal radius that can be assumed. In our approach we rely on the fact that we are in a perturbative regime, i.e. the compactification radius is much larger than the string length and the string coupling is small.

### 3.4 Pati-Salam models

As in the case of a  $SU(3) \times SU(2) \times U(1)$  gauge group, we can try to construct models with a gauge group of Pati-Salam type

$$SU(4) \times SU(2)_L \times SU(2)_R. \quad (3.20)$$

Analogous to the case of a standard model-like gauge group, we analysed the statistical data for Pati-Salam constructions, realised via the intersection of three stacks of branes. One brane with  $N_a = 4$  and two stacks with  $N_{b/c} = 2$ , such that the chiral matter of the model can be realised as

$$Q_L = (\mathbf{4}, \mathbf{2}, \mathbf{1}), \quad Q_R = (\bar{\mathbf{4}}, \mathbf{1}, \mathbf{2}). \quad (3.21)$$

One possibility to obtain the standard model gauge group in this setup is given by breaking the  $SU(4)$  into  $SU(3) \times U(1)$  and one of the  $SU(2)$  groups into  $U(1) \times U(1)$ . This can be achieved by separating the four branes of stack  $a$  into two stacks consisting of three and one branes, respectively, and the two branes of stack  $b$  or  $c$  into two stacks consisting of one brane each. The separation corresponds to giving a vacuum expectation value to the fields in the adjoint representation of the gauge groups  $U(N_a)$  and  $U(N)_{b/c}$ , respectively.

Models of this type have been constructed explicitly in the literature, see e.g [59, 58, 56, 54, 55, 45]. However, one has to be careful comparing these models with our results, since our constraints are stronger compared to those usually imposed. In particular, we do not allow for symmetric or antisymmetric representations of  $SU(4)$ , a constraint that is not always fulfilled for the models that can be found in the references above.

A restriction on the possible models, similar to the standard model case, is provided by the constraint that there should be no additional antisymmetric matter and the number of chiral fermions transforming under  $SU(2)_L$  and  $SU(2)_R$  should be equal.

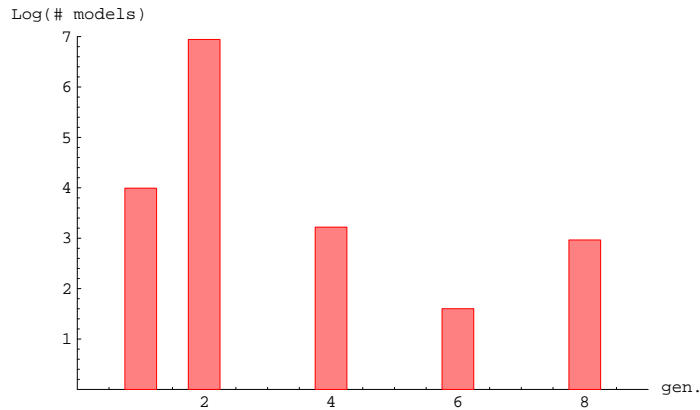


Figure 3.13: Logarithmic plot of the number of Pati-Salam models found, depending on the number of generations. The solutions have been restricted to an equal number of left- and right-handed fermions, i.e.  $gen. = Q_L \stackrel{!}{=} Q_R$

As can be seen in figure 3.13, we found models with up to eight generations, but no three-generation models. The conclusion is the same as in section 3.3 – the suppression of three generation models is extremely large and explicit models show up only at very large values of the complex structure parameters. The distribution differs from the standard model case in the domination of two-generation models. This is an interesting phenomenon, which can be traced back to the specific construction of the models using two  $N = 2$  stacks of branes. This example shows that the number of generations, in contrast to the distribution of gauge groups in the hidden sector (see also section 3.6), does depend on the specific visible sector gauge group we chose.

### 3.5 $SU(5)$ models

From a phenomenological point of view a very interesting class of low-energy models consist of those with a grand unified gauge group<sup>1</sup>, providing a framework for the unification of the strong and electro-weak forces.

The minimal simple Lie group that could be used to achieve this is  $SU(5)$  [86] or also the so-called flipped  $SU(5)$  [13, 65], consisting of the gauge group  $SU(5) \times U(1)_X$ . They represent the two possibilities how to embed an  $SU(5)$  gauge group into  $SO(10)$ . The flipped construction is more interesting phenomenologically, because models based on this gauge group might survive the experimental limits on proton decay. Several explicit constructions of supersymmetric  $SU(5)$  models in the context of intersecting D-brane models are present in the literature [57, 9, 43, 42, 46, 44], as well as some non-supersymmetric ones [24, 80].

In the remainder of this section we present some results on the distribution of the

<sup>1</sup>For an introduction see e.g. [149] or the corresponding chapters in [47, 79].

gauge group properties of  $SU(5)$  and flipped  $SU(5)$  models, using the same  $T^6/\mathbb{Z}_2 \times \mathbb{Z}_2$  orientifold setting as in the previous sections. This part is based on [93].

### 3.5.1 Construction

In the original  $SU(5)$  construction, the standard model particles are embedded in a  $\bar{\mathbf{5}}$  and a  $\mathbf{10}$  representation of the unified gauge group as follows

$$\begin{aligned} SU(5) &\rightarrow SU(3) \times SU(2) \times U(1)_Y, \\ \bar{\mathbf{5}} &\rightarrow (\bar{\mathbf{3}}, \mathbf{1})_{2/3} + (\mathbf{1}, \mathbf{2})_{-1}, \\ \mathbf{10} &\rightarrow (\bar{\mathbf{3}}, \mathbf{1})_{-4/3} + (\mathbf{3}, \mathbf{2})_{1/3} + (\mathbf{1}, \mathbf{1})_2, \end{aligned} \quad (3.22)$$

where the hypercharge is generated by the  $SU(3) \times SU(2)$ -invariant generator

$$Z = \text{diag}(-1/3, -1/3, -1/3, 1/2, 1/2). \quad (3.23)$$

In the flipped  $SU(5)$  construction, the embedding is given by

$$\begin{aligned} SU(5) \times U(1)_X &\rightarrow SU(3) \times SU(2) \times U(1)_Y, \\ \bar{\mathbf{5}}_{-3} &\rightarrow (\bar{\mathbf{3}}, \mathbf{1})_{-4/3} + (\mathbf{1}, \mathbf{2})_{-1}, \\ \mathbf{10}_1 &\rightarrow (\bar{\mathbf{3}}, \mathbf{1})_{2/3} + (\mathbf{3}, \mathbf{2})_{1/3} + (\mathbf{1}, \mathbf{1})_0, \\ \mathbf{1}_5 &\rightarrow (\mathbf{1}, \mathbf{1})_2, \end{aligned} \quad (3.24)$$

including a right-handed neutrino  $(\mathbf{1}, \mathbf{1})_0$ . The hypercharge is in this case given by the combination  $Y = -\frac{2}{5}Z + \frac{2}{5}X$ .

We would like to realise models of both type within our orientifold setup. The  $SU(5)$  case is simpler, since in principle it requires only two branes, a  $U(5)$  brane  $a$  and a  $U(1)$  brane  $b$ , which intersect such that we get the  $\bar{\mathbf{5}}$  representation at the intersection. The  $\mathbf{10}$  is realised as the antisymmetric representation of the  $U(5)$  brane. To get reasonable models, we have to require that the number of antisymmetric representations is equal to the number of  $\bar{\mathbf{5}}$  representations,

$$I_{ab} = -\#\mathbf{Anti}_a. \quad (3.25)$$

In a pure  $SU(5)$  model one should also include a restriction to configurations with  $\#\mathbf{Sym}_a = 0$  to exclude  $\mathbf{15}$  representations from the beginning. Since it has been proven in [57] that in this case no three generation models can be constructed and symmetric representations might also be interesting from a phenomenological point of view, we include these in our discussion<sup>2</sup>.

The flipped  $SU(5)$  case is a bit more involved since in addition to the constraints of the  $SU(5)$  case one has to make sure that the  $U(1)_X$  stays massless and the  $\bar{\mathbf{5}}$  and  $\mathbf{10}$

---

<sup>2</sup>We are grateful to Paul Langacker for discussions about this point.

have the right charges, summarised in (3.24). To achieve this, at least one additional brane  $c$  is needed. Generically, the  $U(1)_X$  can be constructed as a combination of all  $U(1)$ s present in the model

$$U(1)_X = \sum_{a=1}^k x_a U(1)_a. \quad (3.26)$$

The simplest way to construct a combination which gives the right charges would be

$$U(1)_X = \frac{1}{2}U(1)_a - \frac{5}{2}U(1)_b + \frac{5}{2}U(1)_c, \quad (3.27)$$

but a deeper analysis shows [152], that this is in almost all cases not enough to ensure that the hypercharge remains massless. The condition for this can be formulated as

$$\sum_{a=1}^k x_a N_a \vec{Y}_a = 0, \quad (3.28)$$

with the coefficients  $x_a$  from (3.27). To fulfill this requirement we need generically one or more additional  $U(1)$  factors.

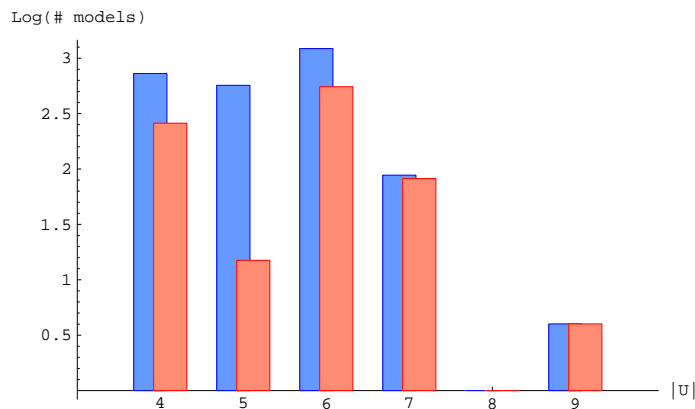


Figure 3.14: Logarithmic plot of the number of solutions with an  $SU(5)$  factor depending on the absolute value of the parameters  $U$ . We give the results with (blue bars to the left) and without (red bars to the right) symmetric representations of  $SU(5)$ .

### 3.5.2 General results

Having specified the additional constraints, we use the techniques described in section 2.2.3 to generate as many solutions to the tadpole, supersymmetry and K-theory conditions as possible. The requirement of a specific set of branes to generate the  $SU(5)$  or flipped  $SU(5)$  simplifies the computation and gives us the possibility to

explore a larger part of the moduli space as compared to the more general analysis we described above.

Before doing an analysis of the gauge sector properties of the models under consideration, we would like to check if the number of solutions decreases exponentially for large values of the  $U_I$ , as we observed in section 3.2.1 for the general solutions. In figure 3.14 the number of solutions with and without symmetric representations are shown. The scaling holds in our present case as well, although the result is a bit obscured by the much smaller statistics. In total we found 2590 solutions without restrictions on the number of generations and the presence of symmetric representations. Excluding these representations reduces the number of solutions to 914. Looking at the flipped  $SU(5)$  models, we found 2600 with and 448 without symmetric representations. Demanding the absence of symmetric representations is obviously a much severer constraint in the flipped case.

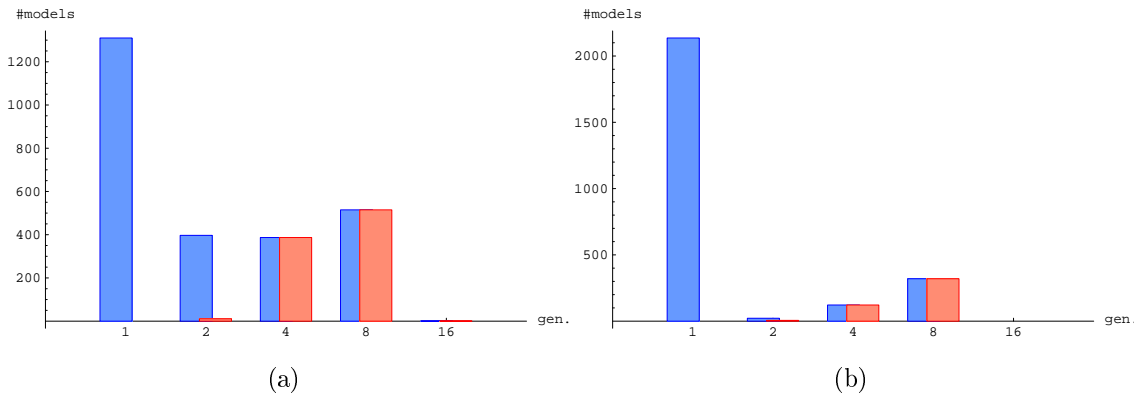


Figure 3.15: Plots of the number of solutions for different numbers of generations for (a)  $SU(5)$  and (b) flipped  $SU(5)$  models with (blue bars to the left) and without (red bars to the right) symmetric representations of  $SU(5)$ .

The correct number of generations turned out to be the strongest constraint on the statistics in our previous work on standard model constructions. The  $SU(5)$  case is not different in this aspect. In figure 3.15 we show the number of solutions for different numbers of generations. We did not find any solutions with three  $\bar{5}$  and  $10$  representations. This situation is very similar to the one we encountered in our previous analysis of models with a standard model gauge group in section 3.3. An analysis of the models which have been explicitly constructed showed that they exist only for very large values of the complex structure parameters. The same is true in the present case. Because the number of models decreases rapidly for higher values of the parameters, we can draw the conclusion that these models are statistically heavily suppressed.

Comparing the standard and the flipped  $SU(5)$  construction the result for models with one generation might be surprising, since there are more one generation models in the flipped than in the standard case. This is due to the fact that there are generically

different possibilities to realise the additional  $U(1)_X$  factor for one geometrical setup, which we counted as distinct models.

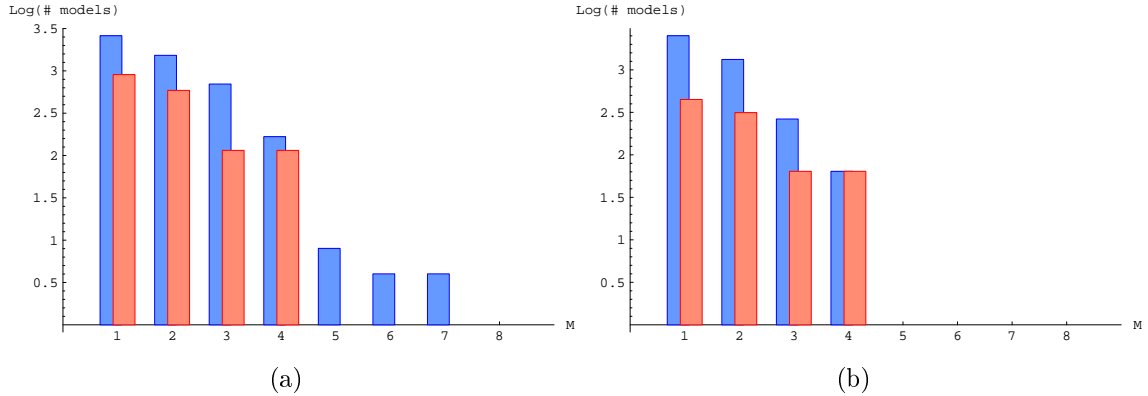


Figure 3.16: Logarithmic plots of the number of solutions with a specific rank  $M$  gauge factor in the hidden sector in (a)  $SU(5)$  and (b) flipped  $SU(5)$  models with (blue bars to the left) and without (red bars to the right) symmetric representations of  $SU(5)$ .

Regarding the hidden sector, we found in total only four  $SU(5)$  models which did not have a hidden sector at all - one with 4, two with 8 and one with 16 generations. For the flipped  $SU(5)$  case such a model cannot exist, because it is not possible to solve the condition for a massless  $U(1)_X$  without hidden sector gauge fields.

The frequency distribution of properties of the hidden sector gauge group, the probability to find a gauge group of specific rank  $M$  and the distribution of the total rank, are shown in figures 3.16 and 3.17. The distribution for individual gauge factors is qualitatively very similar to the one obtained for all possible solutions above (see figures 3.5). One remarkable difference between standard and flipped  $SU(5)$  models is the lower probability for higher rank gauge groups. This is due to the above mentioned necessity to have a sufficient number of hidden branes for the construction of a massless  $U(1)_X$ .

The total rank distribution for both, the standard and the flipped version, differs in one aspect from the one obtained in 3.2.1, namely in the large fraction of hidden sector groups with a total rank of 10 or 9, respectively. This can be explained by just one specific construction which is possible for various values of the complex structure parameters. In this setup the hidden sector branes are all except one on top the orientifold planes on all three tori. If we exclude this specific feature of the  $SU(5)$  construction, the remaining distribution shows the behaviour estimated from the prior results.

Note that while comparing the distributions one has to take into account that the total rank of the hidden sector gauge group in the  $SU(5)$  case is lowered by the contribution from the visible sector branes to the tadpole cancellation conditions. In the flipped case, the additional  $U(1)$ -brane contributes as well.



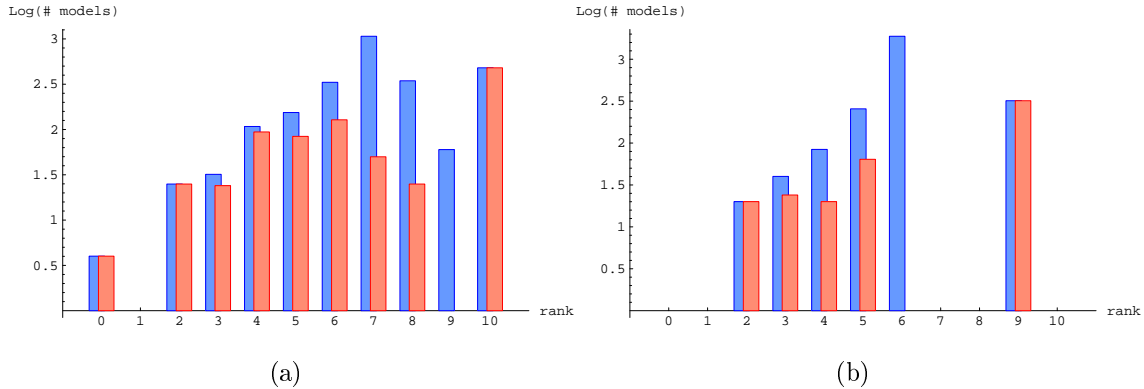


Figure 3.17: Plots of the number of solutions for given values of the total rank of the hidden sector gauge group in (a)  $SU(5)$  and (b) flipped  $SU(5)$  models with (blue bars to the left) and without (red bars to the right) symmetric representations of  $SU(5)$ .

### 3.5.3 Restriction to three branes in the hidden sector

In order to compare our results for the statistics of constructions with a standard model-like gauge group with Gepner models in section 3.3.4, we truncated the full set of models to those with only three stacks of branes in the hidden sector. In the following we also perform a restriction to a maximum of three branes in the hidden sector in the  $SU(5)$  case, but with a different motivation and in a different way. We do not truncate our original results, but instead impose the constraint to a maximum of three branes from the very beginning in the computational process. It turns out that such a restriction can greatly improve the performance of the partition algorithm and allows us therefore to analyse a much bigger range of complex structures. This is highly desirable, since it opens up the possibility to check some claims about the growths of solutions that we made in section 2.3. The method has also some drawbacks. Since we do not compute the full distribution of models, but with an artificial cutoff, we can not be sure that the frequency distributions of properties in the gauge sector are the same as in the full set of models. As we will see in the following, there are indeed some deviations.

In figure 3.18 we plotted the total number of models with a maximum of three stacks of branes in the hidden sector. As in our analysis above we show the models without symmetric representations separately. This plot should be compared with figure 3.14, the number of solutions for  $SU(5)$  models without restrictions. In the restricted case we were able to compute up to much higher values of the complex structures and confirm the assertion of 2.3, that the number of solution drops exponentially with  $|U|$ . This provides another hint that the total number of solutions is indeed finite. In total we found 3275 solutions, which is more then in the case without restrictions, but in contrast to a range of complex structures which is 25 times bigger, the amount of additional solutions is comparably small.

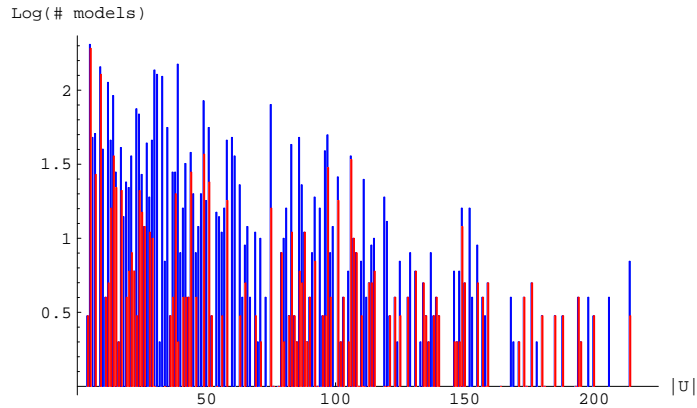


Figure 3.18: Logarithmic plot of the number of solutions with an  $SU(5)$  factor depending on the absolute value of the parameters  $U$ . The number of brane stacks in the hidden sector is restricted to three and the results are shown for models with (blue spikes) and without (red spikes) symmetric representations of  $SU(5)$ .

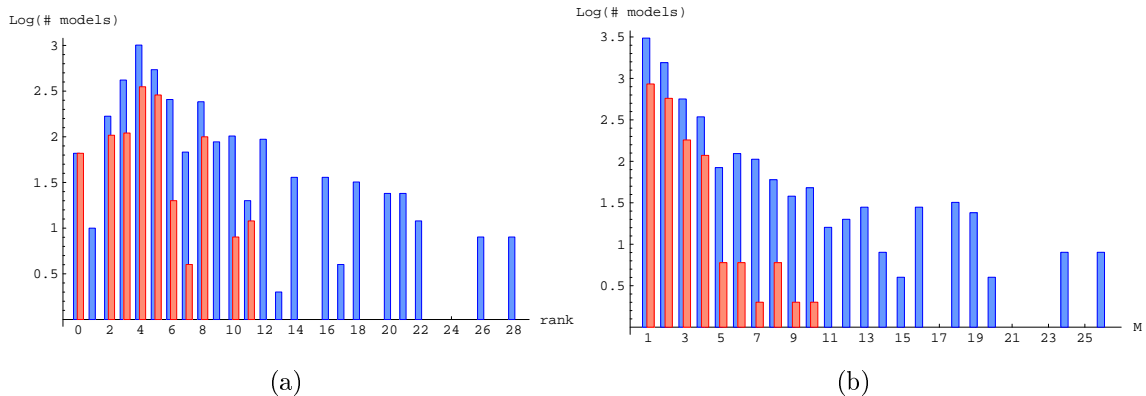


Figure 3.19: Logarithmic plots of the frequency distributions in the hidden sector of  $SU(5)$  models with a maximum of three hidden branes. (a) Specific rank  $M$  gauge factors, (b) Total rank of the hidden sector gauge group.

Comparing the distributions for individual gauge factors (figure 3.19(a)) and the total rank in the hidden sector (figure 3.19(b)), we see some interesting differences to figures 3.16(a) and 3.17(a). The distribution of individual gauge factors is just extended to higher factors in the restricted case. This was to be expected, since larger values for the complex structure parameters allow for larger gauge factors to occur, since they provide us with very long branes with negative wrapping numbers  $X$  that can compensate these large numbers in the tadpole cancellation conditions. The general shape of the distribution remains unchanged. In the case of the total rank the situation is different. The distribution also shows larger values for the total rank, which is directly correlated to the larger individual ranks of the factors, but moreover the

maximum of the distribution is shifted from around seven in the unrestricted case to about four. This can be explained by the fact that the restriction to a maximum of three branes in the hidden sector also restricts the possible contributions from models with many gauge factors of small rank, especially the contribution of  $U(1)$  gauge factors.

What about models with a flipped  $SU(5)$  gauge group? Repeating the analysis for these models in the case of a restriction in the hidden sector can of course be done, but the results might not be very predictive. For a consistent flipped  $SU(5)$  model, we need a massless  $U(1)_X$ , which also depends on a combination of  $U(1)$  factors from the hidden sector. After choosing an additional  $U(1)$  brane for the visible sector of flipped  $SU(5)$  there remain only two hidden sector branes. This restriction is too drastic to give meaningful results, since it turned out in the analysis of flipped  $SU(5)$  models that we need more than two hidden sector branes to solve the equations for the  $U(1)_X$  to be massless.

### 3.5.4 Comments

The analysis in this section showed that three generation models with a minimal grand unified gauge group are heavily suppressed in this specific orientifold setup. This result was expected, since we know that the explicit construction of three generation  $SU(5)$  models using the  $\mathbb{Z}_2 \times \mathbb{Z}_2$  orbifold has turned out to be difficult.

The analysis of the hidden sector showed that the frequency distributions of the total rank of the gauge group and of single gauge group factors are quite similar to the results for generic models in section 3.2.1. Differences in the qualitative picture result from specific effects in the  $SU(5)$  construction.

Comparing the results for the standard and flipped  $SU(5)$  models, we find no significant differences. If we allow for symmetric representations, there is basically no additional suppression factor. If we restrict ourselves to models without these representations, flipped constructions are three times less likely than the standard ones.

## 3.6 Correlations

An interesting question that we raised in the introduction concerns the correlation of observables. If different properties of our models were correlated, independently of the specific visible gauge group, this would provide us with some information about the generic behaviour of this class of models. In the following discussion we would like to clarify this point, emphasizing a crucial difference between correlations of phenomenologically interesting observables in the gauge sector of our models on the one hand, and correlations between basic properties used as constraints to characterize a specific visible sector on the other hand. Finally we use the observations on the second class of correlations to estimate the number of models with a standard model gauge group and three generations of quarks and leptons for the  $T^6/\mathbb{Z}_2 \times \mathbb{Z}_2$  orientifold.

### 3.6.1 Rank and chirality

To give an example of correlations between gauge group observables let us consider the mean chirality  $\chi$ , defined by (3.7), and the total rank of the gauge group. As we already saw using the saddle point approximation on  $T^4$  in section 3.1.3, these two quantities should be correlated. To confirm this in the four-dimensional case, we use our explicit results and compute the frequency distributions for the different visible sectors considered above, standard model-like constructions with and without a massless hypercharge and Pati-Salam models. The result is shown in figure 3.20. Please note that we have normalised the distributions in order to make the results better comparable.

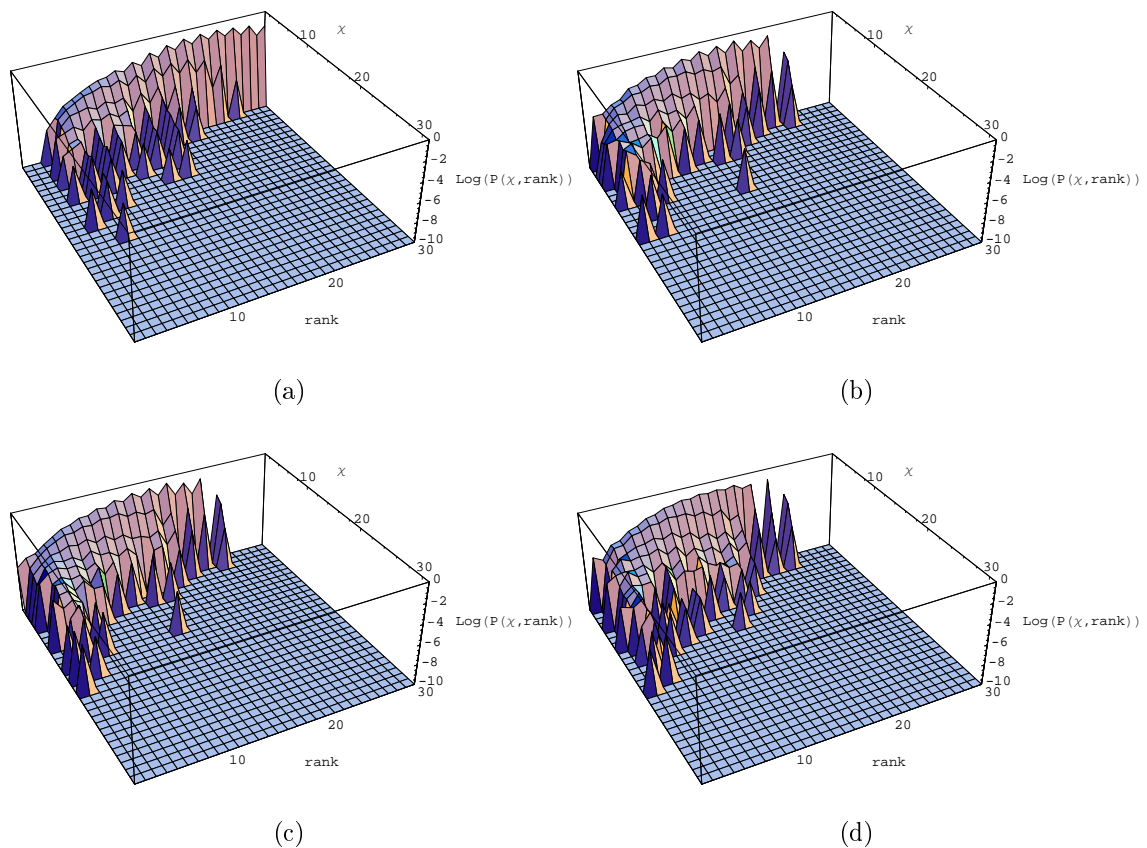


Figure 3.20: Logarithmic plots of the relative frequency distributions of models with specific total rank of the gauge group and mean chirality. Plot (a) shows the analysis for the full gauge group of all models, figures (b), (c) and (d) give the results for the hidden sector gauge groups of standard model-like constructions with and without a massive hypercharge and Pati-Salam models, respectively.

We find two striking results here, which illustrate the two points we made in the introduction to this section. Firstly the two observables are clearly correlated, a large value for the mean chirality is much more likely to find if the total rank is small.

Secondly the results for the full set of models, figure 3.20(a), and the different visible sectors, figures 3.20(b), (c) and (d), show qualitatively very similar results. This last observation is intriguing, since we might use this to conjecture that the specific properties used to define an individual visible sector do not influence the distributions. Put differently, we might speculate that these properties could be regarded independent of each other. If this would be indeed the case, it could simplify some specific analysis dramatically. Instead of constructing solutions for one specific setup with some set of properties it would be enough to know the probabilities for each property. Since they would be independent of each other we could just multiply the results and get an answer to our more difficult question.

### 3.6.2 Estimates

We would like to test this conjecture using the properties of a standard model construction. These include several constraints on the models, in particular the existence of specific  $U(N)$  gauge factors, the vanishing of antisymmetric representations, a massless hypercharge and three generations of chiral matter. How can we check whether two of these properties  $A$  and  $B$ , are independent? A good measure for this would be to calculate the correlation between the probabilities  $P(A)$  and  $P(B)$  to find these properties. This can be expressed as

$$P_{AB} = \frac{P(A)P(B) - P(A \wedge B)}{P(A)P(B) + P(A \wedge B)}, \quad (3.29)$$

where  $P(A \wedge B)$  is the probability to find both properties realised at the same time.

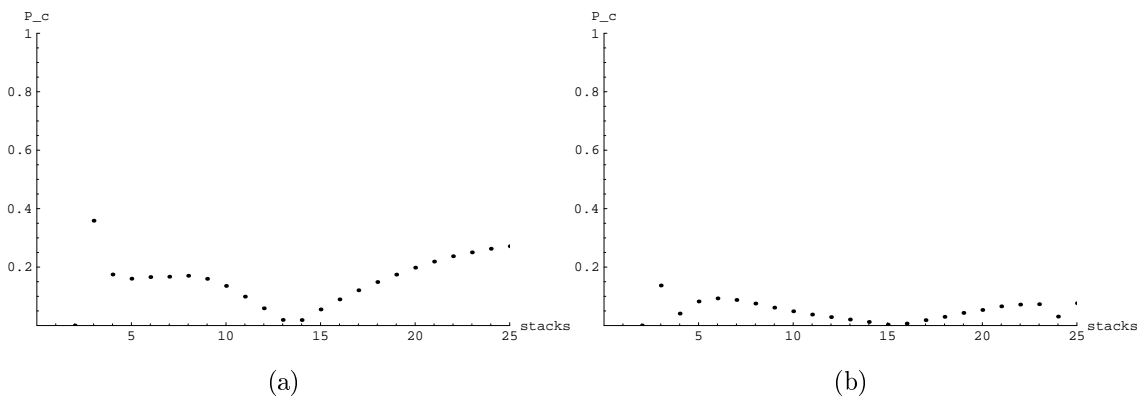


Figure 3.21: Correlations between properties of standard model-like configurations. (a) Correlation between the existence of an  $SU(3)$  and an  $SU(2)$  or  $Sp(2)$  gauge group. (b) Correlation between the existence of an  $SU(3)$  gauge group and the absence of symmetric representations.

For concreteness let us take the following properties as examples: The existence of a  $U(3)$  gauge group, existence of a  $U(2)$  or  $Sp(2)$  gauge group and the vanishing of

antisymmetric representations. In figure 3.21 we plotted the value of  $P_{AB}$  in the set of all models for different values of the number of stacks. As can be derived from these plots the two properties are not really independent, but values of about 0.1 and 0.2, respectively, which are also the order of magnitude for other possible correlations, suggest that one could give it a try and treat these properties as independent in an estimate<sup>3</sup>.

Restriction	Factor
gauge factor $U(3)$	0.0816
gauge factor $U(2)/Sp(2)$	0.992
No symmetric representations	0.839
Massless $U(1)_Y$	0.423
Three generations of quarks	$2.92 \times 10^{-5}$
Three generations of leptons	$1.62 \times 10^{-3}$
<i>Total</i>	$1.3 \times 10^{-9}$

Table 3.4: Suppression factors for various constraints of standard model properties.

In table 3.4 we summarised the properties of a three-generation standard model, including the suppression factor calculated using the probability to find this property in the set of all models and their total number,  $1.66 \times 10^8$ . The two  $U(1)$  gauge groups required for a standard model setup are not included in this, since the probability to find a  $U(1)$  in one of the constructions is essentially one. Multiplying all these factors, we get a probability of  $\approx 1.3 \times 10^{-9}$ , i.e. one in a billion, to find a three-generation standard model in the  $T^6/\mathbb{Z}_2 \times \mathbb{Z}_2$  setup.

# generations	# of models found	estimated #	suppression factor
2	162921	188908	$\approx 10^{-3}$
3	0	0.2	$\approx 10^{-9}$
4	3898	3310	$\approx 2 \times 10^{-5}$

Table 3.5: Comparison between the estimated number of solutions and the actual number of solutions found for models with two, three and four generations.

---

<sup>3</sup>Note that the independence of different properties have been an assumption that was used in the original work on vacuum statistics [75].

**How reliable is this estimate?**

This is of course an important question, since we concluded from the analysis above that the basic properties are only approximately independent and we can not really make a quantitative statement about the possible error in our estimate. So let us compare the result we obtain with this method for models with standard model gauge group and two or four generations of quarks and leptons with the actual numerical results we have obtained in these cases.

The result is shown in table 3.5. As can be read of this table, the estimate for the two- and four-generation case deviates by around 20% from the correct value. Keeping this in mind and further noting that we are making an estimate only at an order-of-magnitude level, a suppression factor of  $\approx 10^{-9}$  seems to be a reliable value.





## Part II

# Generalised geometry



# Chapter 4

## Concepts

In this chapter we give an introduction to generalised complex geometry. We set up the notation and concepts used in the next chapter for applications relevant to string theory. For more background information the reader might also want to consider the theses [103, 161] or the recent lectures [168] for a pedagogical introduction.

The main idea of generalised geometry is to unify complex and symplectic geometry by considering the action of the corresponding structures not on the tangent bundle of the  $n$ -dimensional manifold  $M$ , but on the sum of the tangent and the cotangent bundle. The basic properties of this space  $T \oplus T^*$  are introduced in section 4.1. An important aspect of generalised geometry is the natural identification of forms and spinors, which we describe, together with a general introduction to spinors on  $T \oplus T^*$  in section 4.2.

An important question in the context of differential geometry is about integrability. How this notion can be formulated in the context of generalised geometry is the subject of section 4.3.

In the last three sections, we introduce additional structure. First of all generalised complex structures in 4.4, which we show to contain complex and symplectic structures as special cases. In section 4.5 we deal with generalised metrics, which we combine with generalised complex structures into the notion of generalised Kähler structures and introduce the concept of generalised  $G$ -structures.

### 4.1 The space $\mathbf{T} \oplus \mathbf{T}^*$

Let us establish some facts about the space  $T \oplus T^*$  of dimension  $2n$  with elements

$$(X + \xi) \in T \oplus T^*, \quad (4.1)$$

where  $\xi \in T^*$  is an  $n$ -form. This space has a natural inner product of signature  $(n, n)$ , defined through the inner product of vectors and forms by

$$\langle X + \xi, Y + \eta \rangle = \frac{1}{2}(\xi(Y) + \eta(X)). \quad (4.2)$$

The symmetry group that preserves this inner product is the non-compact group  $O(n, n)$ . We can define a canonical orientation on this space, using the decomposition of the highest exterior power

$$\Lambda^{2n}(T \oplus T^*) = \Lambda^n T \otimes \Lambda^n T^*, \quad (4.3)$$

and the natural pairing between elements of  $v \in \Lambda^n T$  and  $\omega \in \Lambda^n T^*$  given by  $(\omega, v) = \det(\omega(v))$ . This gives us the identification  $\Lambda^{2n} \cong \mathbb{R}$  and by choosing  $\pm 1 \in \mathbb{R}$  we can fix an orientation. This reduces the symmetry group further to  $SO(T \oplus T^*) = SO(n, n)$ .

A generic element  $A$  of the Lie algebra  $\mathfrak{so}(T \oplus T^*) = \mathfrak{so}(n, n)$  can be written in a  $T \oplus T^*$ -basis as

$$A = \begin{pmatrix} \alpha & \beta \\ b & -\alpha^* \end{pmatrix}, \quad (4.4)$$

where  $\alpha$  is an element of  $\text{End}(T)$ ,  $b : T \rightarrow T^*$  and  $\beta : T^* \rightarrow T$ .  $b$  and  $\beta$  are skew-symmetric, which means that we can take  $b \in \Lambda^2 T^*$  and  $\beta \in \Lambda^2 T$ . In the end we get a decomposition

$$\mathfrak{so}(T \oplus T^*) \cong \text{End}(V) \oplus \Lambda^2 T^* \oplus \Lambda^2 T. \quad (4.5)$$

The two-form  $b$  can be identified with the well-known NS-NS b-field in string theory compactifications. We do not deal with  $\beta$  transformations in this thesis, but let us mention that they have been connected in [120] to Poisson structures, responsible for the notion of non-commutativity, and used in [48] to define isotropic A-branes, in analogy to the coisotropic A-branes of [123].

## 4.2 Spinors and forms

To define spinors on  $T \oplus T^*$ , we note first that we have  $GL(n) \leq SO(n, n)$ . This inclusion can be lifted to  $Spin(n, n)$ , which leads to the conclusion that an  $SO(n, n)$  structure is always spinnable.

To construct the associated spin representation  $S$ , we consider the following action of an element  $(X + \xi)$  of  $T \oplus T^*$  on forms  $\rho \in \wedge^\bullet T$ , defined as

$$(X + \xi) \bullet \rho = -X \lrcorner \rho + \xi \wedge \rho. \quad (4.6)$$

For unit vectors this action squares to minus the identity and extends therefore to an algebra isomorphism

$$\text{Cliff}(T \oplus T^*) \cong \text{End}(\wedge^\bullet T^*). \quad (4.7)$$

Under the action of  $Spin(n, n)$  we obtain an invariant decomposition into chiral spinors represented by

$$S^\pm = \Lambda^{ev, od} T^*, \quad (4.8)$$

In practice, we work with orientable manifolds and associate the spin representation with the principal  $GL_+(n)$  bundle via the canonic lift of  $GL_+(n)$  to  $Spin_+(n, n)$ ,

where the notation  $G_+$  always refers to the identity component of a Lie group  $G$ . In particular, we obtain a canonic spin structure. Restricted to  $GL_+(n)$ , we have

$$S^\pm = \Lambda^{ev,od} T^* \otimes (\Lambda^n T)^{1/2}. \quad (4.9)$$

We can define a bilinear form

$$\langle \cdot, \cdot \rangle : S \otimes S \rightarrow \det T^*, \quad (4.10)$$

which acts on elements  $\rho, \tau$  as

$$\langle \rho, \tau \rangle = [\rho \wedge \widehat{\tau}]^n \in \Lambda^n T^* \otimes ((\Lambda^n T)^{1/2})^2 = \mathbb{R}. \quad (4.11)$$

In this definition  $[\cdot]^n$  indicates a projection on the top degree component and  $\widehat{\beta}$  denotes the anti-automorphism defined on  $p$ -forms by

$$\widehat{\rho}^p = (-1)^{p(p+1)/2} \rho^p, \quad (4.12)$$

followed by complex conjugation if the form is complex.

Using this we obtain

$$\langle (X + \xi) \bullet \rho, \tau \rangle = (-1)^n \langle \rho, (X + \xi) \bullet \tau \rangle \quad (4.13)$$

and, in particular, this form is  $Spin_+(n, n)$ -invariant. It is symmetric for  $n \equiv 0, 3 \pmod{4}$  and skew for  $n \equiv 1, 2 \pmod{4}$ , i.e.

$$\langle \rho, \tau \rangle = (-1)^{n(n+1)/2} \langle \tau, \rho \rangle. \quad (4.14)$$

Moreover,  $S^+$  and  $S^-$  are non-degenerate and orthogonal if  $n$  is even and totally isotropic if  $n$  is odd. Because of orientability, we can always choose an isomorphism between spinors and exterior forms induced by a nowhere vanishing volume form. Since this is unique up to a scale, any property of  $S^\pm$  makes also sense for forms.

To put it simply, we can summarise this by saying *forms are spinors*.

### 4.2.1 The action of 2-forms on spinors

The action of a two-form  $b \in \Lambda^2(T \oplus T^*)$  can be naturally lifted to an action on any  $Spin(n, n)$ -representation space by exponentiation, as we can inject  $b = \sum b_{kl} x^k \wedge x^l$  into  $\mathfrak{spin}(n, n) = \Lambda^2(T \oplus T^*) \subset Cliff(T \oplus T^*)$  via  $b \mapsto \sum_{kl} b_{kl} x^k \bullet x^l$ . On spinors, this action is induced by wedging with the exponential

$$e^b \bullet \rho = (1 + b + \frac{1}{2} b \wedge b + \dots) \wedge \rho = (1 + b + \frac{1}{2} b \bullet b + \dots) \wedge \rho = e^b \wedge \rho. \quad (4.15)$$

Note that if  $\pi_0 : Spin(n, n) \rightarrow SO(n, n)$  denotes the usual covering map and  $\pi_{0*}$  its differential, then

$$\pi_0(e^b_{Spin(n, n)}) = e^{\pi_{0*}(b)}_{SO(n, n)} = e^{2b}_{SO(n, n)}. \quad (4.16)$$

As an element of  $\Lambda^2(T \oplus T^*)$ ,  $b$  becomes a skew-symmetric linear operator  $T \rightarrow T^*$  under the identification  $\zeta \wedge \xi(X) = (\zeta, X)\xi - (\xi, X)\zeta = X \lrcorner (\zeta \wedge \xi)/2$  and therefore we have

$$\pi_0(e^b)(X + \xi) = \begin{pmatrix} 1 & 0 \\ b & 1 \end{pmatrix} \cdot \begin{pmatrix} X \\ \xi \end{pmatrix} \quad (4.17)$$

on  $T \oplus T^*$ , where  $b(X) = X \lrcorner b$ .

### 4.2.2 Pure spinors and maximally isotropic subspaces

For a fixed spinor  $\rho$ , we can define the space  $W_\rho$ , consisting of all  $X + \xi \in T \oplus T^*$  which satisfy the property

$$(X + \xi) \bullet \rho = 0. \quad (4.18)$$

The space  $W_\rho$  transforms equivariantly under the action of an element  $g \in Spin(n, n)$  on  $\rho$ ,

$$W_{g\rho} = \rho(g) \bullet W_\rho, \quad \forall g \in Spin(n, n). \quad (4.19)$$

We note that  $W_\rho$  is *isotropic*, since we have

$$\langle X + \xi, Y + \eta \rangle \bullet \rho = \frac{1}{2} ((X + \xi)(Y + \eta) + (Y + \eta)(X + \xi)) \bullet \rho, \quad (4.20)$$

which gives  $\forall (X + \xi), (Y + \eta) \in W_\rho$  that  $\langle X + \xi, Y + \eta \rangle = 0$ . The space  $W_\rho$  is called *maximally isotropic*, iff

$$\dim_{\mathbb{C}}(W_\rho) = \dim_{\mathbb{C}}T = n. \quad (4.21)$$

If equation (4.21) holds, the associated spinor  $\rho$  is called *pure*.

Any maximally isotropic subspace  $W \leq T \oplus T^*$  has a unique representation as

$$W = W_{U,F} = \{X + X \lrcorner F + \eta \mid X \in U, \eta \in N^*U\} = e^{2F}(U \oplus N^*U) \quad (4.22)$$

for some  $p$ -dimensional subspace  $U$  with normal bundle  $N$  and a 2-form  $F \in \Lambda^2 U^*$ . For a given isotropic space  $W$ , define  $U$  to be the image of the projection of  $W$  to  $T$ , so  $w = X + \eta$  with  $X \in U$  for any  $w \in W$ . The projection of  $\eta$  to  $U^*$  is unique and we can define  $F \in \Lambda^2 U^*$  by

$$F(\text{proj}_U(w), y) = y \lrcorner \text{proj}_{U^*}(w). \quad (4.23)$$

This defines indeed a 2-form since  $W$  is isotropic. If  $\alpha^p$  is a  $p$ -form on  $U$ , then  $\star \alpha^p$  is annihilated by  $W_U = U \oplus N^*U$  and because of equivariance, so is  $e^F \wedge \star \alpha^p$  by  $W_{U,F}$ .

An orientation for  $W_{U,F}$  will be the choice of one of the two spinor half-lines spanned by  $\pm e^F \wedge \star \alpha^p$ . If  $U$  is oriented, we have the oriented Riemannian volume form  $\text{vol}_U$  on  $U$  and take  $e^F \wedge \widehat{\star \text{vol}_U}$  as an orientation for  $W$ . Conversely, an orientation for  $W$  in the sense above induces an orientation for  $U$  by requiring  $e^F \wedge \widehat{\star \text{vol}_U}$  to be oriented.

To render the choice of the pure spinor associated with  $W$  unique, we normalise by its norm  $\|\cdot\|_{\hat{g}}$  with respect to  $\mathcal{Q}_{\hat{g}}$  and introduce the notation

$$\rho_{U,F} = \frac{e^F \wedge \widehat{\star vol_U}}{\|\mathcal{Q}_{\hat{g}}(e^F \wedge \widehat{\star vol_U})\|_{\hat{g}}}. \quad (4.24)$$

If we act on  $\rho_{U,F}$  by  $e^b$ , then any leg of  $b$  along  $U^\perp$  does not contribute, so  $b$  acts on  $(U, F)$  by  $(U, F + j^*b)$ .

### 4.3 The Courant bracket and integrability

In the context of differential geometry integrability is defined by the closure of the action of the Lie bracket on smooth sections of the tangent bundle. By replacing the tangent bundle with  $T \oplus T^*$ , we have to use a different notion of integrability, which can be defined in this context using the Courant bracket [51, 52].

The skew-symmetric operation of the Courant bracket on smooth sections of  $T \oplus T^*$  is defined by

$$[X + \xi, Y + \eta] = [X, Y]_L + \mathcal{L}_X \eta - \mathcal{L}_Y \xi - \frac{1}{2}d(\eta(X) - \xi(Y)), \quad (4.25)$$

where  $\mathcal{L}_X = i_X d + di_X$  is the Lie derivative. Acting on vector fields, the Courant bracket reduces to the ordinary Lie bracket  $[\cdot, \cdot]_L$ . This can be expressed using the natural projection  $\pi : T \oplus T^* \rightarrow T$  as

$$\pi([A, B]) = [\pi(A), \pi(B)]_L. \quad (4.26)$$

Besides the invariance under diffeomorphisms, the Courant bracket has another symmetry. It is invariant under the b-field transformation (4.17) iff  $b$  is closed, i.e.  $db = 0$  [109].

Isotropic subbundles, as defined in section 4.2.2, that are closed under the Courant bracket are called *involutive*. The action of  $(X + \xi)$  on a spinor (4.6) maps  $\Lambda^{ev/od}$  to  $\Lambda^{od/ev}$ . Considering this action for the exterior derivative  $d$  gives a correspondence between the notion of involutive isotropic subbundles  $W_\rho$  and smooth sections of the spin bundle. We have that  $W_\rho$  is involutive, iff  $\exists(X + \xi) \in C^\infty(T \oplus T^*)$  such that  $(X + \xi) \bullet \rho = d\rho$ . This setup can be extended by twisting the Courant bracket with a gerbe [110], such that the exterior derivative  $d$  gets replaced by  $d_H = d + H \wedge$ , where  $H \in \Lambda^3 T^*$ .

### 4.4 Generalised complex structures

In analogy to the definition of ordinary complex and symplectic structures, we define a generalised complex structure to be an endomorphism  $\mathcal{J}$  of  $T \oplus T^*$ , satisfying two

conditions,

$$\mathcal{J}^2 = -1 \quad \text{and} \quad \mathcal{J}^* = -\mathcal{J}. \quad (4.27)$$

The demand that a generalised complex structure fulfills both conditions, that of an ordinary complex structure  $J : T \rightarrow T$  with  $J^2 = -1$ , as well as the one for a symplectic structure  $\omega : T \rightarrow T^*$  with  $\omega^* = \omega$ , shows that generalised complex structures comprise both notions in one algebraic structure.

To show this explicitly, we note that a complex structure  $J$  can be embedded in a generalised complex one in the following way

$$\mathcal{J}_J = \begin{pmatrix} -J & 0 \\ 0 & J^* \end{pmatrix}, \quad (4.28)$$

where we use the matrix notation for  $T \oplus T^*$ . Similarly we can embed a symplectic structure  $\omega$  as

$$\mathcal{J}_\omega = \begin{pmatrix} 0 & -\omega^{-1} \\ \omega & 0 \end{pmatrix}. \quad (4.29)$$

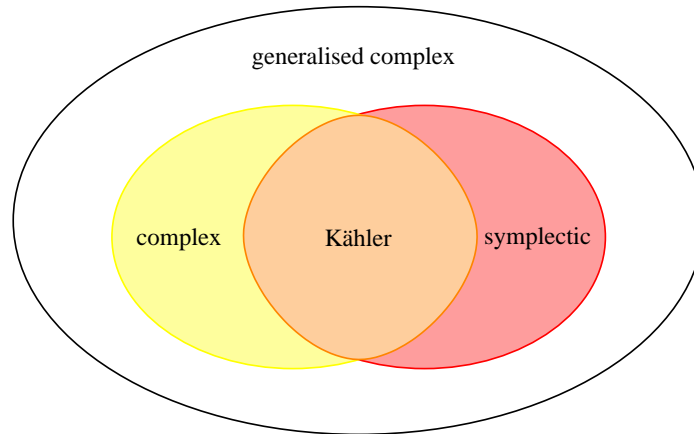


Figure 4.1: Generalised complex spaces include complex and symplectic spaces as special cases.

## 4.5 Generalised metrics

Each additional structure we define on a manifold reduces its structure group. In this section we consider reductions of the principal  $SO(n, n)$ -fibre bundle. The main ingredient to do so is the definition of a generalised metric  $\mathcal{G}$ . We have seen in section 4.1, that  $T \oplus T^*$  carries a natural inner product and metric of signature  $(n, n)$ . If we choose a subgroup  $G$  of  $SO(n, n)$ , which is isomorphic to  $SO(n) \times SO(n)$ , this induces a metric splitting, a decomposition

$$T \oplus T^* = V_+ \oplus V_-. \quad (4.30)$$



The oriented spaces  $V_+$  and  $V_-$  carry a positive or negative definite metric  $g_+$  and  $g_-$ , respectively. Since  $V_{\pm}$  intersect the isotropic spaces  $T$  and  $T^*$  trivially, we can write them as the graph of an isomorphism

$$P_{\pm} : T \rightarrow T^*. \quad (4.31)$$

A dualisation of  $P_{\pm}$  gives an element in  $T^* \otimes T^*$  with a symmetric part  $\pm g$  and an antisymmetric part  $b$ . We can also obtain  $(V_{\pm}, g_{\pm})$  from  $(g, b)$  in a two step procedure. Firstly we define

$$D_{\pm} = \{X \pm g(X) | X \in T\}, \quad (4.32)$$

where we considered  $g$  as a map  $g : T \rightarrow \mathbb{R}$ . In a second step we apply the  $b$ -field transformation, such that we obtain

$$V_{\pm} = e^b D_{\pm}. \quad (4.33)$$

The data  $(g, b)$  defines a reduction from  $SO(n, n)$  to  $(SO(n) \times SO(n))$ . This data can be recast into a *generalised metric*  $\mathcal{G}$ , which acts as an involution on  $V_{\pm}$  with  $\mathcal{G}V_{\pm} = \pm V_{\pm}$ .  $\mathcal{G}$  preserves the natural inner product on  $T \oplus T^*$  and, if  $n$  is even, it also preserves the orientation. Using matrices in  $T \oplus T^*$  we can write

$$\begin{aligned} \mathcal{G} &= e^b \begin{pmatrix} 0 & g^{-1} \\ g & 0 \end{pmatrix} e^{-b} = \begin{pmatrix} 1 & 0 \\ b & 1 \end{pmatrix} \begin{pmatrix} 0 & g^{-1} \\ g & 0 \end{pmatrix} \begin{pmatrix} 1 & 0 \\ -b & 1 \end{pmatrix} \\ &= \begin{pmatrix} -g^{-1}b & g^{-1} \\ g - bg^{-1}b & bg^{-1} \end{pmatrix}. \end{aligned} \quad (4.34)$$

Conversely, every operator that squares to the identity and is compatible with the inner product, in the sense that its eigenspaces are maximal subspaces of  $T \oplus T^*$ , can be decomposed in the same way.

We can also let the generalised metric act on spinors, by lifting it to  $Pin(n, n)$ , which we denote by  $\tilde{\mathcal{G}}$ . Let us consider first the case where  $\mathcal{G}$  is induced by a metric diagonal  $D_{\pm}$  with oriented orthonormal basis  $d_k^{\pm} = e_k \oplus \pm g(e_k)$ . Then  $\mathcal{G}$  is the composition of reflections  $R_{d_k^-}$  along  $d_k^-$ , i.e.  $\mathcal{G} = R_{d_1^-} \circ \dots \circ R_{d_n^-}$ . Therefore,  $\tilde{\mathcal{G}}$  acts via Clifford multiplication as the Riemannian volume form  $vol_{D_-} = d_1^- \wedge \dots \wedge d_n^-$  of  $D_-$ . Next let  $J$  denote the isomorphism between  $Cliff(T)$  and  $\Lambda^* T^*$ . Recall that for any  $X \in T$  and  $a \in Cliff(T)$ , we have that  $J(X \cdot a) = -X \lrcorner J(a) + X \wedge J(a)$ ,  $J(a \cdot X) = (-1)^{\deg(a)} (X \lrcorner J(a) + X \wedge J(a))$  and  $\star J(a) = J(\hat{a} \cdot vol_g)$ , where  $vol_g$  denotes the Riemannian volume form on  $T$ . As a result we obtain for  $\rho \in \Lambda^p \subset S$  that

$$vol_{D_-} \bullet \rho^p = (-1)^{n(n+1)/2+pn} J(J^{-1}(\rho^p) \cdot vol_g) = (-1)^{n(p+1)} \star \hat{\rho}^p. \quad (4.35)$$

For a non-trivial  $b$ -field,  $\mathcal{G}$  gets conjugated by  $\exp(2b)$  and thus  $\tilde{\mathcal{G}}$  by  $\exp(b)$ , which leads to  $vol_{V_-} \bullet \rho^p = e^b \bullet vol_{D_-} \bullet e^{-b} \bullet \rho^p$ , where we used that the lift  $\tilde{g}$  of  $\mathcal{G}$  to  $Pin(n, n)$

acts on  $S^\pm = \Lambda^{ev,od}$  via

$$\tilde{g} \bullet \rho^{ev} = (-1)^n e^b \wedge \star(e^{-b} \wedge \rho^{ev})^\wedge \quad (4.36)$$

$$\tilde{g} \bullet \rho^{od} = e^b \wedge \star(e^{-b} \wedge \rho^{od})^\wedge. \quad (4.37)$$

Up to an exchange of sign, we note that  $\tilde{g}$  coincides with the  $\square$ -operator in [160]. Furthermore we see that  $\tilde{g}^2 = (-1)^{n(n-1)/2}$ , since  $\widehat{\star\rho^p} = (-1)^{p(n-p)+n(n+1)/2} \star \widehat{\rho^p}$  and in particular,  $\tilde{\mathcal{G}}$  defines a complex structure on  $S$  if  $n \equiv 2, 3 \pmod{4}$ . Moreover we find that

$$\langle \tilde{g} \bullet \rho, \tau \rangle = (-1)^{n(n+1)/2} \langle \rho, \tilde{g} \bullet \tau \rangle \quad (4.38)$$

and obtain the inner product

$$\mathcal{Q}_{\tilde{g}}(\rho^{ev,od}, \tau^{ev,od}) = \pm(-1)^{n(n-1)/2} \langle \rho, \tilde{\mathcal{G}} \bullet \tau \rangle = g(e^{-b} \wedge \rho, e^{-b} \wedge \tau), \quad (4.39)$$

which is invariant under the cover

$$\begin{aligned} Spin(V_+) \times Spin(V_-) &\rightarrow Spin_+(T \oplus T^*) \\ \text{of } SO(V_+) \times SO(V_-) &\hookrightarrow SO_+(T \oplus T^*). \end{aligned} \quad (4.40)$$

The operator  $\tilde{g}$  acts as an isometry for  $\mathcal{Q}_{\tilde{g}}$ .

The presence of a generalised metric also implies a very useful description of the complexification  $S^\mathbb{C}$  of  $S$  as a  $Spin(V_+) \times Spin(V_-)$ -module if the manifold is spinnable. The orthogonal decomposition of  $T \oplus T^*$  into  $V_+ \oplus V_-$  makes  $Cliff(T \oplus T^*)$  isomorphic with the twisted tensor product  $Cliff(V_+) \hat{\otimes} Cliff(V_-)$ . Furthermore we have that  $(V_\pm, g_\pm)$  is isometric to  $(T, \pm g)$  via the isometries

$$\begin{aligned} \pi_{b+} &= e^{2b} \circ \pi_+, & \pi_+ &: x \in T \mapsto x \oplus g(x) \in D_+, \\ \pi_{b-} &= e^{2b} \circ \pi_-, & \pi_- &: x \in T \mapsto x \oplus -g(x) \in D_-. \end{aligned} \quad (4.41)$$

We obtain an isomorphism by extending

$$\iota_b : x \hat{\otimes} y \in T^\mathbb{C} \hat{\otimes} T^\mathbb{C} \subset Cliff^\mathbb{C}(T, g) \hat{\otimes} Cliff^\mathbb{C}(T, -g) \mapsto \iota_b(x \hat{\otimes} y) = \pi_{b+}(x) \bullet \pi_{b-}(y). \quad (4.42)$$

The complexification  $Cliff^\mathbb{C}(T, \pm g) \cong Cliff(T \otimes \mathbb{C}, g^\mathbb{C})$  is isomorphic to  $\text{End}(\Delta)$  if the dimension  $n$  is odd and to  $\text{End}(\Delta) \oplus \text{End}(\Delta)$  if  $n$  is even. The module  $\Delta$  is the space of spinors and in the latter case it can be decomposed into the irreducible  $Spin(2m)$ -representations  $\Delta_\pm$ . Moreover, it carries a  $Spin(n)$ -invariant hermitian inner product for which Clifford multiplication is skew. By convention, we take the first argument to be conjugate-linear. In all dimensions, there exists a conjugate-linear endomorphism  $\mathcal{A}$  of  $\Delta$  such that

$$\mathcal{A}(x \cdot \Psi) = (-1)^{n(n-1)/2} x \cdot \mathcal{A}(\Psi), \quad (4.43)$$

and in particular, it is  $Spin(n)$ -equivariant. Moreover,  $\mathcal{A}$  reverses the chirality for  $n = 2m$ ,  $m$  odd [158]. We can inject  $\Delta \otimes \Delta$  into  $\Lambda^*$  in an  $Spin(n)$ -equivariant way

by associating with the product of two spinors  $\Psi_L \otimes \Psi_R$ , where  $\Psi_{L/R} \in Spin(n)$ , the form

$$[\Psi_L \otimes \Psi_R](X_1, \dots, X_n) = (\mathcal{A}(\Psi_L), (X_1 \wedge \dots \wedge X_n) \cdot \Psi_R). \quad (4.44)$$

This is an isomorphism for  $n$  even. In the odd case, we obtain an isomorphism by concatenating  $[\cdot, \cdot]$  with projection on the even or odd forms, which we write as  $[\cdot, \cdot]^{ev,od}$ . The  $b$ -field can be accounted for by defining

$$[\cdot, \cdot]_b := e^b \wedge [\cdot, \cdot]. \quad (4.45)$$

Let  $\sim$  be the involution defined by  $\pm id$  on  $\Lambda^{ev,od}$ . Then we have the following relations

$$\begin{aligned} [x \cdot \Psi_L \otimes \Psi_R]_b &= (-1)^{n(n-1)/2} \iota_b(x \hat{\otimes} 1) \bullet [\Psi_L \otimes \Psi_R]_b, \\ [\Psi_L \otimes y \cdot \Psi_R]_b &= \iota_b(1 \hat{\otimes} y) \bullet [\widetilde{\Psi_L \otimes \Psi_R}]_b. \end{aligned} \quad (4.46)$$

This statement can be proven along the lines of [160]. Let us fix an orthonormal basis  $e_1, \dots, e_n$  of  $(T, g)$ . By definition and the usual rules for Clifford algebras, we get

$$\begin{aligned} [e_k \cdot \Psi_L \otimes \Psi_R] &= \sum_I (\mathcal{A}(e_k \cdot \Psi_L), e_I \cdot \Psi_R) e_I \\ &= (-1)^{n(n-1)/2+1} \sum_I (\mathcal{A}(\Psi_L), e_k \cdot e_I \cdot \Psi_R) e_I \\ &= (-1)^{n(n-1)/2+1} \sum_I (\mathcal{A}(\Psi_L), (-e_k \lrcorner e_I + e_k \wedge e_I) \cdot \Psi_R) e_I \\ &= (-1)^{n(n-1)/2} \left( \sum_{k \in I} (\mathcal{A}(\Psi_L), e_k \lrcorner e_I \cdot \Psi_R) e_k \wedge (e_k \lrcorner e_I) - \right. \\ &\quad \left. \sum_{k \notin I} (\mathcal{A}(\Psi_L), e_k \wedge e_I \cdot \Psi_R) e_k \lrcorner (e_k \wedge e_I) \right) \\ &= (-1)^{n(n-1)/2} \pi_+(e_k) \bullet [\Psi_L \otimes \Psi_R]. \end{aligned} \quad (4.47)$$

The proof for the second equation is completely analogous.

### 4.5.1 Generalised Kähler structures

Before considering reductions of structure groups in general in the next section, we would like to give one important example, that we use later for the description of mirror symmetry for topological sigma models.

Let us take a manifold which carries a generalised complex structure  $\mathcal{J}_1$  that commutes with a generalised metric  $\mathcal{G}$ . We can define a second generalised complex structure by

$$\mathcal{J}_2 := \mathcal{G} \mathcal{J}_1. \quad (4.48)$$

One can easily check that this indeed fulfills the conditions for a generalised complex structure. Since  $\mathcal{G}^2 = 1$  and  $\mathcal{J}_1^2 = -1$ , we have  $\mathcal{J}_2^2 = -1$  and  $\mathcal{J}_2^* = \mathcal{J}_1^* \mathcal{G}^* = -\mathcal{J}_2$ .

Conversely, a pair  $(\mathcal{J}_1, \mathcal{J}_2)$  of commuting generalised complex structures defines a generalised metric via

$$\mathcal{G} = -\mathcal{J}_1\mathcal{J}_2. \quad (4.49)$$

By definition a generalised Kähler structure consists of two commuting generalised complex structures and a generalised metric, that fulfill (4.49). The structure group  $SO(n, n)$  is thereby reduced to  $U(n/2) \times U(n/2)$ .

The relation to an ordinary Kähler structure can be shown as follows. An ordinary Kähler structure consists of a metric  $g$ , a Kähler form  $\omega$  and a complex structure  $J$ , satisfying

$$\omega = gJ. \quad (4.50)$$

By embedding  $J$  and  $\omega$  into generalised complex structures, according to (4.28) and (4.29) as

$$\mathcal{J}_1 = \begin{pmatrix} -J & 0 \\ 0 & J^* \end{pmatrix}, \quad \mathcal{J}_2 = \begin{pmatrix} 0 & -\omega^{-1} \\ \omega & 0 \end{pmatrix}, \quad (4.51)$$

we obtain using (4.50),

$$\mathcal{G} = -\mathcal{J}_1\mathcal{J}_2 = \begin{pmatrix} 0 & g^{-1} \\ g & 0 \end{pmatrix}, \quad (4.52)$$

which we recognise from (4.34) as a simple example of a generalised metric.

## 4.5.2 Generalised $G$ -structures

In the last sections we have already discussed a reduction of the structure group of  $T \oplus T^*$ . Let us consider general reductions to a group  $G_L \times G_R$ , where we already implied that a metric splitting is possible, such that we have a generalised metric  $\mathcal{G} \hat{=} (g, b)$ . Furthermore we want to assume that we have two chiral spinors  $\Psi_L$  and  $\Psi_R$ , which reduces the structure group from  $Spin(n)$  to  $G_L$  and  $G_R$ , respectively. We assume that  $G_{L,R}$  acts irreducibly on  $\mathbb{R}^n$  via the induced vector representation.

There are two different possibilities to define a  $G_L \times G_R$  structure, which by definition is a reduction from the  $Spin_+(n, n)$ -fibre bundle to a  $G_L \times G_R$ -fibre bundle. We can choose a reduction to  $G_L \times G_R$  by  $G_L \times G_R$  invariant spinors  $S^\pm$ , or by a generalised metric and two  $T$ -spinors  $\Psi_{L,R}$ .

It is a remarkable fact that we can represent any  $G_L \times G_R$ -invariant spinor as a decomposable bispinor: Assume that we are given a  $G_L \times G_R$ -invariant pair of spinors. This induces a reduction from  $Spin_+(n, n)$  to  $G_L \times G_R$ . Projecting the inclusion  $G_L \times G_R \subset Spin(n) \times Spin(n)$  down to  $SO_+(n, n)$  gives rise to a metric splitting  $V_+ \oplus V_-$  where  $V_{+,-}$  carries in addition a  $G_{L,R}$ -structure. Pulling this structure back to  $T$  via the isometries  $\pi_{b\pm}$  (4.41) gives rise to a  $G_{L,R}$ -structure inside the  $SO(n)$ -fibre bundle associated with the induced metric. Moreover, the inclusions  $G_{L,R} \subset SO(n)$  can be lifted to  $Spin(n)$  so that we obtain a spin structure which admits reductions

to  $G_L$  and  $G_R$ . As a result there are, on top of the generalised metric  $(g, b)$ , the invariant spinors associated with  $G_L$  and  $G_R$ . By invariance, the  $T \oplus T^*$ -spinors  $([\Psi_L \otimes \Psi_R]_b, [\mathcal{A}(\Psi_L) \otimes \Psi_R]_b)$  must coincide with the  $G_L \times G_R$ -invariant pair of spinors (up to a universal scalar). Interestingly, these  $T \oplus T^*$ -spinors are all self-dual for  $\tilde{g}$  in the following sense. A Riemannian volume form acts on chiral spinors by

$$vol_g \cdot \Psi_{\pm} = \pm(-1)^{m(m+1)/2}(-i)^m \Psi_{\pm}, \quad (4.53)$$

for  $\Psi_{\pm} \in \Delta_{\pm}$ ,  $n = 2m$  and by

$$vol_g \cdot \Psi = (-i)^{m+1} \Psi, \quad (4.54)$$

for  $n = 2m + 1$ . Therefore,

$$\tilde{g} \bullet [\Psi_L \otimes \Psi_R]_b = [\Psi_L \otimes vol_g \cdot \Psi_R]_b = (-1)^{m(m+1)/2}(-i)^m [\Psi_L \otimes \Psi_R]_b \quad (4.55)$$

for  $n = 2m$  and

$$\tilde{g} \bullet [\Psi_L \otimes \Psi_R]_b = [\Psi_L \otimes vol_g \cdot \Psi_R] = (-i)^{m+1} [\Psi_L \otimes \Psi_R]_b \quad (4.56)$$

for  $n = 2m + 1$ .

Note that in low dimensions the group  $Spin(n)$  acts transitively on the sphere of its spin representation. As a result, there is only one orbit of the form  $Spin(n)/G$  and therefore any  $G_L \times G_R$ -structure is actually a  $G \times G$ -structure or *generalised  $G$ -structure*, following the language of [115, 160, 161]. For instance, we find generalised  $SU(3)$ - an  $G_2$ -structures in dimension 6 and 7 and generalised  $Spin(7)$ -structures in dimension 8 and 9, the highest dimension for which the spin group acts transitively.



# Chapter 5

## Applications

Having described the basic concepts of generalised geometry in the last chapter, we are now going to give two applications of this concept to string theory. Very soon after its mathematical formulation it has become clear, that generalised geometry can be used to deepen our understanding of the spaces used to compactify string theory to four dimensions beyond the realm of manifolds with  $SU(3)$  structure. This is based on two basic observations. First of all the  $B$ -field, elementary ingredient of the zero mode spectrum in the NS-NS sector of type II string theory, is embedded in a very natural way. Secondly, generalised Kähler structures, introduced in section 4.5.1, have been proven to be equivalent to a bi-hermitian geometry. This geometry is important for the analysis of nonlinear sigma models, since it has been found that it is the most general geometry of a target space manifold for a nonlinear sigma model with  $\mathcal{N} = (2, 2)$  world-sheet supersymmetry.

In the first section we introduce a description of T-duality in the framework of generalised geometry. We formulate the transformation laws as the action of a map  $\mathcal{M}$  in the  $T \oplus T^*$  basis and show how it acts on pure spinors. In section 5.2 we apply this reasoning to generalised Kähler structures. We derive the mirror symmetry transformation of the two generalised complex structures in the  $T \oplus T^*$  picture and give an alternative description in terms of the spinors associated to the four maximal isotropic subbundles.

In section 5.3, we define generalised topological sigma models with target spaces that carry a generalised Kähler structure. We show that the well-known topological A- and B-models can be found as special cases in the generalised theory. Using the results of section 5.1, we explore the action of mirror symmetry on the generalised topological sigma models. We verify explicitly that the generalised complex structures of the A- and B-model get exchanged by this action. Section 5.4 deals with topological D-branes and we verify that the boundary conditions for topological A- and B-branes are interchanged under the action of mirror symmetry.

Section 5.5 deals with an analysis of the calibration conditions for cycles wrapped by D-branes in generalised complex spaces. We make use of the generalised G-structures introduced in the last chapter and analyse the supersymmetry conditions for D-branes

in the generalised framework. This leads us to the notion of generalised calibrations, which are a natural generalisation of the known calibrations for D-branes in type II string theory. In the last part of this section we investigate the action of T-duality on the generalised calibration conditions.

The content of this chapter is based on [49] and [94].

## 5.1 T-duality and mirror symmetry

Following the reasoning of [154], we would like to describe mirror symmetry as a combination of three T-dualities in a  $T^3$ -fibrated manifold. The formulation of T-duality and mirror symmetry along these lines in the framework of generalised complex geometry has been studied in [114, 14, 94]. We apply the results of this section in the following to topological sigma models and generalised calibrations.

Let us start with a generalised metric  $\mathcal{G} \hat{=} (g, b)$  on the vector space  $T \oplus T^*$  and pick a non-trivial one-form  $\theta$ . Let  $X$  be the vertical vector field (i.e. the projection of  $X$  to the kernel of  $\theta$  is trivial) such that  $\theta(X) = 1$ . We can then extend  $(X, \theta)$  to a basis  $x_1, \dots, x_n = X$  of  $T$  with dual basis  $x^1, \dots, x^n = \theta$ . Consequently,  $x \oplus \theta$  is of unit norm and thus  $\widetilde{\mathcal{M}}_\theta = X \oplus \theta$  is an element of  $Pin(n, n)$ . Its projection to  $O(n, n)$  yields the reflection  $\mathcal{M}_\theta$  along the hyperplane orthogonal to  $X \oplus \theta$ . With respect to the coordinates  $(x_i, x^j)$  the matrix of  $\mathcal{M}_\theta$  is given by

$$\mathcal{M}_\theta = \begin{pmatrix} A & B \\ C & D \end{pmatrix} = \begin{pmatrix} \mathbf{id}_{n-1} & \mathbf{0} & & \\ & 0 & & -1 \\ \mathbf{0} & & \mathbf{id}_{n-1} & \\ & -1 & & 0 \end{pmatrix}. \quad (5.1)$$

Conjugation of  $\mathcal{G}$  by  $\mathcal{M}_\theta$  yields another generalised metric  $\mathcal{G}^T$  induced by  $(g^T, b^T)$ . Calculating these quantities in the fixed basis above yields the well-known Buscher rules [35, 36] (see also [108, 118]).

Let us show this in detail. With respect to the basis  $x_i, x^j$ , the data  $(g^T, b^T)$  are given by

$$\begin{aligned} g_{kl}^T &= g_{kl} - \frac{1}{g_{nn}}(g_{kn}g_{nl} + b_{kn}b_{nl}), & g_{kn}^T &= -\frac{1}{g_{nn}}b_{kn}, & g_{nn}^T &= -\frac{1}{g_{nn}} \\ b_{kl}^T &= b_{kl} - \frac{1}{g_{nn}}(g_{kn}b_{nl} + b_{kn}g_{nl}), & b_{kn}^T &= -\frac{1}{g_{nn}}g_{kn}. \end{aligned} \quad (5.2)$$

In particular, we have  $g^T = M^*g$  where

$$M = \begin{pmatrix} id & \frac{1}{q}(u-v) \\ 0 & \frac{1}{q} \end{pmatrix}. \quad (5.3)$$



This can be proven as follows. By definition, we have

$$\mathcal{G}^T = \begin{pmatrix} -g^{-1T}b^T & g^{-1T} \\ g^T - b^T g^{-1T}b^T & b^T g^{-1T} \end{pmatrix} = \mathcal{M}_\theta \begin{pmatrix} -g^{-1}b & g^{-1} \\ g - bg^{-1}b & bg^{-1} \end{pmatrix} \mathcal{M}_\theta \quad (5.4)$$

and therefore

$$g^{-1T} = Ag^{-1}D - Ag^{-1}bB + B(g - bg^{-1}b)B + Bbg^{-1}D. \quad (5.5)$$

With respect to the splitting  $\langle x^1, \dots, x^{n-1} \rangle \oplus \mathbb{R}\theta$ , the tensors  $g$ ,  $g^{-1}$  and  $b$  are schematically given by

$$g = \begin{pmatrix} \underline{g} & v \\ v^{tr} & q \end{pmatrix}, \quad g^{-1} = \begin{pmatrix} \underline{h} & w \\ w^{tr} & p \end{pmatrix}, \quad b = \begin{pmatrix} \underline{b} & u \\ -u^{tr} & 0 \end{pmatrix}. \quad (5.6)$$

We have to show that

$$g^T = \begin{pmatrix} \underline{g} - \frac{1}{q}(vv^{tr} - uu^{tr}) & \frac{1}{q}u \\ \frac{1}{q}u^{tr} & \frac{1}{q} \end{pmatrix}, \quad b^T = \begin{pmatrix} \underline{b} - \frac{1}{q}(uw^{tr} - vu^{tr}) & \frac{1}{q}v \\ -\frac{1}{q}v^{tr} & 0 \end{pmatrix}. \quad (5.7)$$

From (5.5) we gain

$$g^{-1T} = \begin{pmatrix} \underline{h} & -\underline{h}u \\ -u^{tr}\underline{h} & q + u^{tr}\underline{h}u \end{pmatrix} \quad (5.8)$$

which is the inverse of  $g^T$  as given in (5.2). For instance, the upper left hand block is

$$\underline{g}\underline{h} - \frac{1}{q}vv^{tr}\underline{h} + \frac{1}{q}uu^{tr}\underline{h} - \frac{1}{q}uu^{tr}\underline{h} = \underline{id} - vw^{tr} + vw^{tr} = \underline{id}, \quad (5.9)$$

where we used the relations  $\underline{g}\underline{h} + vw^{tr} = \underline{id}$  and  $v^{tr}\underline{h} + qw^{tr} = 0$  coming from  $gg^{-1} = id$ . To derive the matrix expression for  $b^T$  we consider

$$\begin{aligned} b^T g^{-1T} &= -Cg^{-1}bB + Cg^{-1}D + D(g - bg^{-1}b)B + Dbg^{-1}D \\ &= \begin{pmatrix} \underline{b}\underline{h} + uw^{tr} & v - \underline{b}\underline{h}u - uw^{tr}u \\ w^{tr} & -w^{tr}u \end{pmatrix}. \end{aligned} \quad (5.10)$$

Multiplying from the right by  $g^t$  we find precisely  $b^t$ . Again, we prove this for the upper left hand block. It is given by

$$\begin{aligned} &\underline{b}\underline{h}(\underline{g} - \frac{1}{q}vv^{tr} + \frac{1}{q}uu^{tr} - \frac{1}{q}uu^{tr}) + uw^{tr}(\underline{g} - \frac{1}{q}vv^{tr} + \frac{1}{q}uu^{tr} - \frac{1}{q}uu^{tr}) + \frac{1}{q}vu^{tr} \\ &= \underline{b} - \underline{b}wv^{tr} + \underline{b}wv^{tr} - pvv^{tr} - \frac{1}{q}u(1 - qp)v^{tr} + \frac{1}{q}vu^{tr} \\ &= \underline{b} - \frac{1}{q}uw^{tr} + \frac{1}{q}vu^{tr} \\ &= \underline{b} - \frac{1}{q}(uw^{tr} - vu^{tr}), \end{aligned} \quad (5.11)$$

using the relations  $w^{tr}g + pv^{tr} = 0$  and  $\underline{h}v + qw = 0$ , which can be deduced again from  $gg^{-1} = id$ .

### 5.1.1 T-duality action on spinors

Let us consider the action of  $\widetilde{\mathcal{M}}_\theta$  on spinors. The T-dual of a spinor  $\rho$  can be obtained from

$$\rho^T = \widetilde{\mathcal{M}}_\theta \bullet \rho. \quad (5.12)$$

Note that  $\widetilde{\mathcal{M}}_\theta$  preserves the  $Spin(n, n)$ -orbit structure and defines an isometry between  $(\Lambda^{ev, od}, \mathcal{Q}_{\tilde{g}})$  and  $(\Lambda^{od, ev}, \mathcal{Q}_{\tilde{g}^T})$ . For instance, consider the case of a  $G_L \times G_R$ -invariant spinor

$$\rho = e^{-\phi} [\Psi_L \otimes \Psi_R]_b \otimes \sqrt{vol_g}. \quad (5.13)$$

Since we deal with two different metrics, it is essential to keep track of the volume form defining the identification between spinors and forms. Its T-dual is also  $G_L \times G_R$ -invariant, but now the stabiliser gives rise to the generalised metric  $(g^T, b^T)$ . Therefore we can write the T-dual of (5.13) as

$$\rho^T = e^{-\phi^T} [\Psi_L^T \otimes \Psi_R^T]_{b^T} \otimes \sqrt{vol_{g^T}}. \quad (5.14)$$

From the definition of the T-dual, we obtain  $(-X \lrcorner + \theta \wedge) [\Psi_L \otimes \Psi_R]_b = \|X\| [\Psi_L^T \otimes \Psi_R^T]_{b^T}$  since  $\|X\| \sqrt{vol_g} = \sqrt{vol_{g^T}}$ .

Since T-duality interchanges the chirality of the  $T \oplus T^*$ -spinor, a decomposable bispinor of spinors of equal (opposite) chirality maps to a bispinor of opposite (equal) chirality if  $n$  is even, reflecting the fact that T-duality interchanges type IIB and type IIA string theory.

### 5.1.2 Geometric aspects of T-duality

Let us have a look at a geometrical description of T-duality. We consider a special class of integral three-forms (called ‘‘T-dualisable’’), following [31].

We assume that  $M^n$  is the total space of a principal  $S^1$ -fibre bundle  $p : M^n \rightarrow N^{n-1}$ , endowed with a gauge form  $\theta$ . Moreover,  $M$  comes along with an  $S^1$ -invariant generalised structure  $(g, b)$  and a calibration  $\rho$  which is also invariant under the  $S^1$ -action. Take  $X$  to be the vertical vector field of  $\theta$  such that  $X \lrcorner \theta = 1$  and consider the curvature two-form  $\omega$  which we regard as a two-form on  $N$ , i.e.  $d\theta = \omega$  (we do not write the pull-back  $p^*$  explicitly in the following). Let  $H$  be a closed,  $S^1$ -invariant three-form representing a cohomology class in  $H^3(M, \mathbb{Z})$  such that  $\omega^T = -X \lrcorner H$  is also integral. Integrality of  $\omega^T$  ensures the existence of another principal  $S^1$ -bundle  $M^T$  over  $N$ , the T-dual of  $M$  defined by the choice of a connection form  $\theta^T$  with  $d\theta^T = \omega^T$ . Writing  $H = \theta \wedge \omega^T - \mathcal{H}$  for some three-form  $\mathcal{H} \in \Omega^3(M)$ , we define the T-dual of  $H$  by

$$H^T = \theta^T \wedge \omega - \mathcal{H}. \quad (5.15)$$

T-duality consists then in applying the map  $\mathcal{M}_\theta$  or  $\widetilde{\mathcal{M}}_\theta$ , followed by the substitution  $\theta \rightarrow \theta^T$ . For instance, decomposing

$$\rho = \rho_0 + \theta \wedge \rho_1, \quad (5.16)$$

we have  $\rho^T = \widetilde{-\rho_1} + \theta^T \wedge \rho_0$ . To indicate the coordinate-change, we also use the notation  $\rho^T \cong \widetilde{\mathcal{M}}_\theta$ , meaning that the left hand side coincides with the right hand side upon substituting  $\theta$  by  $\theta^T$ . Explicitly, we obtain for the T-dual of (5.16)

$$\rho^T = [\rho^T]_{g^T} \otimes \sqrt{\text{vol}_{g^T}} \cong (-X \lrcorner [\rho]_g + \theta \wedge [\rho]_g) \otimes \sqrt{\text{vol}_g}, \quad (5.17)$$

such that  $\|X\| [\rho^T]_{g^T} \cong -X \lrcorner [\rho]_g + \theta \wedge [\rho]_g$ .

For later application in section 5.5.6, we establish the following relation

$$X \lrcorner d_H C - \theta \wedge d_H C \cong d_{H^T} (-X \lrcorner C + \theta^T \wedge C), \quad (5.18)$$

where  $C = C_0 + \theta \wedge C_1$  is a differential form of mixed degree that is  $S^1$  invariant. To obtain this relation, we note that the  $S^1$ -invariance of  $C$  yields  $dC = dC_0 + \omega \wedge C_1 - \theta \wedge dC_1$  with  $dC_0 + \omega \wedge C_1 \in \Omega^*(N)$ .

As a particular case, we find for an  $S^1$ -invariant spinor  $\rho$  that

$$X \lrcorner d_H [\rho]_g - \theta \wedge d_H [\rho]_g \cong d_{H^T} \|X\| [\rho^T]_{g^T}. \quad (5.19)$$

## 5.2 The mirror map for generalised Kähler structures

Generically, the two generalised complex structures of a generalised Kähler structure (see section 4.5.1) are given in the  $T \oplus T^*$  basis by

$$\mathcal{J}_{1/2} = \frac{1}{2} \begin{pmatrix} J_+ \pm J_- & -(\omega_+^{-1} \mp \omega_-^{-1}) \\ \omega_+ \mp \omega_- & -(J_+^T \pm J_-^T) \end{pmatrix}, \quad (5.20)$$

where the complex structures  $J_+$  and  $J_-$  are independent sections ( $\forall p \in M^6$ ) in the twistor space  $\mathcal{Z}M^6$ . Note that we always assume integrability for the two complex structures. We can also define a generalised metric by  $G = -\mathcal{J}_1 \mathcal{J}_2$ .

Suppose that we take a trivial fibre bundle  $M^6 = T^6$  with fibre  $F = T^3$  over the base space  $B = T^3$ , thus  $M^6 = T^3 \oplus T^3$ . Therefore we have the following splitting of the generalised tangent space:

$$T \oplus T^* = T_B \oplus T_F \oplus T_B^* \oplus T_F^*. \quad (5.21)$$

This choice is for computational convenience, but one can consider a more general  $M^6$  as a nontrivial  $T^3$  torus fibration over a general three dimensional base space without changing the essence of our argument [154]. Furthermore, we want to consider only generalised complex structures which are adapted in the sense of [14], i.e.

$$\mathcal{J}_{1/2} : T_F \oplus T_F^* \rightarrow T_B \oplus T_B^*. \quad (5.22)$$

Respecting additionally the algebraic properties of the generalised complex structures we take

$$J_+ \pm J_- = \begin{pmatrix} 0 & -(\tilde{J}_+ \pm \tilde{J}_-) \\ \tilde{J}_+ \pm \tilde{J}_- & 0 \end{pmatrix}, \quad (5.23)$$

$$\omega_+ \mp \omega_- = \begin{pmatrix} 0 & -(\tilde{\omega}_+ \mp \tilde{\omega}_-) \\ \tilde{\omega}_+ \mp \tilde{\omega}_- & 0 \end{pmatrix}. \quad (5.24)$$

Note that  $\tilde{J}_+, \tilde{J}_-$  and  $\tilde{\omega}_+, \tilde{\omega}_-$  are not complex structures and Kähler forms, respectively. Note also that to satisfy the properties  $I_{\pm}^2 = -1$  and  $\omega_{\pm}^T = -\omega_{\pm}^T$  one has to require  $\tilde{I}_{\pm}^2 = 1$  and  $\tilde{\omega}_{\pm}^T = \tilde{\omega}_{\pm}$ .

Let us write the specific generalised complex structures explicitly as

$$\mathcal{J}_{1/2} = \frac{1}{2} \begin{pmatrix} 0 & -(\tilde{J}_+ \pm \tilde{J}_-) & 0 & -(\tilde{\omega}_+^{-1} \mp \tilde{\omega}_-^{-1}) \\ \tilde{J}_+ \pm \tilde{J}_- & 0 & \tilde{\omega}_+^{-1} \mp \tilde{\omega}_-^{-1} & 0 \\ 0 & -(\tilde{\omega}_+ \mp \tilde{\omega}_-) & 0 & -(\tilde{J}_+^T \pm \tilde{J}_-^T) \\ \tilde{\omega}_+ \mp \tilde{\omega}_- & 0 & \tilde{J}_+^T \pm \tilde{J}_-^T & 0 \end{pmatrix}. \quad (5.25)$$

By adopting the idea of [154] we describe mirror symmetry as three T-dualities along the  $T^3$ -fibre over a three-dimensional base space. Therefore we formulate mirror map  $\mathcal{M}$  as a map which acts on the generalised tangent bundle  $T \oplus T^*$  as a bundle isomorphism [14, 114]. Moreover, this isomorphism should have the property of an involution,  $\mathcal{M}^2 = 1$ . The mirror map in the generalised tangent space induces naturally a map for the generalised Kähler structure, consisting of mirror transformed generalised complex structures  $\hat{\mathcal{J}}_{1/2}$  and a mirror transformed generalised metric  $\hat{G}$ .

Let us define the mirror map such that it acts as an identity on  $T_B, T_B^*$  and flips  $T_F$  and  $T_F^*$ :

$$\mathcal{M} : T_B \oplus T_F \oplus T_B^* \oplus T_F^* \rightarrow T_B \oplus T_F^* \oplus T_B^* \oplus T_F, \quad (5.26)$$

explicitly

$$\mathcal{M} = \begin{pmatrix} \mathbf{id}_3 & & & \\ & & & -1 \\ & & -1 & \\ & -1 & & \end{pmatrix}. \quad (5.27)$$

We recognise this as the combination of three T-dualities defined according to (5.1) in the direction of the fibres  $T_F$ .

We get a conjugated generalised complex structure in the following way,

$$\hat{\mathcal{J}}_{1/2} = \mathcal{M} \circ \mathcal{J}_{1/2} \circ \mathcal{M}^{-1} : T_B \oplus T_F^* \oplus T_B^* \oplus T_F \rightarrow T_B \oplus T_F \oplus T_B^* \oplus T_F^*. \quad (5.28)$$

Applying this construction explicitly we get

$$\hat{\mathcal{J}}_{1/2} = \frac{1}{2} \begin{pmatrix} 0 & -(\tilde{\omega}_+^{-1} \mp \tilde{\omega}_-^{-1}) & 0 & -(\tilde{J}_+ \pm \tilde{J}_-) \\ \tilde{\omega}_+ \mp \tilde{\omega}_- & 0 & \tilde{J}_+^T \pm \tilde{J}_-^T & 0 \\ 0 & -(\tilde{J}_+^T \pm \tilde{J}_-^T) & 0 & -(\tilde{\omega}_+ \mp \tilde{\omega}_-) \\ \tilde{J}_+ \pm \tilde{J}_- & 0 & \tilde{\omega}_+^{-1} \mp \tilde{\omega}_-^{-1} & 0 \end{pmatrix}. \quad (5.29)$$

To compare  $\hat{\mathcal{J}}_{1/2}$  with  $\mathcal{J}_{1/2}$  we reinterpret  $\hat{\mathcal{J}}_{1/2}$  as a map  $T_B \oplus T_F \oplus T_B^* \oplus T_F^* \rightarrow T_B \oplus T_F \oplus T_B^* \oplus T_F^*$  instead of (5.28). We then use the fiber metric  $g_F$  and its inverse and we write them back into  $\hat{\mathcal{J}}_{1/2}$ . By using the identity  $\omega = gI$ , we get finally

$$\hat{\mathcal{J}}_{1/2} = \frac{1}{2} \begin{pmatrix} 0 & -(\tilde{J}_+ \mp \tilde{J}_-) & 0 & -(\tilde{\omega}_+^{-1} \pm \tilde{\omega}_-^{-1}) \\ \tilde{J}_+ \mp \tilde{J}_- & 0 & \tilde{\omega}_+^{-1} \pm \tilde{\omega}_-^{-1} & 0 \\ 0 & -(\tilde{\omega}_+ \pm \tilde{\omega}_-) & 0 & -(\tilde{J}_+^T \mp \tilde{J}_-^T) \\ \tilde{\omega}_+ \pm \tilde{\omega}_- & 0 & \tilde{J}_+^T \mp \tilde{J}_-^T & 0 \end{pmatrix}, \quad (5.30)$$

where now  $\hat{\mathcal{J}}_{1/2}$  are again maps

$$\hat{\mathcal{J}}_{1/2} : T_B \oplus T_F \oplus T_B^* \oplus T_F^* \rightarrow T_B \oplus T_F \oplus T_B^* \oplus T_F^*. \quad (5.31)$$

This is the mirror transformed complex structure. We see immediately that mirror symmetry interchanges the two generalised complex structures,

$$\begin{aligned} \mathcal{J}_{1/2} &\longleftrightarrow \hat{\mathcal{J}}_{1/2} = \mathcal{J}_{2/1} \\ (J_+, J_-) &\longleftrightarrow (\hat{J}_+, \hat{J}_-) = (J_+, -J_-). \end{aligned} \quad (5.32)$$

When  $M^6$  is a nontrivial torus fibration, using the same remark above, also the mirror manifold  $\hat{M}^6$  is a nontrivial torus fibration.

This result can be equivalently described in terms of pure spinors and their associated maximally isotropic subbundles. This will be the topic of the following section.

### 5.2.1 Description in terms of pure spinors

Let us assume we have a generic generalised Kähler structure, as defined in section 4.5.1, on a 6-manifold  $M^6$ . With the two commuting integrable generalised complex structures,  $\mathcal{J}_{1/2}$ , we get a decomposition of  $(T \oplus T^*)$  into a direct sum of four subbundles. As we have seen in section 4.5, the choice of a generalised metric leads to a decomposition

$$T \oplus T^* = V_+ \oplus V_-. \quad (5.33)$$

In the following we are in fact dealing only with the metric part of these spaces, denoted by  $D_{\pm}$  in section 4.5. As explained there, the introduction of a non-trivial

$b$ -field can be simply accounted for by an application of the  $b$ -field transformation. Since this transformation does not change the formalism, we set  $b = 0$ , but keep the notation  $V_{\pm}$ , to indicate that everything holds in the general case. The elements of  $V_{\pm} = D_{\pm}$  can be written as

$$\begin{aligned} V_+ &= \{X + g(X) | X \in T\} \\ V_- &= \{X - g(X) | X \in T\}. \end{aligned} \quad (5.34)$$

In this case the generalised metric  $G$  is purely Riemannian,

$$\mathcal{G} = \begin{pmatrix} 0 & g^{-1} \\ g & 0 \end{pmatrix}. \quad (5.35)$$

On the other hand, since the generalised complex structures commute with  $\mathcal{G}$ , we can also decompose the generalised tangent bundle with respect to  $\mathcal{J}_{1/2}$ ,

$$\begin{aligned} \mathcal{J}_1 &= \pi|_{V_+}^{-1} J_+ \pi P_+ + \pi|_{V_-}^{-1} J_- \pi P_-, \\ \mathcal{J}_2 &= \pi|_{V_+}^{-1} J_+ \pi P_+ - \pi|_{V_-}^{-1} J_- \pi P_-, \end{aligned} \quad (5.36)$$

where  $\pi : V_{\pm} \rightarrow T$  is a projection.

We denote the  $i$  eigenbundle of  $\mathcal{J}_{1/2}$ , or equivalently the graphs of the maps  $-i\mathcal{J}_{1/2}$ , by  $W_{1/2}$ , respectively,

$$\begin{aligned} W_1 &= \{X + gX | X \in T_+^{1,0}\} \oplus \{X - gX | X \in T_-^{1,0}\}, \\ W_2 &= \{X + gX | X \in T_+^{1,0}\} \oplus \{X - gX | X \in T_-^{0,1}\}. \end{aligned} \quad (5.37)$$

The generalised tangent bundle decomposes therefore in

$$T \oplus T^* = W_1 \oplus \overline{W_1} = W_2 \oplus \overline{W_2}. \quad (5.38)$$

Since the two generalised complex structures commute we can decompose  $W_{1/2}$  further by  $\mathcal{J}_{2/1}$ . With the indices  $\pm$  we indicate the eigenvalues  $\pm i$  corresponding to the second splitting,

$$W_1 \oplus \overline{W_1} = W_1^+ \oplus W_1^- \oplus \overline{W_1^+} \oplus \overline{W_1^-}, \quad (5.39)$$

where

$$\begin{aligned} W_1^+ &= \{X + gX | X \in T_+^{1,0}\}, \\ W_1^- &= \{X - gX | X \in T_-^{1,0}\}, \\ W_2^+ &= \{X + gX | X \in T_+^{1,0}\}, \\ W_2^- &= \{X - gX | X \in T_-^{0,1}\}. \end{aligned} \quad (5.40)$$

We see that  $W_2 = W_1^+ \oplus \overline{W_1^-}$  and

$$V_{\pm} = W_{1/2}^{\pm} \oplus \overline{W_{1/2}^{\pm}}. \quad (5.41)$$

These observations show that by changing  $J_- \rightarrow -J_-$  we do not affect the  $C_+$ -bundle and, moreover, only interchange holomorphic with antiholomorphic objects with respect to  $J_-$  in the  $C_-$ -bundle. We finally obtain the result that mirror symmetry interchanges the subbundles  $W_1^- \leftrightarrow \overline{W_1^-}$ .

Since our subbundles  $W_{1/2}^\pm$  are maximally isotropic we can generate them by pure spinor lines. In the following we show that the mapping  $W_{1/2}^\pm$  is equivalent to a mapping of the associated pure spinors.

It can be proven that  $W_1^+, W_1^-$  can be described by the following four pure spinor lines  $\rho_i, i \in \{1, \dots, 4\}$

$$\begin{aligned} 0 &= W_1^+ \bullet \rho_1 = W_1^+ \bullet \Omega_+^{(3,0)}, \\ 0 &= W_1^- \bullet \rho_2 = W_1^- \bullet \Omega_-^{(3,0)}, \\ 0 &= W_1^+ \bullet \rho_3 = W_1^+ \bullet e^{i\omega_+}, \\ 0 &= W_1^- \bullet \rho_4 = W_1^- \bullet e^{-i\omega_-}, \end{aligned} \tag{5.42}$$

where  $\Omega_\pm^{(3,0)} \in \Lambda^{od}$  are holomorphic top degree forms with respect to  $J_+, J_-$  and  $\omega_\pm \in \Lambda^{ev}$  are the Kähler forms.

We choose an appropriate local trivialisation for the forms in terms of local complex coordinates with respect to either  $J_+$  or  $J_-$ . We split them into an imaginary part  $y^i, i \in \{1, 2, 3\}$ , and a real part  $x^\alpha, \alpha \in \{1, 2, 3\}$ , which are the coordinates in the base and the fibre, respectively.

$$e^{i\omega_+} = 1 + i dx^i dy^i + dx^{12} dy^{12} + dx^{23} dy^{23} + dx^{13} dy^{13} + i dx^{123} dy^{123}, \tag{5.43}$$

$$\Omega_+^{(3,0)} = (dx^1 + i dy^1) \wedge (dx^2 + i dy^2) \wedge (dx^3 + i dy^3). \tag{5.44}$$

The action of the mirror map acting on the pure spinor lines is given explicitly by

$$\widetilde{\mathcal{M}} : \Lambda^{ev/od} \rightarrow \Lambda^{od/ev} \tag{5.45}$$

$$\rho \rightarrow (\partial_{X_3} + dx^3) \bullet (\partial_{X_2} + dx^2) \bullet (\partial_{X_1} + dx^1) \bullet \rho, \tag{5.46}$$

where  $T_F = \text{span}\{\partial_{X_\alpha}\}$ ,  $T_F^* = \text{span}\{dx^\alpha\}$  and  $\rho \in \Lambda^\bullet$ .

Using the property that  $\partial_{X_\alpha} \lrcorner dx^\beta = \delta_\alpha^\beta$ , we apply the mirror map to the pure spinors  $\rho_i$  to get

$$\begin{aligned} \hat{\rho}_1 &= \widetilde{\mathcal{M}} \bullet \Omega_+^{(3,0)} = e^{i\omega_+}, \\ \hat{\rho}_2 &= \widetilde{\mathcal{M}} \bullet \Omega_-^{(3,0)} = e^{i\omega_-}, \\ \hat{\rho}_3 &= \widetilde{\mathcal{M}} \bullet e^{i\omega_+} = -\Omega_+^{(3,0)}, \\ \hat{\rho}_4 &= \widetilde{\mathcal{M}} \bullet e^{-i\omega_-} = -\overline{\Omega_-^{(3,0)}}. \end{aligned} \tag{5.47}$$

Looking at the maximally isotropic bundles that are associated to the mirror transformed pure spinors  $\hat{\rho}_i, i \in \{1, \dots, 4\}$ , we find that  $W_1^+$  is left unchanged by the map  $\mathcal{M}$ , but in the  $V_-$ -bundle  $W_1^-$  is exchanged with  $\overline{W_1^-}$ . This is exactly the same result we obtained in section 5.1.

### 5.3 Topological sigma models

Topological sigma models [164], considerably simpler to analyse than the full nonlinear sigma model, have been widely used to study aspects of mirror symmetry. Starting from an  $\mathcal{N} = (2, 2)$  supersymmetric theory on the world-sheet, they are obtained by the so-called twisting. This twist consists of mixing the spin of the world-sheet fermions with the  $U(1)$ -current, such that they get an integer spin. The motivation to do this comes from the fact that global supersymmetry on the world-sheet cannot be defined on a curved Riemann surface. This global supersymmetry is necessary to make use of the localisation principle, that ensures that amplitudes can be calculated relatively easy by considering only holomorphic or constant maps in the A- and B-model case, respectively. There exist two different models, the A- and the B-model, because there are two different ways to twist the underlying theory, using either the vector or the axial part of the  $U(1)$ -current.

In the classical studies of  $\mathcal{N} = (2, 2)$  theories it is implicitly assumed that the left- and right-moving world-sheet fermions transform according to the same complex structure  $J$  and the target space manifold is Kähler. As has been discovered in [84], this is not the most general case, but one can use two different complex structures for the left- and right-moving fermions. This leads to a bi-hermitian geometry described in terms of a metric  $g$ , the two complex structures  $J_+$  and  $J_-$ , and a three-form  $H$ . It has been shown in [103] that this is equivalent to one generalised Kähler structure, defined in section 4.5.1, that is twisted by  $H$ . The twist of the  $\mathcal{N} = (2, 2)$  sigma model in the more general case of  $J_+ \neq J_-$  was performed in [120, 122] yielding a generalised notion of topological sigma models.

#### 5.3.1 Definition of generalised topological sigma models

Let us give a brief formulation of the topological sigma models in the generalised formalism. We start with the two-dimensional nonlinear sigma model in the  $\mathcal{N} = (1, 1)$  superfield formalism. Using bosonic coordinates  $\sigma$  and fermionic coordinates  $\theta$  and a chiral superfield  $\Phi$ , we can write this as

$$S = \frac{1}{2} \int d^2\sigma d^2\theta (g + B)(D_+\Phi, D_-\Phi), \quad (5.48)$$

where the derivatives  $D_\pm$  are given by

$$D_\pm = \frac{\partial}{\partial\theta^\pm} + i\theta^\pm\partial_\pm, \quad (5.49)$$

using the partial derivatives  $\partial_\pm$ , which are defined as

$$\partial_\pm := \partial_0 \pm \partial_1. \quad (5.50)$$

The  $\mathcal{N} = (1, 1)$  SUSY transformations are generated by  $Q_\pm$ , which read

$$Q_\pm^{(1)} := \frac{\partial}{\partial\theta^\pm} - i\theta^\pm\partial_\pm. \quad (5.51)$$



We can expand the chiral superfield  $\Phi$  in components as

$$\Phi = \phi + \theta^+ \psi_+ + \theta^- \psi_- + \theta^- \theta^+ F. \quad (5.52)$$

Since we want to obtain a theory with  $\mathcal{N} = (2, 2)$  supersymmetry on the world-sheet, we have to define an additional supersymmetry. This can be done introducing two complex structures  $J_{\pm}$  and the generators

$$Q_{\pm}^{(2)} := J_{\pm} D_{\pm}. \quad (5.53)$$

This is a well defined additional  $(1, 1)$  supersymmetry, if the  $J_{\pm}$  are a pair of integrable almost complex structures and the metric  $g$  is hermitian with respect to both,  $J_+$  and  $J_-$ . Furthermore the almost complex structures have to be covariantly constant with respect to the covariant derivatives with connection

$$\Gamma_{\pm bc}^a := \Gamma_{bc}^a \pm g^{ad} H_{dbc}, \quad (5.54)$$

where  $\Gamma$  is the Levi-Civita connection. A non-trivial  $H$ -field modifies this connection differently for  $\psi_+$  and  $\psi_-$ . We get the following relation between the two connections

$$\Gamma_{+bc}^a \psi_+^b \psi_-^c = -\Gamma_{-bc}^a \psi_-^b \psi_+^c. \quad (5.55)$$

Acting with the two supersymmetries on the superfield (5.52) we can write the variations in components as

$$\begin{aligned} \delta_+^{(1)} \phi &= \psi_+, & \delta_-^{(1)} \phi &= \psi_-, \\ \delta_+^{(1)} \psi_+ &= -i \partial_+ \phi, & \delta_-^{(1)} \psi_+ &= F, \\ \delta_+^{(1)} \psi_- &= -F, & \delta_-^{(1)} \psi_- &= -i \partial_- \phi, \\ \delta_+^{(2)} \phi &= J_+ \psi_+, & \delta_-^{(2)} \phi &= J_- \psi_-, \\ \delta_+^{(2)} \psi_+ &= i J_+ \partial_+ \phi, & \delta_-^{(2)} \psi_+ &= J_- F, \\ \delta_+^{(2)} \psi_- &= -J_+ F, & \delta_-^{(2)} \psi_- &= i J_- \partial_- \phi. \end{aligned} \quad (5.56)$$

The auxiliary field  $F$  can be integrated out, using it's equations of motion,

$$F^a = \Gamma_{+bc}^a \psi_+^b \psi_-^c. \quad (5.57)$$

We define the following combinations of the supersymmetry generators<sup>1</sup>.

$$\begin{aligned} Q_+ &= \frac{1}{2}(Q_+^{(1)} - iQ_+^{(2)}), & \bar{Q}_+ &= \frac{1}{2}(Q_+^{(1)} + iQ_+^{(2)}), \\ Q_- &= \frac{1}{2}(Q_-^{(1)} - iQ_-^{(2)}), & \bar{Q}_- &= \frac{1}{2}(Q_-^{(1)} + iQ_-^{(2)}). \end{aligned} \quad (5.58)$$

---

<sup>1</sup>These definitions correspond to those in [111].

	$q_V$	$q_A$	$s$	$s_A$	$s_B$
$\mathcal{P}_+\psi_+$	-1	-1	$-\frac{1}{2}$	-1	-1
$\overline{\mathcal{P}}_+\psi_+$	+1	+1	$-\frac{1}{2}$	0	0
$\mathcal{P}_-\psi_-$	-1	+1	$+\frac{1}{2}$	0	+1
$\overline{\mathcal{P}}_-\psi_-$	+1	-1	$+\frac{1}{2}$	+1	0

Table 5.1: Charges of the fermionic fields before and after the twist.  $q_{V/A}$  denote the vector and axial charges, respectively.  $s$  is the spin before the twist and  $s_{A/B}$  are the spins after performing an A or B twist. The projection operators  $\mathcal{P}$  are defined in (5.60).

Up to this point we are dealing with an ordinary nonlinear sigma model. To obtain a topological theory, we have to twist the spins of the world-sheet fermions. Depending on whether we use the vector or axial part of the  $U(1)$  current to perform the twist, we obtain the topological A- or B-model [164]. The charges of the fields before and after the twist are listed in table 5.1, where the fermionic spins after performing an A or B twist are given by

$$s_{A/B} = s + \frac{1}{2}q_{V/A}. \quad (5.59)$$

In the table we also used projectors on the holomorphic and antiholomorphic parts of the fields with respect to the two complex structures  $J_{\pm}$ . These are defined as

$$\mathcal{P}_{\pm} = \frac{1}{2}(1 - iJ_{\pm}), \quad \overline{\mathcal{P}}_{\pm} = \frac{1}{2}(1 + iJ_{\pm}). \quad (5.60)$$

### 5.3.2 BRST operators

After the twist we obtain fermionic fields with spin 0 and spin 1. We can use the spin 0 fields to construct a BRST operator. As BRST operators for the generalised A- and B-model we take therefore<sup>2</sup>

$$Q_A := \overline{Q}_+ + Q_-, \quad Q_B := \overline{Q}_+ + \overline{Q}_-, \quad (5.61)$$

which act on the scalar fields of the twisted models like

$$\begin{aligned} \delta_A \phi &= \overline{\mathcal{P}}_+\psi_+ + \mathcal{P}_-\psi_-, & \delta_B \phi &= \overline{\mathcal{P}}_+\psi_+ + \overline{\mathcal{P}}_-\psi_-, \\ \delta_A \overline{\mathcal{P}}_+\psi_+ &= \Gamma_+ \overline{\mathcal{P}}_+\psi_+ \mathcal{P}_-\psi_-, & \delta_B \overline{\mathcal{P}}_+\psi_+ &= \Gamma_+ \overline{\mathcal{P}}_+\psi_+ \overline{\mathcal{P}}_-\psi_-, \\ \delta_A \mathcal{P}_-\psi_- &= \Gamma_- \mathcal{P}_-\psi_- \overline{\mathcal{P}}_+\psi_+, & \delta_B \overline{\mathcal{P}}_-\psi_- &= \Gamma_- \overline{\mathcal{P}}_-\psi_- \overline{\mathcal{P}}_+\psi_+. \end{aligned} \quad (5.62)$$

We can rewrite the BRST operator (5.61) in the  $T \oplus T^*$  picture. To do so we define

<sup>2</sup>Note that in [164] a different definition for the world sheet fermions is used, which leads to a different BRST operator for the A-model,  $Q_A = Q_+ + \overline{Q}_-$ .

a fermionic basis

$$\psi := (\psi_+ + \psi_-) \in T, \quad \rho := g(\psi_+ - \psi_-) \in T^*, \quad \Psi := \begin{pmatrix} \psi \\ \rho \end{pmatrix}. \quad (5.63)$$

Using this notation we can write the BRST operators of the generalised A- and B-model as

$$\begin{aligned} Q_A &= \left\langle \begin{pmatrix} \partial_1 \phi \\ g \partial_0 \phi \end{pmatrix}, (1 + i\mathcal{J}_2)\Psi \right\rangle, \\ Q_B &= \left\langle \begin{pmatrix} \partial_1 \phi \\ g \partial_0 \phi \end{pmatrix}, (1 + i\mathcal{J}_1)\Psi \right\rangle, \end{aligned} \quad (5.64)$$

where  $\langle \cdot, \cdot \rangle$  is the natural product on  $T \oplus T^*$ , as defined in (4.2).

In this language the relevant BRST variations (5.62), namely those that vanish because of (5.55), take the simple form

$$\delta_A \frac{1}{2}(1 + i\mathcal{J}_1)\Psi = 0, \quad \delta_B \frac{1}{2}(1 + i\mathcal{J}_2)\Psi = 0. \quad (5.65)$$

The classical  $U(1)_{A/V}$  symmetry can be broken by quantum effects. This anomaly is given in terms of the first Chern class of the  $L_{1/2}$  bundle for the  $B/A$  model [122]. The cancellation of this anomaly constraints the target space geometry via  $c_1(L_{1/2}) = 0$ .

### 5.3.3 The action of mirror symmetry

It is well known that mirror symmetry exchanges the topological A-model on one Calabi-Yau with the B-model on the mirror Calabi-Yau, characterised by the exchange of complex and symplectic moduli. We want to apply the mirror map as defined in sections 5.1 and 5.2.1 to the generalised B-model with target space  $M^6$  and show that it is mapped to the generalised A-model with the mirror target space  $\hat{M}^6$ .

In section 5.2 we found that  $\mathcal{M} : \mathcal{J}_1 \rightarrow \mathcal{J}_2$ , such that  $\mathcal{M} : Q_B \rightarrow Q_A$ . We also know that the complex structures  $(J_+, J_-)$  are mapped to  $(J_+, -J_-)$  under the mirror map and equation (5.40) tells us that  $\mathcal{M} : L_1 \rightarrow L_2$ . Therefore,  $\mathcal{M} : c_1(L_1) \rightarrow c_1(L_2)$  and the anomaly cancellation of the generalised B-model gets mapped to that of the generalised A-model.

The next step is to show that the observables of the generalised B- and A-model are mirrors of each other. We show this for the local observables of the closed topological sector, but first let us remember how they were constructed in [120]. Following [164], one has to construct scalar BRST invariant field configurations. Writing the BRST

variations in the  $T \oplus T^*$  bundle, we get<sup>3</sup>

$$\delta_{B/A}\Phi = \Psi_{1/2} := \frac{1}{2}(1 + i\mathcal{J}_{1/2})\Psi \in \bar{L}_{1/2}, \quad \Phi := \begin{pmatrix} \phi \\ g\phi \end{pmatrix}. \quad (5.66)$$

The nilpotency properties  $\delta_{B/A}^2 = 0$  of the BRST variations then yield  $\delta_{B/A}\Psi_{1/2} = 0$ , which was also obtained in (5.65). Thus,  $\Psi_{1/2}$  are the configurations we are looking for in the generalised B/A-model. The space of observables is then given by

$$(\mathcal{O}_f)_{B/A} = f_{a_1 \dots a_n}(\phi)\Psi_{1/2}^{a_1} \dots \Psi_{1/2}^{a_n}, \quad (5.67)$$

which can be mapped to the exterior algebra bundle  $\Lambda^k \bar{L}_{1/2}^* \simeq \Lambda^k L_{1/2}$  since  $f$  is skew symmetric in the indices  $a$ . Performing the BRST variation of  $(\mathcal{O}_f)_{B/A}$ , one realizes that the map is actually an isomorphism,

$$\{Q_{B/A}, (\mathcal{O}_f)_{B/A}\} = (\mathcal{O}_{d_{\bar{L}_{1/2}} f})_{B/A}, \quad (5.68)$$

where  $d_{\bar{L}_{1/2}} = \partial_{\bar{L}_{1/2}}^+ + \partial_{\bar{L}_{1/2}}^-$  is the Lie algebroid derivative such that

$$d_{\bar{L}_{1/2}} : C^\infty(\Lambda^k L_{1/2}) \rightarrow C^\infty(\Lambda^{k+1} L_{1/2}). \quad (5.69)$$

Since  $\mathcal{M} : \bar{L}_1 \rightarrow \bar{L}_2$ , the cohomologies of the differential complexes for the generalised A- and B-models are mirror pairs.

We want to do the same for the generalised instantons [120]. The instantons are the fixed points of the BRST transformations. Performing the Wick rotation  $\partial_0 \phi \rightarrow i\partial_2 \phi$  on the Riemann surface, one gets the instanton equations

$$\delta_{B/A}\Psi = (1 - i\mathcal{J}_{1/2}) \begin{pmatrix} i\partial_2 \phi \\ g\partial_1 \phi \end{pmatrix} = 0, \quad (5.70)$$

from which we conclude that the instantons of the generalised B model are mapped to those of the generalised A model under the mirror map.

## 5.4 Topological branes

Branes in the topological A- or B-model (A- or B-branes) can be defined by a gluing matrix  $R : T \rightarrow T$ , which encodes information about the mapping of left- and right-moving fermions at the boundary  $\partial\Sigma$  of the worldsheet [2, 3]. The gluing conditions read

$$\psi_- = R\psi_+. \quad (5.71)$$

---

<sup>3</sup>Here  $\Phi$  is an element of  $T \oplus T^*$  and should not be confused with the chiral superfield defined in (5.48).

In the generalised picture this translates to [166]

$$\mathcal{R} : T \oplus T^* \rightarrow T \oplus T^*, \quad \mathcal{R}\Psi = \Psi, \quad (5.72)$$

where  $\Psi$  is defined in (5.63).  $\mathcal{R}$  respects the natural metric  $\langle \cdot, \cdot \rangle$  on  $T \oplus T^*$ , squares to one, i.e.  $\mathcal{R}^2 = 1$ , and anticommutes with  $\mathcal{G}$ , i.e.  $\mathcal{G}\mathcal{R} + \mathcal{R}\mathcal{G} = 0$ .

In the physical framework the operator  $\mathcal{R}$  contains the information about Dirichlet and Neumann boundary conditions. It defines a smooth distribution  $\mathcal{D} \subset T$  which has rank equal to the dimension of the brane. In case of an integrable distribution we even have a maximal integral submanifold  $\mathcal{D}$ .

From a different point of view, the above properties of  $\mathcal{R}$  serve to consider the projection operator  $\frac{1}{2}(1 + \mathcal{R})$  to define a special almost Dirac structure  $\tau_{\mathcal{D}}^0$  (a real, maximal isotropic sub-bundle),

$$\tau_{\mathcal{D}}^0 = T\mathcal{D} \oplus \text{Ann}(T\mathcal{D}) \subset T \oplus T^*, \quad (5.73)$$

which is Courant integrable iff  $\mathcal{D}$  is integrable.

The extension of  $\mathcal{R}$  by a closed two-form  $F \in \Omega^2(\mathcal{D})$ ,  $dF = 0$ , on the submanifold  $\mathcal{D}$  corresponds to

$$\tau_{\mathcal{D}}^F = \left\{ \frac{1}{2}(1 + \mathcal{R})(X + \xi) = (X + \xi) : (X + \xi) \in T\mathcal{D} \oplus T^*M|_{\mathcal{D}}, \xi|_{\mathcal{D}} = X \lrcorner F \right\} \quad (5.74)$$

and is equivalent to the definition of a generalised tangent bundle given in [103]. This gluing matrix is given by

$$\mathcal{R} = \begin{pmatrix} 1 & \\ F & 1 \end{pmatrix} \begin{pmatrix} r & \\ & -r^t \end{pmatrix} \begin{pmatrix} 1 & \\ -F & 1 \end{pmatrix} = \begin{pmatrix} & r \\ F r + r^t F & -r^t \end{pmatrix}, \quad (5.75)$$

where  $r$  is an operator which carries the gluing information for the fermions (see [2, 3]).

Let us focus on the A/B branes in the corresponding A/B-model. This means that the  $U(1)$  currents  $j_{\pm} = \omega_{\pm}(\psi_{\pm}, \psi_{\pm})$ ,  $\psi_{\pm} \in T$ , have to fulfill the matching conditions

$$0 = j_+ \pm j_- = \frac{1}{2} \langle \Psi, \mathcal{J}_{2/1} \Psi \rangle \quad (5.76)$$

for the A- or B-model, respectively.

Moreover, combining this with the gluing conditions for the fermions, we obtain a stability condition for  $\mathcal{R}$ , or equivalently, a stability condition for  $\tau_{\mathcal{D}}^F$ . Using also  $\{\mathcal{G}, \mathcal{R}\} = 0$ , one gets:

$$\begin{aligned} \text{A branes: } \mathcal{R}\mathcal{J}_1 &= -\mathcal{J}_1\mathcal{R} & \text{and} & & \mathcal{R}\mathcal{J}_2 &= \mathcal{J}_2\mathcal{R} \\ \text{B branes: } \mathcal{R}\mathcal{J}_1 &= \mathcal{J}_1\mathcal{R} & \text{and} & & \mathcal{R}\mathcal{J}_2 &= -\mathcal{J}_2\mathcal{R}. \end{aligned} \quad (5.77)$$

We will call the (anti)commuting constraints  $\mp$ -stability with respect to a certain generalised complex structure. Thus, the A/B-model is  $\mathcal{J}_{1/2}^-$  stable and additionally

$\mathcal{J}_{2/1}^+$  stable. This reflects the fact that the generalized tangent bundle  $\tau_{\mathcal{D}}^F$  in the A/B model splits into  $\pm i$  eigenbundles of  $\mathcal{J}_{2/1}$  or, in other words, it becomes a stable subbundle of  $L_{2/1} \oplus \overline{L_{2/1}}$ , respectively:

$$\text{A/B-model: } \tau_{\mathcal{D}}^F = \tau_{\mathcal{D}}^{F+} \oplus \tau_{\mathcal{D}}^{F-}, \quad \text{w.r.t. } L_{2/1} \oplus \overline{L_{2/1}}. \quad (5.78)$$

### 5.4.1 Transformation under mirror symmetry

Let us apply the mirror map  $\mathcal{M}$ , in the same way as for the topological models, on the topological branes. The gluing operator  $\mathcal{R}$  gets mapped to  $\hat{\mathcal{R}} = \mathcal{M}\mathcal{R}\mathcal{M}^{-1}$  and one can show that the properties for  $\hat{\mathcal{R}}$  are the same as for  $\mathcal{R}$ . Again we take  $M^6$  with a  $T^3$  fibration, such that mirror symmetry interchanges Neumann with Dirichlet boundary conditions in the fibre, being nothing else then three applications of T-duality.

The conditions on the  $U(1)$  currents get naturally exchanged, since we found in section 5.2 that the generalised complex structures  $\mathcal{J}_1$  and  $\mathcal{J}_2$  get exchanged. It is important to note however, that the stability conditions on the mirror symmetric side have to be formulated in terms of the transformed gluing matrix  $\hat{\mathcal{R}}$ .

## 5.5 Generalised Calibrations

In this section we define a special class of submanifolds that generalises the well-known notion of a calibrated submanifold. This is a direct extension of the last section on generalised topological D-branes, putting the notion of stability for generalised branes in a mathematical context.

### 5.5.1 Definition

Before we discuss the global notion, we first deal with the algebraic aspects of the theory and assume to work over a real,  $n$ -dimensional space  $T \cong \mathbb{R}^n$ . Let us start with the classical notion of calibrations and calibrated subplanes [107]. The data are a Riemannian metric  $g$  on  $T \cong \mathbb{R}^n$  and a  $p$ -form  $\rho^p$ . Restricted to an oriented  $p$ -plane  $j : U^p \hookrightarrow T$ ,  $\rho^p$  becomes a volume form which can be compared in an obvious sense with the Riemannian volume  $vol_U$ . One says that  $\rho^p$  defines a *calibration* iff

$$j^* \rho^p \leq vol_U \quad (5.79)$$

and the bound is met for at least one  $p$ -plane, which is said to be *calibrated*. Equivalently, we can require  $g(\rho, vol_U) \leq 1$ .

We immediately conclude from the definition that if  $\rho$  defines a calibration, so does  $\star_g \rho$ . If  $U$  is a calibrated plane with respect to  $\rho$ , then so is  $U^\perp$  with respect to  $\star_g \rho$ . Moreover, the calibration condition is  $GL(n)$ -equivariant in the sense that if  $A \in GL(n)$  and  $\rho$  defines a calibration, then so does  $A^* \rho$  with respect to  $A^* g$ . If  $U$  is

calibrated for  $\rho$ , then so is  $A(U)$  for  $A^*\rho$ . In particular, if  $\rho$  is  $G$ -invariant, then so is the calibration condition. Therefore, the calibrated subplanes live in special  $G$ -orbits of the Grassmannian  $Gr_p(T)$ .

Let us introduce an analogous concept for generalised metrics. The role of  $p$ -forms is now assured by even or odd forms which we view as spinors for  $Spin(n, n)$ . The orbits of interest to us are given by the maximally isotropic subplanes. These can be equivariantly identified with lines of pure spinors, as explained in section 4.2.2. For a generalised structure  $(g, b)$  a spinor  $\rho^{ev,od}$  of even or odd parity is defined to be a calibration, iff for any spinor  $\rho_{U,F}$ , induced by the pair  $(U, F)$ , consisting of an oriented subspace  $U$  and a two-form  $F \in \Lambda^2 T^*U$ , the inequality

$$\langle \rho, \rho_{U,F} \rangle \leq e^{-\phi} \quad (5.80)$$

holds and there exists at least one pair for which the bound is met. This pair is said to be calibrated by  $\rho^{ev,od}$ .

The condition (5.80) is clearly  $Spin_+(n, n)$ -equivariant, since if  $\rho_{U,F}$  is of unit norm for  $\mathcal{Q}_{\tilde{g}}$ , then so is  $A \bullet \rho_{U,F}$  for  $A \bullet \tilde{g} \bullet A^{-1}$ . Hence  $\rho$  defines a calibration if and only if  $A \bullet \rho$  does and a pair  $(U, F)$  is calibrated for  $\rho$  if and only if the pair  $(U_A, F_A)$  associated with  $A \bullet \rho_{U,F}$  and its induced orientation is for  $A \bullet \rho$ . Furthermore,  $\tilde{g}$  is an isometry for  $\mathcal{Q}_{\tilde{g}}$ , so  $\rho$  defines a calibration if and only if  $\tilde{g} \bullet \rho$  does; if  $(U, F)$  is calibrated for  $\rho$ , then the pair  $(U_{\tilde{g}}, F_{\tilde{g}})$  associated with  $(-1)^{n(n-1)/2} \tilde{g} \bullet \rho_{U,F}$  is calibrated for  $\tilde{g} \bullet \rho$ .

Let us show that this generalised calibration condition is the formal analogue of (5.79) and make the appearance of the data  $(g, b)$  explicit. A spinor  $\rho \in \Lambda^{ev,od}$  defines a calibration if and only if for any pair  $(U, F)$  with  $j^* : U \hookrightarrow T$  a  $p$ -dimensional oriented subspace, the inequality

$$[e^{-F} \wedge j^* \rho]^p \leq e^{-\phi} \sqrt{\det(j^*(g+b) - F)} vol_U \quad (5.81)$$

holds and is met for at least one pair  $(U, F)$  which is then calibrated. The right hand side of 5.81 can be recognised as the Dirac-Born-Infeld energy for D-branes.

To show that (5.81) holds, let us contract it with  $vol_U$ , which gives

$$\begin{aligned} g([e^{-F} \wedge j^* \rho]^p, vol_U) &= \star[e^{-F} \wedge \rho \wedge \star vol_U]^n \\ &= \langle \rho, e^F \bullet \widehat{\star vol_U} \rangle \\ &\leq e^{-\phi} \sqrt{\det(j^*(g+b) - F)}. \end{aligned} \quad (5.82)$$

Furthermore, note that for  $j : U \hookrightarrow T$  an oriented subspace and  $b \in \Lambda^2 T^*$  we have

$$g(e^b \wedge \star vol_U, e^b \wedge \star vol_U) = \det(j^*(g+b)) = \det(j^*(g-b)). \quad (5.83)$$

In particular, we have

$$\mathcal{Q}_{\tilde{g}}(e^F \wedge \widehat{\star vol_U}) = \det(j^*g + \mathcal{F}) = \det(j^*g - \mathcal{F}), \quad (5.84)$$

where  $\mathcal{F} = F - j^*b$ .

As the determinant of a bilinear form is invariant under orthogonal transformations, it is sufficient to show (5.83) for a special choice of an oriented orthonormal basis  $e_1, \dots, e_n$ . Since any leg of  $b$  inside  $U^\perp$  does not survive the wedging,  $b \wedge \star vol_U = j^*b \wedge \star vol_U$  and we choose an orthonormal basis on  $U$  in such a way that  $j^*b = \sum_{k=1}^{\lfloor p/2 \rfloor} b_k e_{2k-1} \wedge e_{2k}$ . Then

$$\begin{aligned} \det(j^*(g-b)) &= \det(j^*(g+b)) \\ &= \prod_{k=1}^{\lfloor p/2 \rfloor} (1+b_k^2) \\ &= 1 + \sum_{k=1}^{\lfloor p/2 \rfloor} b_k^2 + \sum_{k_1 < k_2} b_{k_1}^2 \cdot b_{k_2}^2 + \dots + b_1^2 \cdot \dots \cdot b_{\lfloor p/2 \rfloor}^2. \end{aligned} \quad (5.85)$$

On the other hand

$$\frac{1}{k!} j^* b^k = \sum_{l_1 < \dots < l_k} b_{l_1} \cdot \dots \cdot b_{l_k} e_{2l_1-1} \wedge e_{2l_1} \wedge \dots \wedge e_{2l_k-1} \wedge e_{2l_k}, \quad (5.86)$$

so that

$$g\left(\frac{1}{k!} j^* b^k \wedge \star vol_U, \frac{1}{k!} j^* b^k \wedge \star vol_U\right) = \sum_{l_1 < \dots < l_k} b_{l_1}^2 \dots b_{l_k}^2, \quad 2k \leq p. \quad (5.87)$$

Summing yields precisely (5.85) and thus (5.83). (5.84) follows from (4.39).

In particular, the generalised notion of a calibration encapsulates the classical case. Let  $\rho^q$  be a classical calibration for a Euclidean vector space  $(T, g)$  and  $U$  a calibrated subspace. Then  $(U, 0)$  is calibrated with respect to  $\rho = \rho^q$  and the generalised metric  $(g, b = 0)$ .

### 5.5.2 Connection with G-structures

As for the classical case, calibrations can be defined from special geometric structures. In order to make contact with the  $G_L \times G_R$ -structures from section 4.5.2, we rephrase the calibration condition in terms of  $T$ -spinors. For this, some preliminary work is needed. To start, assume  $F = b = 0$  and represent the isotropic subspace  $W_U$  as the graph of an isometry  $P_U : D_+ \rightarrow D_-$ , using the metric splitting  $T \oplus T^* = D_+ \oplus D_-$  ( $W_U$  intersects the definite spaces  $D_\pm$  trivially). If we choose an adapted orthonormal basis  $e_1, \dots, e_p \in U, e_{p+1}, \dots, e_n \in U^\perp$ , then the matrix of  $P_U$  associated with the basis  $d_k^\pm = \pi_\pm(e_k) = e_k \oplus \pm g(e_k)$  of  $D_\pm$  is

$$P_U = \begin{pmatrix} id_p & 0 \\ 0 & -id_{n-p} \end{pmatrix}. \quad (5.88)$$

Pulling this back via the isometries  $\pi_\pm$  to  $T$  gives rise to the isometry

$$R_U = \pi_-^{-1} \circ P_U \circ \pi_+ : (T, g) \rightarrow (T, -g), \quad (5.89)$$



which we call the gluing matrix of  $U$ , since it encapsulates exactly the same information as (5.71).

Its matrix representation with respect to an orthonormal basis adapted to  $U$  is (5.88). Next we allow for a non-trivial  $b$ - and  $F$ -field and consider the isotropic space  $W_{U,F}$  which annihilates  $\rho_{U,F}$ . Here, we consider the graph  $P_{U,F}^b$  as a map  $V_+ \rightarrow V_-$  which is indicated by the superscript  $b$ . The associated gluing matrix  $R_{U,F}^b$  is then defined as

$$R_{U,F}^b = \pi_{b-}^{-1} \circ P_{U,F}^b \circ \pi_{b+}. \quad (5.90)$$

Note that if we let  $\mathcal{F} = F - j^*b$ , then  $e^{2b}W_{U,\mathcal{F}} = \{v \oplus e^{2b}P_{U,\mathcal{F}}e^{-2b}v \mid v \in V_+\}$ , hence  $P_{U,F}^b = e^{2b}P_{U,\mathcal{F}}e^{-2b}$  and thus  $R_{U,F}^b = R_{U,\mathcal{F}}$ . With respect to an adapted basis for  $U$ , the matrix of  $R_{U,\mathcal{F}}$  can be computed as follows. Changing, if necessary, the orthonormal basis on  $U$  such that  $\mathcal{F} = \sum_{k=1}^{\lfloor p/2 \rfloor} f_k e_{2k-1} \wedge e_{2k}$ .

$$e_1 \oplus f_1 e^2, e_2 \oplus -f_1 e^1, \dots, e^{p+1}, \dots, e^n. \quad (5.91)$$

is a basis of  $W_{U,\mathcal{F}}$  by (4.22). Decomposing the first  $p$  basis vectors into the  $D_{\pm}$ -basis  $d_k^{\pm} = \pi_{\pm}(e_k)$  yields

$$\begin{aligned} 2(e_{2k-1} \oplus f_k e^{2k}) &= d_{2k-1}^+ + f_k d_{2k}^+ \oplus d_{2k-1}^- - f_k d_{2k}^- \\ 2(e_{2k} \oplus -f_k e^{2k-1}) &= -f_k d_{2k-1}^+ + d_{2k}^+ \oplus f_k d_{2k-1}^- + d_{2k}^-, \end{aligned} \quad (5.92)$$

while  $2e^k = d_k^+ \oplus -d_k^-$  for  $k = p+1, \dots, n$ . Written in the  $D_{\pm}$ -basis we have

$$\begin{aligned} w_{2k-1}^+ &= d_{2k-1}^+ + f_k d_{2k}^+, \\ w_{2k}^+ &= -f_k d_{2k-1}^+ + d_{2k}^+, & k \leq p, \\ w_k^+ &= d_k^+, & k > p, \\ \text{and} \quad w_{2k-1}^- &= d_{2k-1}^- - f_k d_{2k}^-, \\ w_{2k}^- &= f_k d_{2k-1}^- + d_{2k}^-, & k \leq p, \\ w_k^- &= d_k^-, & k > p. \end{aligned} \quad (5.93)$$

The matrix  $R_{U,\mathcal{F}}$  is just (5.88). The change of base matrix for  $d_k^+ \rightarrow w_k^+$  is given by the block matrix  $A = (A_1, \dots, A_p, id_{n-p})$ , where for  $(d_{2k-1}^+, d_{2k}^+) \rightarrow (w_{2k-1}^+, w_{2k}^+)$ ,  $k \leq p$ ,

$$A_k = \begin{pmatrix} 1 & f_k \\ -f_k & 1 \end{pmatrix}. \quad (5.94)$$

For  $w_k^- \rightarrow d_k^-$  it is given by the block matrix  $B = (B_1, \dots, B_p, id_{n-p})$ , where for  $(d_{2k-1}^-, d_{2k}^-) \rightarrow (w_{2k-1}^-, w_{2k}^-)$ ,  $k \leq p$ ,

$$B_k = \begin{pmatrix} 1 & -f_k \\ f_k & 1 \end{pmatrix}. \quad (5.95)$$

Computing  $B \circ (id_p, id_{n-p}) \circ A^{-1}$  and pulling back to  $T$  via  $\pi_{\pm}$  we finally find

$$R_{U,\mathcal{F}} = \begin{pmatrix} (j^*g + \mathcal{F})(j^*g - \mathcal{F})^{-1} & 0 \\ 0 & -id_{n-p} \end{pmatrix} \quad (5.96)$$

with respect to some orthonormal basis adapted to  $U$ .

Using this insight, we can make the following statement: The element  $J^{-1}(e^{-b} \bullet \rho_{U,\mathcal{F}})$  lies in  $Spin(T, g)$ . Moreover, its projection to  $SO(T, g)$  equals  $R_{U,\mathcal{F}}$ . This can be shown as follows. Again let  $e_1, \dots, e_n$  be an adapted orthonormal basis so that  $\mathcal{F} = \sum_{k=1}^{\lfloor p/2 \rfloor} f_k e_{2k-1} \wedge e_{2k}$ . Applying a trick from [16], we define

$$\begin{aligned} \arctan \tilde{\mathcal{F}} &= \sum_k \arctan(f_k) e_{2k-1} \cdot e_{2k} \\ &= \frac{1}{2i} \sum_k \ln \frac{1 + if_k}{1 - if_k} e_{2k-1} \cdot e_{2k} \in \mathfrak{spin}(n) \subset Cliff(T), \end{aligned} \quad (5.97)$$

and show that

$$J(\exp(\arctan \tilde{\mathcal{F}}) \cdot \widehat{\star vol_U}) = e^{-b} \bullet \rho_{U,\mathcal{F}} \in \Lambda^*, \quad (5.98)$$

where the exponential takes values in  $Spin(T)$ . Since the elements  $e_{2k-1} \cdot e_{2k}$ ,  $e_{2l-1} \cdot e_{2l}$  commute, exponentiation yields

$$\begin{aligned} &e^{\arctan \tilde{\mathcal{F}}} \\ &= \prod_k e^{\arctan(f_k) e_{2k-1} \cdot e_{2k}} \\ &= \prod_k (\cos(\arctan(f_k)) + \sin(\arctan(f_k)) e_{2k-1} \cdot e_{2k}) \\ &= \prod_k \left( \frac{1}{\sqrt{1+f_k^2}} + \frac{f_k}{\sqrt{1+f_k^2}} e_{2k-1} \cdot e_{2k} \right) \\ &= \frac{1}{\prod_k (\sqrt{1+f_k^2})} \left( 1 + \sum_l f_l e_{2l-1} \cdot e_{2l} + \sum_{l < m} f_l \cdot f_m e_{2l-1} \cdot e_{2l} \cdot e_{2m-1} \cdot e_{2m} + \dots \right) \\ &= \frac{1}{\sqrt{\det(j^*g - \mathcal{F})}} J^{-1} \left( 1 + \mathcal{F} + \frac{1}{2} \mathcal{F} \wedge \mathcal{F} + \dots \right), \end{aligned} \quad (5.99)$$

using the classical identities  $\cos \arctan x = 1/\sqrt{1+x^2}$  and  $\sin \arctan x = x/\sqrt{1+x^2}$ . Applying (5.83), we finally get

$$J(e^{\arctan \tilde{\mathcal{F}}} \cdot \widehat{\star vol_U}) = J(e^{\arctan \tilde{\mathcal{F}}}) \wedge J(\widehat{\star vol_U}) = e^b \wedge \rho_{U,\mathcal{F}}. \quad (5.100)$$

The projection down to  $SO(T)$  via  $\pi_0$  gives indeed the induced gluing matrix. Indeed, we have

$$\pi_0 \left( \exp(\arctan \tilde{\mathcal{F}}) \cdot \widehat{\star vol_U} \right) = e_{SO(T)}^{\pi_{0*}(\arctan \tilde{\mathcal{F}})} \circ \pi_0(\widehat{\star vol_U}). \quad (5.101)$$

Now we find

$$\begin{aligned}
& e^{\pi_0^*(\arctan(f_k)e_{2k-1} \cdot e_{2k})} \\
&= e^{2 \arctan(f_k)e_{2k-1} \wedge e_{2k}} \\
&= \cos(2 \arctan(f_k)) + \sin(2 \arctan(f_k)) e_{2k-1} \wedge e_{2k} \\
&= \frac{1 - f_k^2}{1 + f_k^2} + \frac{2f_k}{1 + f_k^2} e_{2k-1} \wedge e_{2k} \\
&= \frac{1}{1 + f_k^2} \left( \begin{pmatrix} 1 - f_k^2 & 0 \\ 0 & 1 - f_k^2 \end{pmatrix} + \begin{pmatrix} 0 & -2f_k \\ 2f_k & 0 \end{pmatrix} \right), \tag{5.102}
\end{aligned}$$

which yields the matrix  $(j^*g + \mathcal{F})(j^*g - \mathcal{F})^{-1}$  while  $-id_{n-p}$  in the gluing matrix is accounted for by the projection of the volume form.

The fact that  $e^{-b} \bullet \rho_{U,F}$  can be identified as an element of  $Spin(T)$  enables us to show a generalisation of [60] to the case of  $G_L \times G_R$ -structures. Let  $\Psi_L, \Psi_R$  be two chiral unit spinors of the  $Spin(T)$ -representation  $\Delta$ . The real  $T \oplus T^*$ -spinor  $\rho^{ev,od} = e^{-\phi} \Re[\Psi_L \otimes \Psi_R]_b^{ev,od}$  satisfies  $|\langle \rho, \rho_{U,F} \rangle| \leq e^{-\phi}$ . Moreover, a pair  $(U^p, F)$  is calibrated if and only if

$$\mathcal{A}(\Psi_L) = \pm(-1)^{m(m+1)/2+p}(-i)^m e^{-b} \bullet \rho_{U,F} \cdot \Psi_R. \tag{5.103}$$

for  $n = 2m$  and  $\Psi_R \in \Delta_{\pm}$  and

$$\mathcal{A}(\Psi_L) = (-i)^{m+1} e^{-b} \bullet \rho_{U,F} \cdot \Psi_R. \tag{5.104}$$

for  $n = 2m + 1$ .

This can be proven as follows. Since  $e^{\mathcal{F}} \wedge \widehat{\star vol_U} = (\star e^{\mathcal{F}} \lrcorner vol_U)^\wedge$ , we have

$$\begin{aligned}
\langle \Re[\Psi_L \otimes \Psi_R]_b^{ev,od}, \rho_{U,F} \rangle &= \frac{1}{\sqrt{\det(j^*g - \mathcal{F})}} \langle \Re[\Psi_L \otimes \Psi_R]_b^{ev,od}, e^{\mathcal{F}} \wedge \widehat{\star vol_U} \rangle \\
&= \frac{1}{\sqrt{\det(j^*g - \mathcal{F})}} g(\Re[\Psi_L \otimes \Psi_R]^{ev,od}, e^{\mathcal{F}} \lrcorner vol_U) \\
&= \frac{1}{\sqrt{\det(j^*g - \mathcal{F})}} \sum \Re(\mathcal{A}(\Psi_L), e_I \cdot \Psi_R) g(e_I, e^{\mathcal{F}} \lrcorner vol_U) \\
&= \frac{1}{\sqrt{\det(j^*g - \mathcal{F})}} \Re(\mathcal{A}(\Psi_L), e^{\mathcal{F}} \lrcorner vol_U \cdot \Psi_R) \\
&\leq \frac{1}{\sqrt{\det(j^*g - \mathcal{F})}} \|\mathcal{A}(\Psi_L)\|_p \|e^{\mathcal{F}} \lrcorner vol_U \cdot \Psi_R\|_p, \tag{5.105}
\end{aligned}$$

On the other hand

$$\begin{aligned}
e^{\mathcal{F}} \lrcorner vol_U \cdot \Psi_R &= (-1)^{p(n-p)} (e^{\mathcal{F}} \lrcorner \star \star vol_U) \cdot \Psi_R \\
&= (-1)^{p(n-p)} \star (e^{-\mathcal{F}} \wedge \star vol_U) \cdot \Psi_R \\
&= (-1)^{p(n-p)} e^{\mathcal{F}} \wedge \widehat{\star vol_U} \cdot \text{Vol}_g \cdot \Psi_R \\
&= (-1)^{p(n-p)} \sqrt{\det(j^*g - \mathcal{F})} (e^{-b} \bullet \rho_{U,F}) \cdot vol_g \cdot \Psi_R. \tag{5.106}
\end{aligned}$$

Recall from above that a Riemannian volume form acts on chiral spinors by  $vol_g \cdot \Psi_{\pm} = \pm(-1)^{m(m+1)/2}(-i)^m \Psi_{\pm}$  for  $\Psi_{\pm} \in \Delta_{\pm}$ ,  $n = 2m$  and by  $vol_g \cdot \Psi = (-i)^{m+1} \Psi$  for  $n = 2m + 1$ . Since  $e^{-b} \wedge \rho_{U,F} \in Spin(T)$ , we have

$$\|e^{\mathcal{F}} \lrcorner vol_U \cdot \Psi_R\|_p = \sqrt{\det(j^*g - \mathcal{F})} \|e^{-b} \bullet \rho_{U,F}\|_g \|\Psi_R\|_p = \sqrt{\det(j^*g - \mathcal{F})}. \quad (5.107)$$

and consequently, (5.105) is less than or equal to 1 by the Cauchy-Schwarz inequality. Moreover, equality holds precisely if  $\mathcal{A}(\Psi_L) = (-1)^{p(n-p)}(e^{-b} \bullet \rho_{U,F}) \cdot vol_g \cdot \Psi_R$ . As there always exists a subspace  $U$  such that  $\mathcal{A}(\Psi_R) = vol_U \cdot \Psi_L$ , we can choose  $(U, j_U^*b)$  as a calibrated pair and choose the spinor

$$\rho^{ev,od} = e^{-\phi} \Re[\Psi_L \otimes \Psi_R]_b^{ev,od} \quad (5.108)$$

to define a calibration.

### 5.5.3 Examples

Let us give some examples of the generalised calibrations defined above, in particular how we obtain the well-known examples for branes in type IIA and type IIB string theory and the examples for  $G_2$ - and  $Spin(7)$ -structures of [160].

#### Generalised $SU(3)$ -structures

In the case of  $n = 6$  and  $\Psi_l = \Psi_r =: \Psi$  we are dealing with a classical  $SU(3)$  structure. In this case  $\rho^{ev} = e^{i\omega}$  where  $\omega$  is the Kähler form and  $\rho^{od} = \Omega$ , the holomorphic  $(3, 0)$  form. We can distinguish two cases, depending on the choice of the calibration form. If we choose  $\rho = \rho^{ev}$  as calibration form we are dealing with B-branes and get<sup>4</sup>

$$[e^{-F} \wedge j^*e^{i\omega}]^p = i^{(n-p)(n-p+1)} e^{i\alpha} \sqrt{\det(j^*g + F)} Vol_p. \quad (5.109)$$

We find that the dimension of the branes has to be even  $p =: 2k$  and find

$$\frac{1}{k!} (ij^*\omega + F)^k = i^{-k} e^{i\alpha} \sqrt{\det(j^*g + F)} Vol_p, \quad (5.110)$$

which also agrees with the results of [121, 137].

Calibrating with respect to  $\rho = \rho^{od}$  we are treating A-branes and find

$$[e^{-F} \wedge j^*\Omega]^p = i^{(n-p)(n-p+1)} e^{i\alpha} \sqrt{\det(j^*g + F)} Vol_p. \quad (5.111)$$

In this case  $p$  has to be odd, in fact it has to be equal to 3 or 5. For  $p = 3$  we get

$$j^*\Omega = e^{i\alpha} Vol_3, \quad (5.112)$$

---

<sup>4</sup>We set  $b = 0$  in the following. Including a nonvanishing  $b$ -field is straightforward as can be seen from (5.81).

which is nothing else but the condition for a special Lagrangian cycle that we used in the first part of this thesis to obtain supersymmetric D6-branes.

In the case  $p = 5$  we notice that we need a non-vanishing field strength  $F$  and obtain

$$j^*\Omega \wedge F = e^{i\alpha} \sqrt{\det(j^*g + F)} \text{Vol}_5, \quad (5.113)$$

which is the condition for a coisotropic A-brane, also found in [121].

If we are weakening our assumptions and go to the more general case of a  $SU(3) \times SU(3)$  structure  $\rho^{od}$  can also contain a one- and five-form part. For a related discussion on this aspect see also section 4 of [15].

### Generalised $G_2$ -structures

In dimension 7, the spinor  $\rho = e^{-\phi}[\Psi_L \otimes \Psi_R]_b$  gives rise to a  $G_2 \times G_2$ - or generalised  $G_2$ -structure. Since the  $Spin(7)$ -module  $\Delta$  carries a real structure,  $\rho^{ev,od}$  is real and therefore defines a calibration. If the spinors  $\Psi_L$  and  $\Psi_R$  are linearly independent, their stabilisers intersect in  $SU(3)$ .

Besides a one-form  $\alpha \in \Lambda^1$ ,  $SU(3)$  also fixes a symplectic two-form  $\omega$  and the real and imaginary parts of a holomorphic volume form on the orthogonal complement of the dual of  $\alpha$ . Letting  $c = \cos(\angle(\Psi_L, \Psi_R))$  and  $s = \sin(\angle(\Psi_L, \Psi_R))$ , we can write

$$\begin{aligned} [\Psi_L \otimes \Psi_R]^{ev} &= c + s\omega + c(\alpha \wedge \psi_- - \frac{1}{2}\omega^2) - s\alpha \wedge \psi_+ - \frac{1}{6}s\omega^3 \\ [\Psi_+ \otimes \Psi_-]^{od} &= s\alpha - c(\psi_+ + \alpha \wedge \omega) - s\psi_- - \frac{1}{2}s\alpha \wedge \omega^2 + c\text{vol}_g. \end{aligned} \quad (5.114)$$

Note that the forms  $\alpha$ ,  $\omega$  and  $\psi_{\pm}$  have no global meaning on a manifold. It follows

$$[\Psi \otimes \Psi]^{ev} = 1 - \star\varphi, \quad [\Psi \otimes \Psi]^{od} = -\varphi + \text{vol}_g, \quad (5.115)$$

for the straight case, where  $\varphi$  is the stable three-form associated with  $G_2$ . In the even case, the calibration condition reads

$$e^{-F} \wedge j^*(1 - \star\varphi) \leq \sqrt{\det(j^*g - F)} \text{vol}_U. \quad (5.116)$$

A co-associative four-plane (i.e.  $j^*\star\varphi = \text{vol}_U$ ) is calibrated for  $F = 0$ . For a non-trivial gauge field we find

$$g(F \wedge F/2 - \star\varphi, \text{vol}_{U^4}) = \sqrt{\det(j^*g - F)}. \quad (5.117)$$

We have  $F \wedge F/2 = \text{Pf}(F)\text{vol}_U$  and  $\det(j^*g - F) = 1 - \text{Tr}(F^2)/2 + \det(F)$ , so squaring yields the condition  $2\text{Pf}(F) = \text{Tr}(F^2)/2$  which holds if  $F$  is anti-self-dual (see [137]).

### Generalised $Spin(7)$ -structures

In dimension 7, the spinor  $\rho = e^{-\phi}[\Psi_L \otimes \Psi_R]_b$  gives rise to a  $Spin(7) \times Spin(7)$ - or generalised  $Spin(7)$ -structure. Here we consider the even case where both spinors are of equal chirality. In particular,  $\rho$  is even and therefore defines a calibration as the  $Spin(8)$ -space  $\Delta$  carries a real structure. If the spinors  $\Psi_L$  and  $\Psi_R$  are linearly independent, their stabilisers intersect in  $SU(4)$ . Written in the  $SU(4)$ -invariants  $\omega$  and  $\psi_{\pm}$  we find similarly to the  $G_2$ -case that

$$[\Psi_L \otimes \Psi_R] = c + s\omega + c(\psi_+ - \frac{1}{2}\omega^2) - s\psi_- \frac{s}{6}\omega^3 + c\text{vol}_g. \quad (5.118)$$

In the straight case we obtain  $[\Psi \otimes \Psi] = 1 - \Omega + \text{vol}_g$ , where  $\Omega$  is the self-dual 4-form. Again, Cayley four-planes (i.e.  $j^*\Omega = \text{vol}_{U^4}$ ) are calibrated with  $F = 0$  and, as above, Cayley planes are still calibrated if they carry an anti-self-dual two-form.

#### 5.5.4 Calibrations over manifolds

Let  $(M^n, g, b)$  be an oriented generalised Riemannian manifold. An even or odd spinor  $\rho^{ev,od} \in S^{\pm}$  is called a calibration if for any a pair  $(U, F)$  consisting of an oriented submanifold  $U$  and a two-form  $F \in \Omega^2(U)$ , the associated spinor

$$\rho_{U,F} = \frac{e^F \wedge \widehat{\star \text{vol}_U} \otimes \sqrt{\text{vol}_g}}{\sqrt{\det(j_U^*g - \mathcal{F})}}, \quad (5.119)$$

with  $\mathcal{F} = F - j_U^*b$  satisfies the inequality  $\langle \rho, \rho_{U,F} \rangle \leq 1$  over  $U$  and there exists at least one spinor  $\rho_{U,F}$  for which the bound is met. Such pairs  $(U, F)$  or spinors  $\rho_{U,F}$  are said to be calibrated by  $\rho^{ev,od}$ .

All results obtained in section 5.5.1 can be carried over to the global case, especially (5.81), (5.103) and (5.104). It follows that in particular, special Lagrangian, associative, co-associative or Caley submanifolds for classical  $SU(3)$ -,  $G_2$ - or  $Spin(7)$ -structures are calibrated in the sense above with respect the induced generalised structure.

For  $G_L \times G_R$ -structures, (5.103) and (5.104) assert that the  $G_L$ - and  $G_R$ -invariant spinors are related over a calibrated submanifold  $U$  by a section in the associated fibre bundle with fibre  $Spin(n)$ . This is the mathematical formulation of the notion that D-branes break part of the supersymmetry. In our context of  $G_L \times G_R$ -structures, calibrated pairs provide a natural notion of structured manifolds.

The key aspect of classical calibrated submanifolds is that they are volume minimising in their homology class if the calibration form is closed [107]. In presence of a non-trivial  $B$ - and  $F$ -field, closure of the calibration – now considered as a form – induces the calibrated submanifold  $(U, F)$  to maximise the quantity

$$I_{\phi}(U, F) = \int_U e^{-\phi} \sqrt{\det(j^*g - \mathcal{F})}, \quad (5.120)$$

where we introduced an additional scalar field – the dilaton.  $I_\phi$  can be identified as the DBI action for D-branes. Including the R-R potentials  $C$ , we get an additional term, namely

$$I_C(U, F) = - \int_U e^{-\mathcal{F}} \wedge C. \quad (5.121)$$

With  $C$  we are referring to even or odd differential forms.

### 5.5.5 Adding R-R fields

As observed in [105], the additional term (5.121) can be accounted for by non-closed calibration forms. This idea gave rise to minimising theorems of various flavours (see [104]). The following theorem is a straightforward generalisation of these ideas (see also [138], [139]).

Let  $d_H = d + H \wedge$  be the twisted differential induced by a closed three-form  $H$ , introduced in section 4.3, and  $(M^n, g, b)$  an oriented generalised Riemannian manifold,  $\phi \in C^\infty(M)$  and  $C \in \Omega^{ev,od}(M)$ . If  $\rho$  is a calibration such that

$$d_H e^{-\phi} \rho = d_H(e^b \wedge C), \quad (5.122)$$

then any calibrated pair  $(U, F)$  with  $j_U^* H = dj_U^* b$  is locally energy-minimising for  $I = I_\phi + I_C$  in the following sense. For given open discs  $D \subset U$ ,  $D' \subset M$  with  $\partial D = \partial D'$  and  $j_{D,D'}^* H = dj_{D,D'}^* b$ , together with two-forms  $F, F'$  such that  $F_{\partial D} = F'_{\partial D'}$ , we have  $I(D, F) \leq I(D', F')$ .

To show this we note the following. From the calibration condition we deduce

$$[e^{-F} \wedge j_U^* e^{-\phi} \rho]^p \leq e^{-\phi} \sqrt{\det(j_U^* g - \mathcal{F})}, \quad (5.123)$$

while the integrability condition implies

$$e^{-\phi} \rho - e^b \wedge C = d_H A \quad (5.124)$$

for some differential form  $A$ . By Stokes' theorem we obtain

$$\begin{aligned} I(D, F) &= \int_D e^{-F} \wedge j_D^* e^{-\phi} \rho - \int_D e^{-F} \wedge j_D^* (e^b \wedge C^\bullet) \\ &= \int_D e^{-F} \wedge j_D^* dA \\ &= \int_{\partial D} e^{-\mathcal{F}} \wedge j_D^* A, \end{aligned} \quad (5.125)$$

since  $(D, F)$  is calibrated and  $e^{-\mathcal{F}} \wedge j^* d_H A = d(e^{-\mathcal{F}} \wedge j_D^* A)$  for  $j_D^* H = dj_D^* b$ . On the

other hand, we have

$$\begin{aligned} I(D', F') &\geq \int_{D'} e^{-F'} \wedge j_{D'}^* e^{-\phi} \rho - \int_{D'} e^{-F'} \wedge j_{D'}^* (e^b \wedge C^\bullet) \\ &= - \int_{\partial D'} e^{-F'} \wedge j_{D'}^* A = I(D, F). \end{aligned} \quad (5.126)$$

For calibrations of the form  $\rho = [\Psi_L \otimes \Psi_R]_b$ , condition (5.122) is equivalent to

$$d_H e^{-\phi} [\Psi_L \otimes \Psi_R] = F^{RR}, \quad (5.127)$$

where  $F^{RR} = d_H C$  are the R-R fields associated with the potential  $C$ . In [116], this type of equation was shown to be equivalent to the compactification to six or seven dimensions of the spinor field equations as given by the democratic formulation of supergravity in [17].

### 5.5.6 T-duality transformation of calibrations

Using the results of section 5.1, we can investigate how a generalised calibration transforms under T-duality. Let  $\rho$  define a calibration for a generalised metric  $(g, b)$  and  $\theta \in T^*$ . According to section 5.5.1, we have for submanifolds  $\rho_{U,F}$  that

$$\langle \rho, \rho_{U,F} \rangle \leq 1. \quad (5.128)$$

Applying T-duality and denoting the T-dual calibration with  $\rho^T$ , as defined in (5.12), we get

$$(-1)^{n+1} \langle \rho^T, \widetilde{\mathcal{M}}_\theta \bullet \rho_{U,F} \rangle \leq 1. \quad (5.129)$$

Since T-duality is orbit and norm preserving, we have that  $(-1)^{n+1} \rho_{U,F}^T$  is pure and of unit norm, so it equals  $\rho_{U^T, F^T}$  for some suitably oriented pair  $(U^T, F^T)$ .

Including the R-R fields, we can use our considerations from section 5.1.2 and extend the T-duality transformation to include non-trivial R-R potentials  $C$ . Let  $(g, b, \phi)$  be an  $S^1$ -invariant generalised metric,  $\phi$  a scalar dilaton and  $\rho$  an  $S^1$ -invariant calibration that satisfies

$$d_H e^{-\phi} [\rho]_g = d_H (e^b \wedge C). \quad (5.130)$$

If  $(U, F)$  is a calibrated cycle that locally minimises the energy-functional, including  $I_C$  as defined in (5.121). We define the T-dual forms by

$$C^T = e^{-b^T} \wedge (-X_\perp + \theta \wedge) e^b \wedge C \quad (5.131)$$

and have that the T-dualised submanifold  $(U^T, F^T)$  minimises the T-dualised energy-functional  $I_{C^T}$ .



This can be seen by the following reasoning. Using (5.129) we have

$$\langle \rho^T, \rho_{U^T, F^T} \rangle \leq 1, \quad (5.132)$$

and therefore

$$e^{-F^T} \wedge j_{U^T}^* e^{-\phi + \ln \|X\|} \rho^T \leq e^{-\phi + \ln \|X\|} \sqrt{\det(j_{U^T}^* g^T - \mathcal{F}^T)}. \quad (5.133)$$

Applying (5.19), we calculate

$$\begin{aligned} d_{H^T} e^{-\phi^T} [\rho^T]_{g^T} &= d_{H^T} \|X\| e^{-\phi} [\rho^T]_{g^T} \\ &\cong (X_{\perp} - \theta \wedge) d_H e^{-\phi} [\rho]_g \\ &= (X_{\perp} - \theta \wedge) d_H (e^b \wedge C) \\ &\cong d_{H^T} (-X_{\perp} + \theta \wedge) e^b \wedge C \\ &= d_{H^T} (e^{b^T} \wedge C^T). \end{aligned} \quad (5.134)$$

This shows that the T-dualised spinor  $\rho^T$  indeed minimises the T-dualised energy functional.



# Appendix A

## Orientifold models

In this chapter we summarise the concrete examples of orientifold models that are used in the statistical analysis in chapters 2 and 3. We fix the notation and translate the conditions explained in general in section 2.1 into variables that suit the specific cases and simplify the computations.

### A.1 $T^2$

For compactification on  $T^2$ , a special Lagrangian submanifold is specified by two wrapping numbers  $(n_a, m_a)$  around the fundamental one-cycles. In this case these numbers are precisely identical to the numbers  $(X_a, Y_a)$  used in section 2.1.

The tadpole cancellation condition (2.6) reads

$$\sum_a N_a X_a = L, \tag{A.1}$$

where the physical value is  $L = 16$ .

The first supersymmetry condition of (2.7) reads just

$$Y_a = 0, \tag{A.2}$$

and is independent of the complex structure  $U = R_2/R_1$  on the rectangular torus. This implies that all supersymmetric branes must lie along the x-axis, i.e. on top of the orientifold plane. The second supersymmetry condition in (2.7) becomes

$$X_a > 0. \tag{A.3}$$

From these conditions we can immediately deduce that if one does not allow for multiple wrapping, as it is usually done in this framework, there would only exist one supersymmetric brane, namely the one with  $(X, Y) = (1, 0)$ .

## A.2 $\mathbf{T}^4/\mathbb{Z}_2$

In this case a class of special Lagrangian branes is given by so-called factorisable branes, which can be defined by two pairs of wrapping numbers  $(n_i, m_i)$  on two  $T^2$ s. The wrapping numbers  $(X^i, Y^i)$  with  $i = 1, 2$  for the  $\mathbb{Z}_2$  invariant two-dimensional cycles are then given by

$$\begin{aligned} X^1 &= n_1 n_2, & X^2 &= m_1 m_2, \\ Y^1 &= n_1 m_2, & Y^2 &= m_1 n_2. \end{aligned} \quad (\text{A.4})$$

To simplify matters we sometimes use a vector notation  $\vec{X} = (X^1, X^2)^T$  and  $\vec{Y} = (Y^1, Y^2)^T$ .

Note that these branes do not wrap the most general homological class, for the 2-cycle wrapping numbers satisfy the relation

$$X^1 X^2 = Y^1 Y^2. \quad (\text{A.5})$$

However, for a more general class we do not know how the special Lagrangians look like. Via brane recombination it is known that there exist flat directions in the D-brane moduli space, corresponding to branes wrapping non-flat special Lagrangians. Avoiding these complications, we use the well understood branes introduced above only.

The untwisted tadpole cancellation conditions read

$$\begin{aligned} \sum_a N_a X_a^1 &= L^1, \\ \sum_a N_a X_a^2 &= -L^2, \end{aligned} \quad (\text{A.6})$$

with the physical values  $L_1 = L_2 = 8$ . In order to put these equations on the same footing, we change the sign of  $X_2$  to get

$$\begin{aligned} \sum_a N_a X_a^1 &= L^1, \\ \sum_a N_a X_a^2 &= L^2. \end{aligned} \quad (\text{A.7})$$

Note that in contrast to models discussed for example in [89], we are only considering bulk branes without any twisted sector contribution for simplicity<sup>1</sup>. Defining the two form  $\Omega_2 = (dx_1 + iU_1 dy_1)(dx_2 + iU_2 dy_2)$ , the supersymmetry conditions become

$$\begin{aligned} U_1 Y^1 + U_2 Y^2 &= 0, \\ X^1 + U_1 U_2 X^2 &> 0. \end{aligned} \quad (\text{A.8})$$

The intersection number between two bulk branes has an extra factor of two

$$I_{ab} = -2 (X_a^1 X_b^2 + X_2^a X_b^1 + Y_a^1 Y_b^2 + Y_a^2 Y_b^1). \quad (\text{A.9})$$

<sup>1</sup>For a treatment of fractional branes in this framework see e.g. [19, 20].

### A.2.1 Multiple wrapping

In the case of  $T^2$  it made no sense to restrict the analysis of supersymmetric branes to those which are not multiply wrapped around the torus, because there would have been just one possible construction. In the case of  $T^4/\mathbb{Z}_2$  the situation is different and we would like to derive the constraints on the wrapping numbers  $\vec{X}$  and  $\vec{Y}$ .

For the original wrapping numbers  $n_i, m_i$  the constraint to forbid multiple wrapping is  $\gcd(n_i, m_i) = 1 \ \forall i = 1, 2$ . Without losing information we can multiply these two to get

$$\gcd(n_1, m_1) \gcd(n_2, m_2) = 1. \quad (\text{A.10})$$

Using the definitions (A.4) of  $\vec{X}$  and  $\vec{Y}$ , we can rewrite this as

$$\gcd(X^1, Y^2) \gcd(X^2, Y^2) = Y_2, \quad (\text{A.11})$$

which is invariant under an exchange of  $X$  and  $Y$ .

## A.3 $T^6/\mathbb{Z}_2 \times \mathbb{Z}_2$

In the case of compactifications on this six-dimensional orientifold, which has been studied by many authors (see e.g. [82, 59, 58, 129, 78, 22]) the situation is very similar to the four-dimensional case above. We can describe factorisable branes by their wrapping numbers  $(n_i, m_i)$  along the basic one-cycles  $\pi_{2i-1}, \pi_{2i}$  of the three two-tori  $T^6 = \prod_{i=1}^3 T_i^2$ . To preserve the symmetry generated by the orientifold projection  $\Omega\bar{\sigma}$ , only two different shapes of tori are possible, which can be parametrised by  $b_i \in \{0, 1/2\}$  and transform as

$$\Omega\bar{\sigma} : \begin{cases} \pi_{2i-1} & \rightarrow \pi_{2i-1} - 2b_i\pi_{2i} \\ \pi_{2i} & \rightarrow -\pi_{2i} \end{cases}. \quad (\text{A.12})$$

For convenience we work with the combination  $\tilde{\pi}_{2i-1} = \pi_{2i-1} - b_i\pi_{2i}$  and modified wrapping numbers  $\tilde{m}_i = m_i + b_in_i$ . Furthermore we introduce a rescaling factor

$$c := \left( \prod_{i=1}^3 (1 - b_i) \right)^{-1} \quad (\text{A.13})$$

to get integer-valued coefficients. These are explicitly given by  $(i, j, k \in \{1, 2, 3\}$  cyclic)

$$\begin{aligned} X^0 &= cn_1n_2n_3, & X^i &= -cn_i\tilde{m}_j\tilde{m}_k, \\ Y^0 &= c\tilde{m}_1\tilde{m}_2\tilde{m}_3, & Y^i &= -c\tilde{m}_i n_j n_k. \end{aligned} \quad (\text{A.14})$$

The wrapping numbers  $\vec{X}$  and  $\vec{Y}$  are not independent, but satisfy the following relations:

$$\begin{aligned} X_I Y_I &= X_J Y_J, \\ X_I X_J &= Y_K Y_L, \\ X_L (Y_L)^2 &= X_I X_J X_K, \\ Y_L (X_L)^2 &= Y_I Y_J Y_K, \end{aligned} \tag{A.15}$$

for all  $I, J, K, L \in \{0, \dots, 3\}$  cyclic.

Using these conventions the intersection numbers can be written as

$$I_{ab} = \frac{1}{c^2} \left( \vec{X}_a \vec{Y}_b - \vec{X}_b \vec{Y}_a \right). \tag{A.16}$$

The tadpole cancellation conditions read

$$\sum_{a=1}^k N_a \vec{X}_a = \vec{L}, \quad \vec{L} = \begin{pmatrix} 8c \\ \{8/(1-b_i)\} \end{pmatrix}, \tag{A.17}$$

where we used that the value of the physical orientifold charge is 8 in our conventions.

The supersymmetry conditions can be written as

$$\begin{aligned} \sum_{I=0}^3 \frac{Y^I}{U_I} &= 0, \\ \sum_{I=0}^3 X^I U_I &> 0, \end{aligned} \tag{A.18}$$

where we used that the complex structure moduli  $U_I$  can be defined in terms of the radii ( $R_i^{(1)}, R_I^{(2)}$ ) of the three tori as

$$\begin{aligned} U_0 &= R_1^{(1)} R_1^{(2)} R_1^{(3)}, \\ U_i &= R_1^{(i)} R_2^{(j)} R_2^{(k)}, \quad i, j, k \in \{1, 2, 3\} \text{ cyclic.} \end{aligned} \tag{A.19}$$

Finally the K-theory constraints can be expressed as

$$\sum_{a=1}^k N_a Y_a^0 \in 2\mathbb{Z}, \quad \frac{1-b_i}{c} \sum_{a=1}^k N_a Y_a^i \in 2\mathbb{Z}, \quad i \in \{1, 2, 3\}. \tag{A.20}$$

### A.3.1 Multiple wrapping

We can define the condition to exclude multiple wrapping in a way similar to the  $T^4$ -case. A complication that arises is the possibility to have tilted tori. In the definition

of  $\vec{X}$  and  $\vec{Y}$  in (A.14) we used the wrapping numbers  $\tilde{m}_i$ , which have been defined to include the possible tilt. To analyse coprime wrapping numbers, however, we have to deal with the original wrapping numbers  $m_i$ , such that

$$\prod_{i=1}^3 \gcd(n_i, m_i) = 1. \quad (\text{A.21})$$

We can express this condition in terms of the variables  $\vec{\tilde{X}}$  and  $\vec{\tilde{Y}}$ , defined as

$$\begin{aligned} \tilde{X}^0 &= n_1 n_2 n_3, & \tilde{Y}^0 &= m_1 m_2 m_3, \\ \tilde{X}^i &= n_i n_j n_k, & \tilde{Y}^i &= m_i n_j n_k, \end{aligned} \quad (\text{A.22})$$

where  $i, j, k \in \{1, 2, 3\}$  cyclic, analogous to section A.2.1

$$\prod_{i=1}^3 \gcd(\tilde{Y}^0, \tilde{X}^i) = (\tilde{Y}^0)^2. \quad (\text{A.23})$$

The  $\vec{\tilde{X}}$  and  $\vec{\tilde{Y}}$  can be expressed in terms of the  $\vec{X}$  and  $\vec{Y}$  of (A.14), using their definition (A.21) and the rescaling factor (A.13), as

$$\begin{aligned} \tilde{X}^0 &= c^{-1} X^0, \\ \tilde{X}^i &= c^{-1} (-X^i + b_j Y^k + b_k Y^j + b_j b_k X^0), \\ \tilde{Y}^0 &= c^{-1} \left( Y^0 + \sum_{i=1}^3 b_i X^i - \sum_{i=1}^3 b_j b_k Y^i - b_1 b_2 b_3 X^0 \right), \\ \tilde{Y}^i &= c^{-1} (-Y^i - b_i X^0). \end{aligned} \quad (\text{A.24})$$





# Appendix B

## Partition algorithm

In this part of the appendix we briefly outline the partition algorithm used in the computer analysis of vacua<sup>1</sup>. It is designed to calculate the unordered partition of a natural number  $n$ , restricted to a maximal number of  $m$  factors, using only a subset  $F \subset \mathbb{N}$  of allowed factors to appear in the partition.

To describe the main idea, let us drop the additional constraints on the length and factors of the partition. They can be added easily to the algorithm, for details see the comments in listing B.2. The result is stored in a list  $\{a_i\}$ , which is initialized with  $a_i = n\delta_{1,i}$ . An internal pointer  $q$  is set to the first element at the beginning and after each call of the main routine the list  $a$  contains the next partition. The length of this partition is stored in a variable  $m$ , which is set to  $m = 0$ , after the last partition has been generated.

The main routine contains the following steps. It checks if the element  $a_q$  is equal to 1 – if yes, it sets  $q = q - 1$ . This is repeated until  $a_q > 1$  or  $q = 0$  – in this case no new partitions exist,  $m$  is set to 0 and the algorithm terminates. In the second step the routine sets  $a_q = a_q - 1$ ,  $a_{q+1} = a_{q+1} + 1$  and  $q = q + 1$ . But this operation is only performed if  $a_{q+1} < a_q$  and  $a_q > 1$ , otherwise the counter  $q$  is reduced by one and the algorithm starts over.

Let us give an example to illustrate this procedure. Consider the unordered partitions of 5:

$$\{ \{5\}, \{4, 1\}, \{3, 2\}, \{3, 1, 1\}, \{2, 2, 1\}, \{2, 1, 1, 1\}, \{1, 1, 1, 1, 1\} \}. \quad (\text{B.1})$$

Starting with 5 itself, the first time we call the algorithm, it decreases  $a_1$  to  $a_1 = 4$ , increases  $a_2$  to  $a_2 = 1$ , which generates the partition  $\{4, 1\}$ . The pointer  $q$  is increased to  $q = 2$ . The next time we call the routine, the element  $a_q = a_2$  is equal to 1, which leads to  $q = 1$ . Now the condition  $a_q > 1$  is satisfied and the result of  $a_q = a_q - 1$ ,  $a_{q+1} = a_{q+1} + 1$  gives the partition  $\{3, 2\}$ . Continuing in this way, four more partitions of 5 are generated, until we reach  $\{1, 1, 1, 1, 1\}$ . We have  $a_i = 1$  for all  $i = 1, \dots, 5$ , which leads to the termination of the algorithm in the first step.

---

<sup>1</sup>The complete program used to generate the solutions, which is written in C, can be obtained from the author upon request.

## B.1 Implementation

The algorithm uses a data structure `partition` to collect the necessary parameters and internal variables:

```
typedef struct _partition { long n,m,q,*fac,*a,min; } partition;
```

Here  $n \in \mathbb{N}$  is the number to be partitioned and `m` holds the length of the partition list `a`. The array `fac` contains the set  $F$  of allowed values of partition factors. `min` and `q` are internal variables to be explained below. Besides these internal variables, a global variable `maxp` is used, which contains the maximal length of the partition.

The algorithm itself is split into two parts. The function `apartitions_first` is called once at the beginning of the program loop that runs through all partitions. It initializes the internal variables `n` and `fac` and calculates the minimum possible value for a partition factor from the list `fac`. Finally it checks if `n` itself is contained in `fac` and calls the main routine `apartitions_next` if this is not the case.

```
void apartitions_first(long n, long *f, partition *p) {
    long i;
    /* check if we're supposed to do anything */
    if ((n>0)&&(maxp==0)) {
        p->m=0;
        return;
    }
    /* find minimum and check consistency */
    p->min=n+1;
    i=1;
    while (i<=n) {
        if (f[i]>0) {
            p->min=i;
            i=n+1;
        } else {
            i++;
        }
    }
    if (p->min>n) {
        p->m=0;
        return;
    }
    /* init data structure */
    p->n=n;
    p->fac=f;
    p->a=malloc((n+1)*sizeof(long));
    p->a[0]=p->n;
    p->m=1;
    p->a[1]=p->n;
    p->q=1;
    /* generate first partition (check if n is allowed...) */
    if (f[n]<=0) {
        apartitions_next(p);
    }
}
```

Listing B.1: Partition algorithm, initial routine

The main routine can be called subsequently as long as the length `m` of the partition list `a` is positive. Each call will produce a new partition of `n`. Special care has to be

taken if elements of the partition are not contained in `fac` – see the comments in the source code for these subtleties.

```

void apartitions_next(partition *p) {
    /* set the number n what we have to distribute to 0. */
    p->n=0;
    /* go back until there is a value bigger then the minimum min to distribute
    and the partition doesn't get too long. */
    while (((p->q>=maxp)||((p->q>0)&&(p->a[p->q]==p->min)))) {
        p->n=p->n+p->a[p->q];
        p->q=p->q-1;
    }
    /* loop through the distribution process as long as we're not back at the
    beginning of the factor list. */
    while (p->q>0) {
        /* lower the actual value at q we're trying to distribute by 1 and add 1 to
        the distribution account. then increase the list-length m by one. */
        p->a[p->q]=p->a[p->q]-1;
        p->n=p->n+1;
        p->m=p->q+1;
        /* as long as the new factor is > then the one before or it is not in
        fac, subtract 1 from it (and add 1 to n). do this as long as it is >
        then the minimum. */
        while (((p->a[p->q]>p->a[p->q-1])||((p->fac[p->a[p->q]]<=0))
            &&(p->a[p->q]>=p->min)) {
            p->a[p->q]=p->a[p->q]-1;
            p->n=p->n+1;
        }
        /* check if the new factor is lower or equal then the one before and it's
        in fac (the loop above might have terminated on the minimum condition).
        if yes, add the distribution sum to the new factor at q+1. if not, add the
        whole factor at q to n and go one step back in the list. */
        if ((p->a[p->q]<=p->a[p->q-1])&&(p->fac[p->a[p->q]]>0)) {
            p->q=p->q+1;
            p->a[p->q]=p->n;
        }
        /* if the new factor is < then the one before and in our list return. */
        if ((p->a[p->q]<=p->a[p->q-1])&&(p->fac[p->a[p->q]]>0)) {
            return;
        } else {
            /* so the new factor is not smaller or in our list – means we have to
            redistribute some of it to a new factor. but if we are already at the
            maximum length of the partition we have to go one step back! */
            if (p->q < maxhidden) {
                p->n=0;
            } else {
                p->q=p->q-1;
            }
        }
    } else {
        p->n=p->n+p->a[p->q];
        p->q=p->q-1;
    }
}
/* if the pointer is q is 0 there is nothing left to do – free memory and
return 0 for the length of the partition */
if (p->q <= 0) {
    free(p->a); p->m=0;
}
}

```

Listing B.2: Partition algorithm, main routine



# Bibliography

- [1] B. S. ACHARYA, F. DENEFF, AND R. VALANDRO. Statistics of M theory vacua. *JHEP* **06** (2005) 056, [[hep-th/0502060](#)].
- [2] C. ALBERTSSON, U. LINDSTRÖM, AND M. ZABZINE.  $N = 1$  supersymmetric sigma model with boundaries. I. *Commun. Math. Phys.* **233** (2003) 403–421, [[hep-th/0111161](#)].
- [3] C. ALBERTSSON, U. LINDSTRÖM, AND M. ZABZINE.  $N = 1$  supersymmetric sigma model with boundaries. II. *Nucl. Phys.* **B678** (2004) 295–316, [[hep-th/0202069](#)].
- [4] G. E. ANDREWS. The theory of partitions. in *Encyclopedia of Mathematics and its Applications, Vol. 2*. Addison Wesley, 1976.
- [5] I. ANTONIADIS, E. KIRITSIS, AND T. N. TOMARAS. A D-brane alternative to unification. *Phys. Lett.* **B486** (2000) 186–193, [[hep-ph/0004214](#)].
- [6] H. ARFAEI AND M. M. SHEIKH JABBARI. Different D-brane interactions. *Phys. Lett.* **B394** (1997) 288–296, [[hep-th/9608167](#)].
- [7] N. ARKANI-HAMED, S. DIMOPOULOS, AND S. KACHRU. Predictive landscapes and new physics at a TeV. [hep-th/0501082](#).
- [8] S. ASHOK AND M. R. DOUGLAS. Counting flux vacua. *JHEP* **01** (2004) 060, [[hep-th/0307049](#)].
- [9] M. AXENIDES, E. FLORATOS, AND C. KOKORELIS.  $SU(5)$  unified theories from intersecting branes. *JHEP* **10** (2003) 006, [[hep-th/0307255](#)].
- [10] V. BALASUBRAMANIAN AND R. G. LEIGH. D-branes, moduli and supersymmetry. *Phys. Rev.* **D55** (1997) 6415–6422, [[hep-th/9611165](#)].
- [11] T. BANKS. Landskepticism or why effective potentials don't count string models. [hep-th/0412129](#).
- [12] T. BANKS, M. DINE, AND E. GORBATOV. Is there a string theory landscape? *JHEP* **08** (2004) 058, [[hep-th/0309170](#)].

- [13] S. M. BARR. A New Symmetry Breaking Pattern For  $SO(10)$  and Proton Decay. *Phys. Lett.* **B112** (1982) 219.
- [14] O. BEN-BASSAT. Mirror symmetry and generalized complex manifolds. *J. Geom. Phys.* **56** (2006) 533–558, [[math.ag/0405303](#)].
- [15] I. BENMACHICHE AND T. W. GRIMM. Generalized  $N = 1$  orientifold compactifications and the Hitchin functionals. [hep-th/0602241](#).
- [16] E. BERGSHOEFF, R. KALLOSH, T. ORTIN, AND G. PAPADOPOULOS. Kappa-symmetry, supersymmetry and intersecting branes. *Nucl. Phys.* **B502** (1997) 149–169, [[hep-th/9705040](#)].
- [17] E. BERGSHOEFF, R. KALLOSH, T. ORTIN, D. ROEST, AND A. VAN PROEYEN. New formulations of  $D = 10$  supersymmetry and  $D8 - O8$  domain walls. *Class. Quant. Grav.* **18** (2001) 3359–3382, [[hep-th/0103233](#)].
- [18] M. BERKOOZ, M. R. DOUGLAS, AND R. G. LEIGH. Branes intersecting at angles. *Nucl. Phys.* **B480** (1996) 265–278, [[hep-th/9606139](#)].
- [19] R. BLUMENHAGEN, V. BRAUN, B. KÖRS, AND D. LÜST. Orientifolds of  $K3$  and Calabi-Yau manifolds with intersecting D-branes. *JHEP* **07** (2002) 026, [[hep-th/0206038](#)].
- [20] R. BLUMENHAGEN, V. BRAUN, B. KÖRS, AND D. LÜST. The standard model on the quintic. [hep-th/0210083](#).
- [21] R. BLUMENHAGEN, M. CVETIČ, P. LANGACKER, AND G. SHIU. Toward Realistic Intersecting D-Brane Models. [hep-th/0502005](#).
- [22] R. BLUMENHAGEN, M. CVETIČ, F. MARCHESANO, AND G. SHIU. Chiral D-brane models with frozen open string moduli. *JHEP* **03** (2005) 050, [[hep-th/0502095](#)].
- [23] R. BLUMENHAGEN, F. GMEINER, G. HONECKER, D. LÜST, AND T. WEIGAND. The statistics of supersymmetric D-brane models. *Nucl. Phys.* **B713** (2005) 83–135, [[hep-th/0411173](#)].
- [24] R. BLUMENHAGEN, B. KÖRS, D. LÜST, AND T. OTT. The standard model from stable intersecting brane world orbifolds. *Nucl. Phys.* **B616** (2001) 3–33, [[hep-th/0107138](#)].
- [25] R. BLUMENHAGEN, D. LÜST, AND S. STIEBERGER. Gauge unification in supersymmetric intersecting brane worlds. *JHEP* **07** (2003) 036, [[hep-th/0305146](#)].
- [26] R. BLUMENHAGEN, D. LÜST, AND T. R. TAYLOR. Moduli stabilization in chiral type IIB orientifold models with fluxes. *Nucl. Phys.* **B663** (2003) 319–342, [[hep-th/0303016](#)].

- [27] R. BLUMENHAGEN, S. MOSTER, AND T. WEIGAND. Heterotic GUT and standard model vacua from simply connected Calabi-Yau manifolds. [hep-th/0603015](#).
- [28] R. BLUMENHAGEN AND T. WEIGAND. Chiral supersymmetric Gepner model orientifolds. *JHEP* **02** (2004) 041, [[hep-th/0401148](#)].
- [29] V. BOUCHARD, M. CVETIC, AND R. DONAGI. Tri-linear couplings in an heterotic minimal supersymmetric standard model. [hep-th/0602096](#).
- [30] R. BOUSSO AND J. POLCHINSKI. Quantization of four-form fluxes and dynamical neutralization of the cosmological constant. *JHEP* **06** (2000) 006, [[hep-th/0004134](#)].
- [31] P. BOUWKNEGT, J. EVSLIN, AND V. MATHAI. T-Duality: Topology Change from H-flux. *Comm. Math. Phys.* **249** (2004) 383–415, [[hep-th/0306062](#)].
- [32] V. BRAUN, Y.-H. HE, B. A. OVRUT, AND T. PANTEV. The exact MSSM spectrum from string theory. [hep-th/0512177](#).
- [33] A. BREDTHAUER, U. LINDSTRÖM, J. PERSSON, AND M. ZABZINE. Generalized Kähler geometry from supersymmetric sigma models. [hep-th/0603130](#).
- [34] I. BRUNNER, K. HORI, K. HOSOMICHI, AND J. WALCHER. Orientifolds of Gepner models. [hep-th/0401137](#).
- [35] T. H. BUSCHER. A symmetry of the string background field equations. *Phys. Lett.* **B194** (1987) 59.
- [36] T. H. BUSCHER. Path integral derivation of quantum duality in nonlinear sigma models. *Phys. Lett.* **B201** (1988) 466.
- [37] P. CANDELAS, G. T. HOROWITZ, A. STROMINGER, AND E. WITTEN. Vacuum configurations for superstrings. *Nucl. Phys.* **B258** (1985) 46–74.
- [38] G. L. CARDOSO, G. CURIO, G. DALL’AGATA, D. LÜST, P. MANOUSSELIS, AND G. ZOUPANOS. Non-Kähler String Backgrounds and their Five Torsion Classes. *Nucl. Phys.* **B652** (2003) 5–34, [[hep-th/0211118](#)].
- [39] G. L. CARDOSO, D. LÜST, AND J. PERZ. Entropy maximization in the presence of higher-curvature interactions. [hep-th/0603211](#).
- [40] J. F. G. CASCALES AND A. M. URANGA. Chiral 4d  $N = 1$  string vacua with D-branes and NSNS and RR fluxes. *JHEP* **05** (2003) 011, [[hep-th/0303024](#)].
- [41] G. CAVALCANTI. New aspects of the ddc-lemma. DPhil thesis, Oxford University, 2005. [math.DG/0501406](#).

- [42] C.-M. CHEN, G. V. KRANIOTIS, V. E. MAYES, D. V. NANOPOULOS, AND J. W. WALKER. A K-theory anomaly free supersymmetric flipped SU(5) model from intersecting branes. *Phys. Lett.* **B625** (2005) 96–105, [[hep-th/0507232](#)].
- [43] C.-M. CHEN, G. V. KRANIOTIS, V. E. MAYES, D. V. NANOPOULOS, AND J. W. WALKER. A supersymmetric flipped SU(5) intersecting brane world. *Phys. Lett.* **B611** (2005) 156–166, [[hep-th/0501182](#)].
- [44] C.-M. CHEN, T. LI, AND D. V. NANOPOULOS. Flipped and Unflipped SU(5) as Type IIA Flux Vacua. [hep-th/0604107](#).
- [45] C.-M. CHEN, T. LI, AND D. V. NANOPOULOS. Type IIA Pati-Salam flux vacua. *Nucl. Phys.* **B740** (2006) 79–104, [[hep-th/0601064](#)].
- [46] C.-M. CHEN, V. E. MAYES, AND D. V. NANOPOULOS. Flipped SU(5) from D-branes with type IIB fluxes. *Phys. Lett.* **B633** (2006) 618–626, [[hep-th/0511135](#)].
- [47] T. CHENG AND L. LI. Gauge Theory of Elementary Particle Physics. Oxford Science Publications. Oxford, UK: Clarendon, 1984.
- [48] S. CHIANTESE. Isotropic A-branes and the stability condition. *JHEP* **02** (2005) 003, [[hep-th/0412181](#)].
- [49] S. CHIANTESE, F. GMEINER, AND C. JESCHEK. Mirror symmetry for topological sigma models with generalized Kähler geometry. *Int. J. Mod. Phys.* **A21** (2006) 2377–2389, [[hep-th/0408169](#)].
- [50] J. P. CONLON AND F. QUEVEDO. On the explicit construction and statistics of Calabi-Yau flux vacua. *JHEP* **10** (2004) 039, [[hep-th/0409215](#)].
- [51] T. COURANT. Dirac manifolds. *Trans. Amer. Math. Soc.* **319** (1990) 631–661.
- [52] T. COURANT AND A. WEINSTEIN. Beyond Poisson structures. in *Action hamiltoniennes de groupes. Troisième théorème de Lie (Lyon 1986)*, Vol. 27 of Travaux en Cours, pp. 39–49. Paris, France: Hermann, 1988.
- [53] E. CREMMER, B. JULIA, AND J. SCHERK. Supergravity theory in 11 dimensions. *Phys. Lett.* **B76** (1978) 409–412.
- [54] M. CVETIČ, T. LI, AND T. LIU. Supersymmetric Pati-Salam models from intersecting D6-branes: A road to the standard model. *Nucl. Phys.* **B698** (2004) 163–201, [[hep-th/0403061](#)].
- [55] M. CVETIČ, T. LI, AND T. LIU. Standard-like models as type IIB flux vacua. *Phys. Rev.* **D71** (2005) 106008, [[hep-th/0501041](#)].
- [56] M. CVETIČ AND I. PAPANIMITRIOU. More supersymmetric standard-like models from intersecting D6-branes on type IIA orientifolds. *Phys. Rev.* **D67** (2003) 126006, [[hep-th/0303197](#)].



- [57] M. CVETIČ, I. PAPADIMITRIOU, AND G. SHIU. Supersymmetric three family SU(5) grand unified models from type IIA orientifolds with intersecting D6-branes. *Nucl. Phys.* **B659** (2003) 193–223, [[hep-th/0212177](#)].
- [58] M. CVETIČ, G. SHIU, AND A. M. URANGA. Chiral four-dimensional  $N = 1$  supersymmetric type IIA orientifolds from intersecting D6-branes. *Nucl. Phys.* **B615** (2001) 3–32, [[hep-th/0107166](#)].
- [59] M. CVETIČ, G. SHIU, AND A. M. URANGA. Three-family supersymmetric standard like models from intersecting brane worlds. *Phys. Rev. Lett.* **87** (2001) 201801, [[hep-th/0107143](#)].
- [60] J. DADOK AND F. HARVEY. Calibrations and spinors. *Acta Math.* **170** (1993), no. 1 83–120.
- [61] F. DENEFF AND M. R. DOUGLAS. Distributions of flux vacua. *JHEP* **05** (2004) 072, [[hep-th/0404116](#)].
- [62] F. DENEFF AND M. R. DOUGLAS. Distributions of nonsupersymmetric flux vacua. *JHEP* **03** (2005) 061, [[hep-th/0411183](#)].
- [63] F. DENEFF AND M. R. DOUGLAS. Computational complexity of the landscape. I. [hep-th/0602072](#).
- [64] F. DENEFF, M. R. DOUGLAS, AND B. FLOREA. Building a better racetrack. *JHEP* **06** (2004) 034, [[hep-th/0404257](#)].
- [65] J. P. DERENDINGER, J. E. KIM, AND D. V. NANOPOULOS. Anti - SU(5). *Phys. Lett.* **B139** (1984) 170.
- [66] O. DEWOLFE, A. GIRYAVETS, S. KACHRU, AND W. TAYLOR. Enumerating flux vacua with enhanced symmetries. *JHEP* **02** (2005) 037, [[hep-th/0411061](#)].
- [67] D.-E. DIACONESCU, A. GARCIA-RABOSO, AND K. SINHA. A D-brane landscape on Calabi-Yau manifolds. [hep-th/0602138](#).
- [68] K. R. DIENES. Statistics on the heterotic landscape: Gauge groups and cosmological constants of four-dimensional heterotic strings. [hep-th/0602286](#).
- [69] K. R. DIENES, E. DUDAS, AND T. GHERGHETTA. A calculable toy model of the landscape. *Phys. Rev.* **D72** (2005) 026005, [[hep-th/0412185](#)].
- [70] T. P. T. DIJKSTRA, L. R. HUISZON, AND A. N. SCHELLEKENS. Chiral supersymmetric standard model spectra from orientifolds of Gepner models. *Phys. Lett.* **B609** (2005) 408–417, [[hep-th/0403196](#)].
- [71] T. P. T. DIJKSTRA, L. R. HUISZON, AND A. N. SCHELLEKENS. Supersymmetric standard model spectra from RCFT orientifolds. *Nucl. Phys.* **B710** (2005) 3–57, [[hep-th/0411129](#)].

- [72] M. DINE, D. O'NEIL, AND Z. SUN. Branches of the landscape. *JHEP* **07** (2005) 014, [[hep-th/0501214](#)].
- [73] M. DINE, E. GORBATOV, AND S. D. THOMAS. Low energy supersymmetry from the landscape. [hep-th/0407043](#).
- [74] J. DISTLER AND U. VARADARAJAN. Random polynomials and the friendly landscape. [hep-th/0507090](#).
- [75] M. R. DOUGLAS. The statistics of string / M theory vacua. *JHEP* **05** (2003) 046, [[hep-th/0303194](#)].
- [76] M. R. DOUGLAS. Understanding the landscape. [hep-th/0602266](#).
- [77] M. R. DOUGLAS AND Z. LU. Finiteness of volume of moduli spaces. [hep-th/0509224](#).
- [78] E. DUDAS AND C. TIMIRGAZIU. Internal magnetic fields and supersymmetry in orientifolds. *Nucl. Phys.* **B716** (2005) 65–87, [[hep-th/0502085](#)].
- [79] PARTICLE DATA GROUP, S. EIDELMAN *et al.* Review of particle physics. *Phys. Lett.* **B592** (2004) 1.
- [80] J. R. ELLIS, P. KANTI, AND D. V. NANOPOULOS. Intersecting branes flip  $SU(5)$ . *Nucl. Phys.* **B647** (2002) 235–251, [[hep-th/0206087](#)].
- [81] S. FÖRSTE. Strings, branes and extra dimensions. *Fortsch. Phys.* **50** (2002) 221–403, [[hep-th/0110055](#)].
- [82] S. FÖRSTE, G. HONECKER, AND R. SCHREYER. Supersymmetric  $Z(N) \times Z(M)$  orientifolds in 4D with D-branes at angles. *Nucl. Phys.* **B593** (2001) 127–154, [[hep-th/0008250](#)].
- [83] M. R. GAREY AND D. S. JOHNSON. Computers and Intractability, a Guide to the Theory of NP-Completeness. San Francisco, USA: Freeman, 1979.
- [84] J. GATES, S. J., C. M. HULL, AND M. ROCEK. Twisted multiplets and new supersymmetric nonlinear sigma models. *Nucl. Phys.* **B248** (1984) 157.
- [85] J. P. GAUNTLETT, D. MARTELLI, S. PAKIS, AND D. WALDRAM. G-structures and wrapped NS5-branes. *Commun. Math. Phys.* **247** (2004) 421–445, [[hep-th/0205050](#)].
- [86] H. GEORGI AND S. L. GLASHOW. Unity Of All Elementary Particle Forces. *Phys. Rev. Lett.* **32** (1974) 438–441.
- [87] D. GEPNER. Exact Solvable String Compactifications On Manifolds Of  $SU(N)$  Holonomy. *Phys. Lett.* **B199** (1987) 380–388.

- [88] D. GEPNER. Space-Time Supersymmetry In Compactified String Theory And Superconformal Models. *Nucl. Phys.* **B296** (1988) 757.
- [89] E. G. GIMON AND J. POLCHINSKI. Consistency Conditions for Orientifolds and D-Manifolds. *Phys. Rev.* **D54** (1996) 1667–1676, [[hep-th/9601038](#)].
- [90] A. GIRYAVETS, S. KACHRU, AND P. K. TRIPATHY. On the taxonomy of flux vacua. *JHEP* **08** (2004) 002, [[hep-th/0404243](#)].
- [91] F. GMEINER. Standard model statistics of a type II orientifold. *Fortsch. Phys.* **54** (2006) 391–398, [[hep-th/0512190](#)].
- [92] F. GMEINER, R. BLUMENHAGEN, G. HONECKER, D. LÜST, AND T. WEIGAND. One in a billion: MSSM-like D-brane statistics. *JHEP* **01** (2006) 004, [[hep-th/0510170](#)].
- [93] F. GMEINER AND M. STEIN. Statistics of SU(5) D-brane models on a type II orientifold. *Phys. Rev.* **D73** (2006) 126008, [[hep-th/0603019](#)].
- [94] F. GMEINER AND F. WITT. Calibrated cycles and T-duality. [math.dg/0605710](#).
- [95] M. GRAÑA. Flux compactifications in string theory: A comprehensive review. *Phys. Rept.* **423** (2006) 91–158, [[hep-th/0509003](#)].
- [96] M. GRAÑA, J. LOUIS, AND D. WALDRAM. Hitchin functionals in  $N = 2$  supergravity. *JHEP* **01** (2006) 008, [[hep-th/0505264](#)].
- [97] M. GRAÑA, R. MINASIAN, M. PETRINI, AND A. TOMASIELLO. Supersymmetric backgrounds from generalized Calabi-Yau manifolds. *JHEP* **08** (2004) 046, [[hep-th/0406137](#)].
- [98] M. GRAÑA, R. MINASIAN, M. PETRINI, AND A. TOMASIELLO. Type II strings and generalized Calabi-Yau manifolds. *Comptes Rendus Physique* **5** (2004) 979–986, [[hep-th/0409176](#)].
- [99] M. GRAÑA, R. MINASIAN, M. PETRINI, AND A. TOMASIELLO. Generalized structures of  $N = 1$  vacua. *JHEP* **11** (2005) 020, [[hep-th/0505212](#)].
- [100] P. GRANGE AND R. MINASIAN. Tachyon condensation and D-branes in generalized geometries. *Nucl. Phys.* **B741** (2006) 199–214, [[hep-th/0512185](#)].
- [101] M. B. GREEN, J. H. SCHWARZ, AND E. WITTEN. Superstring theory vol. 1: Introduction. Cambridge Monographs On Mathematical Physics. Cambridge, UK: University Press, 1987.
- [102] M. B. GREEN, J. H. SCHWARZ, AND E. WITTEN. Superstring theory vol. 2: Loop amplitudes, anomalies and phenomenology. Cambridge Monographs On Mathematical Physics. Cambridge, UK: University Press, 1987.

- [103] M. GUALTIERI. Generalized complex geometry. DPhil thesis, Oxford University, 2003. [math.DG/0401221](#).
- [104] J. GUTOWSKI, S. IVANOV, AND G. PAPADOPOULOS. Deformations of generalized calibrations and compact non-Kähler manifolds with vanishing first Chern class. *Asian J. Math.* **7** (2003), no. 1 39–79, [[math.dg/0205012](#)].
- [105] J. GUTOWSKI AND G. PAPADOPOULOS. AdS calibrations. *Phys. Lett.* **B462** (1999) 81–88, [[hep-th/9902034](#)].
- [106] G. N. HARDY AND S. RAMANUJAN. Asymptotic formulae in combinatory analysis. *Proc. Lond. Math. Soc.* **2** (1918) 75.
- [107] R. HARVEY AND H. LAWSON. Calibrated geometries. *Acta Math.* **148** (1982) 47.
- [108] S. F. HASSAN. T-duality, space-time spinors and R-R fields in curved backgrounds. *Nucl. Phys.* **B568** (2000) 145–161, [[hep-th/9907152](#)].
- [109] N. HITCHIN. Generalized Calabi-Yau manifolds. *Q. J. Math.* **54 no. 3** (2003) 281–308, [[math.dg/0209099](#)].
- [110] N. HITCHIN. Brackets, forms and invariant functionals. [math.dg/0508618](#).
- [111] K. HORI, S. KATZ, A. KLEMM, R. PANDHARIPANDE, R. THOMAS, C. VAFA, R. VAKIL, AND E. ZASLOW. Mirror Symmetry. Clay Mathematics Monographs, Vol. 1. AMS, 2003.
- [112] L. E. IBANEZ, J. E. KIM, H. P. NILLES, AND F. QUEVEDO. Orbifold compactifications with three families of  $SU(3) \times SU(2) \times U(1)^n$ . *Phys. Lett.* **B191** (1987) 282–286.
- [113] L. E. IBANEZ, H. P. NILLES, AND F. QUEVEDO. Orbifolds and Wilson lines. *Phys. Lett.* **B187** (1987) 25–32.
- [114] C. JESCHEK. Generalized Calabi-Yau structures and mirror symmetry. [hep-th/0406046](#).
- [115] C. JESCHEK AND F. WITT. Generalised  $G_2$ -structures and type IIB superstrings. *JHEP* **0503** (2005) 053, [[hep-th/0412280](#)].
- [116] C. JESCHEK AND F. WITT. Generalised geometries, constrained critical points and Ramond-Ramond fields. [math.DG/0510131](#).
- [117] C. V. JOHNSON. D-branes. Cambridge, USA: University Press, 2003.
- [118] S. KACHRU, M. B. SCHULZ, P. K. TRIPATHY, AND S. P. TRIVEDI. New supersymmetric string compactifications. *JHEP* **03** (2003) 061, [[hep-th/0211182](#)].

- [119] R. KALLOSH AND A. LINDE. M-theory, cosmological constant and anthropic principle. *Phys. Rev.* **D67** (2003) 023510, [[hep-th/0208157](#)].
- [120] A. KAPUSTIN. Topological strings on noncommutative manifolds. *Int. J. Geom. Meth. Mod. Phys.* **1** (2004) 49–81, [[hep-th/0310057](#)].
- [121] A. KAPUSTIN AND Y. LI. Stability Conditions For Topological D-branes: A Worldsheet Approach. [hep-th/0311101](#).
- [122] A. KAPUSTIN AND Y. LI. Topological sigma-models with H-flux and twisted generalized complex manifolds. [hep-th/0407249](#).
- [123] A. KAPUSTIN AND D. ORLOV. Remarks on A-branes, mirror symmetry, and the Fukaya category. *J. Geom. Phys.* **48** (2003) [[hep-th/0109098](#)].
- [124] P. KOERBER. Stable D-branes, calibrations and generalized Calabi-Yau geometry. *JHEP* **08** (2005) 099, [[hep-th/0506154](#)].
- [125] J. KUMAR. A review of distributions on the string landscape. [hep-th/0601053](#).
- [126] J. KUMAR AND J. D. WELLS. Landscape cartography: A coarse survey of gauge group rank and stabilization of the proton. *Phys. Rev.* **D71** (2005) 026009, [[hep-th/0409218](#)].
- [127] J. KUMAR AND J. D. WELLS. Surveying standard model flux vacua on  $T^6/Z_2 \times Z_2$ . *JHEP* **09** (2005) 067, [[hep-th/0506252](#)].
- [128] J. KUMAR AND J. D. WELLS. Multi-brane recombination and standard model flux vacua. [hep-th/0604203](#).
- [129] M. LAROSA AND G. PRADISI. Magnetized four-dimensional  $Z_2 \times Z_2$  orientifolds. *Nucl. Phys.* **B667** (2003) 261–309, [[hep-th/0305224](#)].
- [130] W. LERCHE, D. LÜST, AND A. N. SCHELLEKENS. Chiral Four-dimensional Heterotic Strings from Self-dual Lattices. *Nucl. Phys.* **B287** (1987) 477.
- [131] U. LINDSTRÖM, R. MINASIAN, A. TOMASIELLO, AND M. ZABZINE. Generalized complex manifolds and supersymmetry. *Commun. Math. Phys.* **257** (2005) 235–256, [[hep-th/0405085](#)].
- [132] U. LINDSTRÖM, M. ROCEK, R. VON UNGE, AND M. ZABZINE. Generalized Kähler geometry and manifest  $N = (2,2)$  supersymmetric nonlinear sigma-models. *JHEP* **07** (2005) 067, [[hep-th/0411186](#)].
- [133] U. LINDSTRÖM, M. ROCEK, R. VON UNGE, AND M. ZABZINE. Generalized Kähler manifolds and off-shell supersymmetry. [hep-th/0512164](#).
- [134] D. LÜST. Intersecting brane worlds: A path to the standard model? *Class. Quant. Grav.* **21** (2004) 1399–1424, [[hep-th/0401156](#)].

- [135] D. LÜST AND S. THEISEN. Lectures on String Theory. Lecture Notes in Physics. Berlin, Germany: Springer, 1989.
- [136] F. MARCHESANO AND G. SHIU. Building mssm flux vacua. *JHEP* **11** (2004) 041, [[hep-th/0409132](#)].
- [137] M. MARINO, R. MINASIAN, G. W. MOORE, AND A. STROMINGER. Non-linear instantons from supersymmetric p-branes. *JHEP* **01** (2000) 005, [[hep-th/9911206](#)].
- [138] L. MARTUCCI. D-branes on general N=1 backgrounds: Superpotentials and D-terms. [hep-th/0602129](#).
- [139] L. MARTUCCI AND P. SMYTH. Supersymmetric D-branes and calibrations on general N=1 backgrounds. *JHEP* **11** (2005) 048, [[hep-th/0507099](#)].
- [140] A. MISRA AND A. NANDA. Flux vacua statistics for two-parameter Calabi-Yau's. *Fortsch. Phys.* **53** (2005) 246–259, [[hep-th/0407252](#)].
- [141] W. NAHM. Supersymmetries and their representations. *Nucl. Phys.* **B135** (1978) 149.
- [142] H. OOGURI, C. VAFA, AND E. P. VERLINDE. Hartle-Hawking wavefunction for flux compactifications. *Lett. Math. Phys.* **74** (2005) 311–342, [[hep-th/0502211](#)].
- [143] J. POLCHINSKI. Dirichlet-Branes and Ramond-Ramond Charges. *Phys. Rev. Lett.* **75** (1995) 4724–4727, [[hep-th/9510017](#)].
- [144] J. POLCHINSKI. Lectures on D-branes. [hep-th/9611050](#).
- [145] J. POLCHINSKI. String theory. Vol. 1: An introduction to the bosonic string. Cambridge, UK: University Press, 1998.
- [146] J. POLCHINSKI. String theory. Vol. 2: Superstring theory and beyond. Cambridge, UK: University Press, 1998.
- [147] J. POLCHINSKI. The cosmological constant and the string landscape. [hep-th/0603249](#).
- [148] J. POLCHINSKI, S. CHAUDHURI, AND C. V. JOHNSON. Notes on D-Branes. [hep-th/9602052](#).
- [149] G. G. ROSS. Grand Unified Theories. Frontiers in Physics, 60. Reading, USA: Benjamin / Cummings, 1984.
- [150] A. N. SCHELLEKENS. The landscape “avant la lettre”. [physics/0604134](#).
- [151] M. M. SHEIKH JABBARI. Classification of different branes at angles. *Phys. Lett.* **B420** (1998) 279–284, [[hep-th/9710121](#)].

- [152] M. STEIN. Master's thesis, LMU Munich, 2006.
- [153] A. STROMINGER. Superstrings with torsion. *Nucl. Phys.* **B274** (1986) 253.
- [154] A. STROMINGER, S.-T. YAU, AND E. ZASLOW. Mirror symmetry is T-duality. *Nucl. Phys.* **B479** (1996) 243–259, [[hep-th/9606040](#)].
- [155] L. SUSSKIND. The anthropic landscape of string theory. [hep-th/0302219](#).
- [156] A. M. URANGA. D-brane probes, RR tadpole cancellation and K-theory charge. *Nucl. Phys.* **B598** (2001) 225–246, [[hep-th/0011048](#)].
- [157] C. VAFA. The string landscape and the swampland. [hep-th/0509212](#).
- [158] M. WANG. Parallel spinors and parallel forms. *Ann. Global Anal. Geom.* **7** (1989) 59–68.
- [159] S. WEINBERG. Anthropic bound on the cosmological constant. *Phys. Rev. Lett.* **59** (1987) 2607.
- [160] F. WITT. Generalised  $G_2$ -manifolds. [math.DG/0411642](#).
- [161] F. WITT. Special metric structures and closed forms. DPhil thesis, Oxford University, 2005. [math.DG/0502443](#).
- [162] E. WITTEN. Search for a realistic Kaluza-Klein theory. *Nucl. Phys.* **B186** (1981) 412.
- [163] E. WITTEN. An  $SU(2)$  anomaly. *Phys. Lett.* **B117** (1982) 324–328.
- [164] E. WITTEN. Mirror manifolds and topological field theory. in *Mirror symmetry I* (S. T. Yau, ed.), pp. 121–160. AMS, 1998. [hep-th/9112056](#).
- [165] R. WONG. Asymptotic Approximations of Integrals. New York, USA: Academic Press, 1989.
- [166] M. ZABZINE. Geometry of D-branes for general  $N=(2,2)$  sigma models. *Lett. Math. Phys.* **70** (2004) 211–221, [[hep-th/0405240](#)].
- [167] M. ZABZINE. Hamiltonian perspective on generalized complex structure. *Commun. Math. Phys.* **263** (2006) 711–722, [[hep-th/0502137](#)].
- [168] M. ZABZINE. Lectures on Generalized Complex Geometry and Supersymmetry. [hep-th/0605148](#).
- [169] R. ZUCCHINI. A sigma model field theoretic realization of Hitchin's generalized complex geometry. *JHEP* **11** (2004) 045, [[hep-th/0409181](#)].
- [170] R. ZUCCHINI. Generalized complex geometry, generalized branes and the Hitchin sigma model. *JHEP* **03** (2005) 022, [[hep-th/0501062](#)].

- [171] R. ZUCCHINI. A topological sigma model of biKähler geometry. *JHEP* **01** (2006) 041, [[hep-th/0511144](#)].
- [172] B. ZWIEBACH. A first course in string theory. Cambridge, UK: University Press, 2004.



# Curriculum Vitae

## General Information

Date of birth:	04/12/1977	Marital status:	Single
Place of birth:	Berlin	Citizenship:	German

## Education

06/03 - 07/06	PhD thesis, supervised by Prof. D. Lüst, Humboldt University, Berlin, Max Planck Institute for Physics and Arnold Sommerfeld Center for Theoretical Physics, Munich
02/03 - 06/03	Study trip to Southamerica
01/03	Language course Spanish, Madrid
11/02 - 12/02	Practical training at the Moscow State Aviation Institute
10/01 - 10/02	Diploma thesis, supervised by Prof. H. P. Nilles, Bonn University; Master in physics
07/01 - 09/01	DESY summer student program, Hamburg
03/00 - 07/01	Graduate studies in physics, Heidelberg University
09/99 - 02/00	ERASMUS scholarship, Università degli Studi di Torino
09/97 - 08/99	Undergraduate studies in physics, Heidelberg University
08/87 - 08/97	Secondary school and civil service, Osnabrück

## Special qualifications

04/01	Lecturer at the university computer center (Introduction to Linux), Heidelberg
09/00 - 12/01	Freelance web designer for "novalis media" company, Heidelberg
04/00 - 06/00	Scientific assistant at the European Media Laboratory, Heidelberg
12/98 - 06/99	Scientific assistant at the university computer center (Linux system administration), Heidelberg
08/98	Scientific assistant at the "Leonardo da Vinci" project for interactive learning of the European Union, Marseille

**Teaching**

- 10/05 - 02/06 TA for theoretical physics (quantum mechanics), LMU Munich  
 04/04 - 09/04 TA for theoretical physics (theoretical mechanics), HU Berlin  
 10/01 - 09/02 TA for theoretical physics (theoretical mechanics, electrodynamics, quantum mechanics), Bonn U.  
 04/01 - 09/01 TA for theoretical physics (electrodynamics), Heidelberg U.

**Invited talks***Conferences*

- 09/25/05 *Statistics of MSSM-like models in type II String Theory* (RTN conference, Corfu)  
 06/15/05 *Statistical aspects of type II orientifold models* (String Phenomenology 2005 conference, Munich)  
 10/27/04 *Generalized complex geometry and topological sigma models* (MPI Young Scientists Workshop, Ringberg Castle)

*Seminars*

- 12/05-02/06 *One in a Billion: MSSM-like D-Brane Statistics* (Bonn, Torino, UPenn, Rutgers, Princeton, MIT, UNC, Cornell)  
 12/07/04 *String Statistics* (LMU Munich)  
 04/27/04 *Scherk-Schwarz compactifications and D-branes* (HU Berlin)  
 10/01/02 *Anomalies on Orbifolds* (Bonn U.)

**Conferences**

- 06/06 Workshop on "String Vacua and The Landscape", ICTP, Trieste  
 09/05 RTN conference "The Quantum Structure of Spacetime and the Geometric Nature of Fundamental Interactions", Corfu  
 07/05 "Strings 2005" conference, Toronto  
 06/05 "String Phenomenology 2005" conference, Munich  
 11/04 "String Vacuum Workshop", MPI, Munich  
 10/04 MPI Young Scientists' Workshop "Hot Topics in Particle and Astroparticle Physics", Ringberg  
 09/04 RTN conference "The Quantum Structure of Spacetime and the Geometric Nature of Fundamental Interactions", Kolymbari  
 09/03 RTN conference "The Quantum Structure of Spacetime and the Geometric Nature of Fundamental Interactions", Copenhagen

**Schools**

01/06	RTN Winter school on “Strings, Supergravity and Gauge Theories”, CERN
03/05	Spring school “Superstring Theory and Related Topics”, ICTP, Trieste
02/05	RTN Winter school on “Strings, Supergravity and Gauge Theories”, ICTP, Trieste
03/04	Spring School ”Superstring Theory and Related Topics”, ICTP, Trieste
01/04	RTN Winter school on “Strings, Supergravity and Gauge Theories”, Barcelona
10/03	Workshop ”Advanced Topics in String Theory”, DESY, Hamburg
09/02	National Summer School for Graduate Students ”Basics and new methods in theoretical physics”, Wolfersdorf

**Languages**

German:	native	Italian:	good knowledge
English:	fluent	French:	basic knowledge
Spanish:	good knowledge	Dutch:	basic knowledge

**Computer skills**

Operating systems:	Unix/Linux, Windows
Programming:	C(++), Java, Pascal/Delphi, Perl, PHP, XML
Applications:	L <sup>A</sup> T <sub>E</sub> X, Maple/Mathematica, MS Office

I have experiences as system administrator of Linux networks and in the fields of numerical-, cluster- and web-programming.